AN ABSTRACT OF THE THESIS OF

David Lloyd Vernier for the degree of Master of Science

in General Science presented on August 11, 1975
(Date)

Title: THE SOLID STATE PHOTOCHEMISTRY AND PHOTOPHYSICS OF A TRIPHENYLMETHYL DYE CYANIDE

Redacted for Privacy

Abstract approved: Dr. Malcolm Daniels

Triphenylmethyl dye cyanides have been known to be sensitive to ultraviolet radiation since early in this century. Under appropriate conditions, exposure to uv leads to heteropolar fission of the C-CN bond (photoionization) and intense coloration due to dye formation.

Thin homogeneous films of hexahydroxyethyl pararosaniline cyanide in a nylon matrix (Far West Technology) have been used to study the photochemistry of the dye cyanide in a solid medium and also to investigate its potential as a uv dosimeter.

The dye cyanide in nylon absorbs strongly in the uv ($\varepsilon_{max}$ = 6.25 x $10^4$ liter $mole^{-1}$ $cm^{-1}$ at 277 nm) and dye is produced by excitation at wavelengths < 340 nm. The dye absorbs strongly in the red region ($\varepsilon_{max}$ = 7.0 x $10^4$ liter $mole^{-1}$ $cm^{-1}$ at 608 nm). The extent of photoioniza-

tion may thus be determined from the optical density in the red region. In addition, the dye has been found to fluoresce when excited with a helium-neon laser at 633 nm and this property may also be used to follow the course of photolysis.

The film response is reproducible, stable after exposure for many days, and dose-rate independent. However, at room temperature the partitioned quantum yield for dye formation varies from 0.4 at 260 nm to about 1 at 340 nm. Furthermore, the quantum yield is strongly dependent on the temperature during photolysis. These features limit the use of the film as an integrating actinometer for erythemal uv, but it should be valuable as a routine laboratory actinometer for monochromatic radiation.

A model is presented to account for the observed photochemical behavior.

# The Solid State Photochemistry and Photophysics of a Triphenylmethyl Dye Cyanide

by

David Lloyd Vernier

A THESIS

submitted to

Oregon State University

in partial fulfillment of
the requirements for the
degree of

Master of Science

Commencement June 1976

APPROVED:

Redacted for Privacy

Professor of Chemistry

in charge of major

Redacted for Privacy

Chairman of Department of General Science

Redacted for Privacy

Dean of Graduate School

Date thesis is presented Aug 11 1975

Typed by Janet L. White for David Lloyd Vernier

TABLE OF CONTENTS

LIST OF FIGURES

# LIST OF TABLES

# THE SOLID STATE PHOTOCHEMISTRY AND PHOTOPHYSICS OF A TRIPHENYLMETHYL DYE CYANIDE

## INTRODUCTION

Triphenylmethane compounds were first reported to be photochromic (colored by light) early in the twentieth century. Lifschitz (1919) noticed that colorless solutions of crystal violet cyanide in ethanol became intensely colored upon exposure to ultraviolet radiation. He immediately recognized that this system might be a useful actinometer for uv. Since Lifschitz's discovery the photochromism of triphenylmethyl dyes has been studied extensively and applied in dosimetry of both uv and ionizing radiation.

Triphenylmethyl dyes consist of a central carbon atom surrounded by three phenyl rings. The characteristic color (i.e., position of visible absorption bands) of the dye is determined by the substituents, which are in positions para to the methane carbon atom. The formulae of several triphenylmethyl dyes are shown in Figure 1.

Colored solutions of triphenylmethyl dyes in polar solvents are decolorized when treated with various anions, especially cyanide, hydroxide, and bisulfite. In some solvents the solution will become intensely colored again upon exposure to uv, the color formed being that of the original dye. Upon removal of the radiation the color

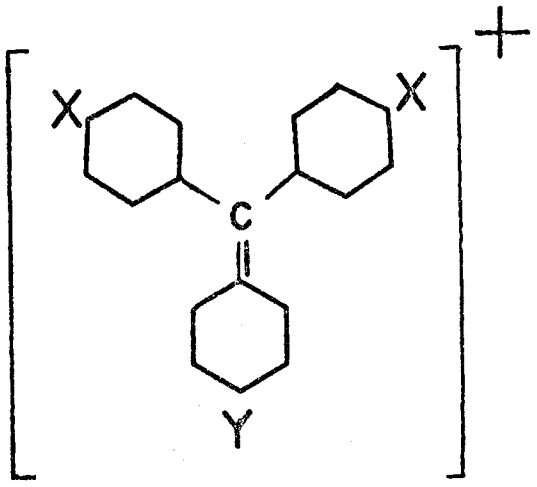

| | X | Y |
|---|---|---|
| Crystal Violet | $N(CH_3)_2$ | $N(CH_3)_2$ |
| Pararosaniline | $NH_2$ | $NH_2$ |
| Magenta III | $NH_2(OCH_3)$ | $NH_2(OCH_3)$ |
| Malachite Green | $N(CH_3)_2$ | H |
| Brilliant Green | $N(C_2H_5)_2$ | H |
| Hexahydroxylethyl Pararosaniline | $N(C_2H_5O)_2$ | $N(C_2H_5O)_2$ |

Figure 1. Classical formulae of some triphenylmethyl dyes. (Based on Oster and Oster, 1962)

fades and the cycle can be repeated. The reverse (fading) reaction rate increases with temperature and may also be increased by addition of the appropriate anion. Weyde and Frankenburger (1931) proposed crystal violet cyanide in ethanol as a reusable actinometer of uv. The equilibrium of the dye cyanide and the dye was dependent on the intensity of the ultraviolet light. The equilibrium was also affected by temperature since the reverse reaction rate is temperature dependent.

The reverse reaction was found to be strongly inhibited by the presence of acid in the solution and Harris and Kaminsky (1935b) proposed an acidified solution of malachite green cyanide in ethanol as an integrating actinometer of uv. Their actinometer, unlike Frankenburger's, measured uv exposure rather than light intensity and showed little temperature response[1].

In the solutions described above the purpose of the ethanol was not just to affect solution but also to render the dye cyanide sensitive to light. Pure crystalline dye cyanide is insensitive to uv (Chalkley, 1952), as are many solutions (e.g., nonpolar solutions) of the dyestuff. The

---

[1]The terms "exposure" and "intensity" will be used in this thesis with the following definitions. Exposure refers to the number of quanta incident per $cm^2$. Intensity refers to the number of quanta per unit time per $cm^2$.

presence of a photoactivating agent is required for photochromism. The term photoactivating agent is used here to refer to any substance which when used as a solvent or added in small amounts as an additive causes the dye cyanide to become photochromic. Several classes of compounds have been found to be effective as photoactivating agents (Bishop, et al, 1973 and Chalkley, 1952):

1. nitriles, in which there is a hydrogen atom attached
2. amines
3. aromatic carbinols
4. polyoxy compounds
5. alcohols
6. hydroxy compounds
7. carboxylic acids
8. ethers especially poly ethers
9. esters of phosphoric acid and some other inorganic acids

Chalkley (1952, 1959) found that in solid solution, various triphenylmethyl dye cyanides with certain organic activator additives (e.g., ß-(p-tert.-butyl-phenoxy) ethyl alcohol) were both uv sensitive and stable after irradiation. He produced uv sensitive impregnated papers and gelatine films. Chalkley (1955, 1961) also discovered that certain solutions, both liquid and solid, of dye cyanides were sensitive to ionizing radiation as well as uv. Since

this discovery most research with triphenylmethyl dye derivatives has been aimed at perfecting the system as an integrating chemical dosimeter of gamma and X rays and high energy particles. This research has lead to the development of thin films of various plastics containing dye cyanide which are sold as dosimeters of ionizing radiation (Humpherys and Wilcox, 1970).

## The Photochemistry of Triphenylmethyl Dye Cyanides

The ultraviolet absorption spectra of triphenylmethyl dye cyanides are basically the sum of the spectra of the individual aryl groups. This indicates that the three aryl groups are non-interacting electronic systems. This is consistent with the molecular structure usually given for the dye cyanide which has the three phenyl rings widely separated, forming, with the CN group, the four corners of a regular tetrahedron around the central carbon atom. The spectra show strong absorption ($\epsilon_{max} \approx 4 \times 10^4$ liter mole$^{-1}$cm$^{-1}$) in the region 250-275 nm probably due to a $\pi \rightarrow \pi^*$ transition.[2] A

---

[2]The extinction coefficients($\varepsilon$) used in this thesis are decadic molar extinction coefficients determined from the following form of Beer's law:

$$\frac{I}{I_o} = 10^{-\varepsilon c l}$$

Where $I_o$ represents incident light intensity
$I$ represents transmitted light intensity
$c$ is the molar concentration of the absorbing species
$l$ is the path length in cm

This decadic molar extinction coefficient is sometimes called molar absorptivity, absorption coefficient or molar absorbancy index.

weaker absorption band ($\varepsilon \approx 0.8 \times 10^4$ liter $mole^{-1} cm^{-1}$) in the area of 295-310 nm is probably due to $n \rightarrow \pi^*$ transitions in the ring substituents. A weaker absorption band at 240-250 nm in both the dye cyanide and the dye is assumed to be associated with the benzene nucleus (McLaughlin, 1966). The ultraviolet sensitivity of the triphenylmethyl dye cyanide typically extends to about 350 nm (Brown, 1971, page 311).

The dye cyanides are not very thermochromic, unlike the dye bisulfites and dye hydroxides (Brown, 1971, page 322), and this is one of the reasons why cyanide dye derivatives are almost exclusively used for actinometry and dosimetry.

The mechanism by which the photochromism occurs is not fully understood. The conversion from leucodye to dye is usually assumed to take place via at least one intermediate state, but the nature of these intermediate states is disputed. Lifschitz and his colleagues (1919) proposed a simple mechanism for the reactions involving an ionized, nonsolvated intermediate state based on studies of the conductivity of solutions before, during, and after photolysis. They found that the conductivity of the photolysed solutions was not as high as would have been expected if all of the dye cyanide was completely dissociated. They therefore proposed an intermediate which was nonsolvated and therefore did not enhance conductivity. The suggested

mechanism was then:

$$\underset{\text{colorless}}{D\text{-}CN} \overset{h\nu}{\rightleftharpoons} \underset{\substack{\text{colorless}\\ \text{nonsolvated}\\ \text{intermediate}}}{[D^{+}CN^{-}]} \rightleftharpoons \underset{\text{colored}}{D^{+} + CN^{-}}$$

Harris and Kaminsky (1935a) showed that the thermal reverse reaction was complicated by reaction with the solvent. By varying the solvent they found the decoloration reaction can result in the formation of products other than the dye cyanide. In solutions containing water they suggested that the colorless dye hydroxide was formed. Their reaction mechanism also included a colorless intermediate species although they offered no evidence for the existence of this species.

Holmes (1957) used malachite green leucocyanide in various solvents to show that the photochromism was still more complex. He proposed that the reaction path depended upon the dielectric constant of the solvent, the wavelength of exciting light, and in some cases the dipole moment of solvent. His proposed mechanism is shown in Figure 2. In this proposed scheme, irradiation of the dye cyanide in a solvent with a dielectric constant > about 4.5 leads to formation of dye cations. In solvents of lower dielectric constant Holmes noticed that irradiation produced a decrease in the absorption at the 270-280nm region and an increase at other wavelengths not associated with the dye. His conclusion was that in solvents of low dielectric con-

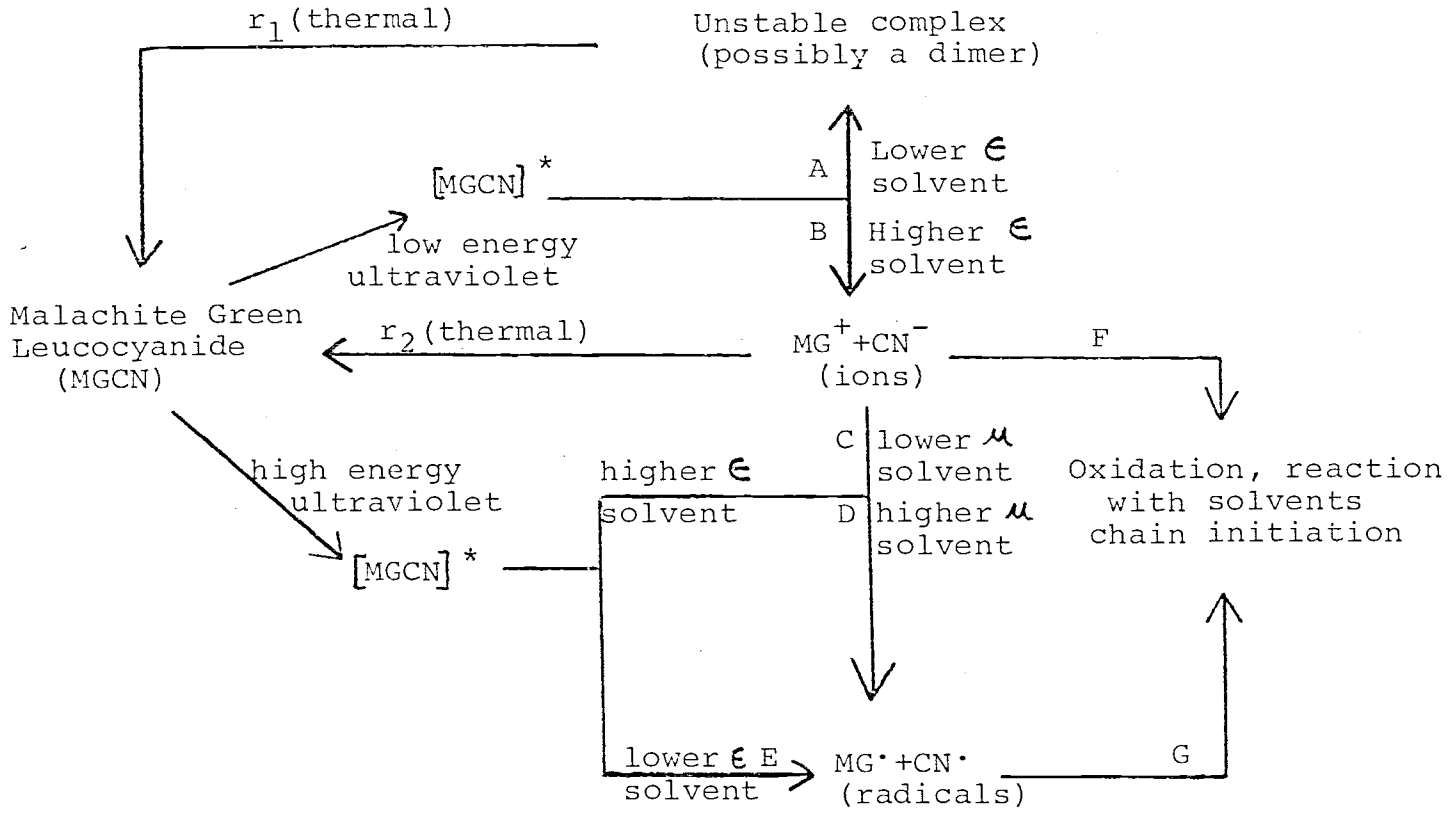


Figure 2. Photochromic scheme for malachite green leucocyanide proposed by Holmes (1957).

stant the photoreaction may be cleavage of substituents on the amine nitrogens and formation of the triphenylmethyl free radical. This conclusion was reached solely on the basis of absorption spectra of photolysed solutions with various solvents. Sporer (1961) claimed to observe the cleavage reaction and the formation of the triphenylmethyl free radical. The free radicals were detected by electron spin resonance techniques. He suggested that this reaction occurs in all media, but in solvents of higher dielectric constant it is masked by the dye formation reaction which occurs with a much higher quantum yield. Sporer proposed that the cleavage reaction occurs in photoexcited molecules in the triplet state and dye formation occurs when the excited molecule undergoes internal conversion to a high vibrational level of the ground electronic state.

The conclusions of Brown, et al (1962) based on a study of kinetics of the reaction of methyl violet with KCN in various solvents, generally conflict with the ideas of Holmes and Sporer. They concluded that free radicals are never formed but ion-pair complexes are formed as intermediates in all photoreactions. In solvents of lower dielectric constant these complexes never completely dissociate to form the dye cation and cyanide anion.

The quantum yield for dye formation based on photons absorbed by the dye cyanide of alcoholic solutions of triphenylmethyl dye cyanide has been measured by several

researchers. The usual result is that the quantum yield is unity within the limits of experimental error over the range of ultraviolet absorption. This was the result obtained by Weyde and Frankenburger (1931), Harris and Kaminsky (1935b), and Calvert and Rechen (1952) all using triphenylmethyl dye cyanides in ethanol. A more recent study by Fisher, et al (1967) gives a quantum yield for dye formation of 0.91 ± 0.01 using malachite green cyanide in ethanol. In addition, Fisher and his associates showed that the quantum yield was independent of intensity when the intensity was varied by a factor of ten. The apparent quantum yield may decrease as the dye concentration increases due to internal filtering by the dye (which absorbs in the uv). The quantum yield for dye formation may also vary with solvent as mentioned above. In water, Sporer (1961) found a quantum yield of 0.25. In solvents like cyclohexane with a low dielectric constant the quantum yield for dye formation may be zero (Holmes, 1957).

## The Photochemistry of Triphenylmethyl Dyes

The visible absorption spectra of triphenylmethyl dyes may consist of one or two absorption bands. All of the dyes exhibit intense absorption ($\varepsilon_{max} \approx 8 \times 10^4$ liter mole$^{-1}$ cm$^{-1}$) in the region 540-610 nm. Diamino-triphenylmethyl dyes have in addition a less intense absorption band

($\varepsilon_{max} \simeq 5 \times 10^4$ liter $mole^{-1}$ $cm^{-1}$) at 408-426 nm. These two absorption bands at either end of the visible spectrum give diamino-triphenylmethyl dyes a green color. Trimino-triphenylmethyl dyes have only one absorption band in the visible, generally in the red region, and hence appear blue or violet (Brown, 1971).

The triphenylmethyl dyes also absorb in the ultra-violet region. This absorption, which is less intense than the visible absorption ($\varepsilon_{max} \simeq 2 \times 10^4$ liter $mole^{-1} cm^{-1}$) is typically in the wavelength regions 300-318nm and 240-260nm. Triamino-triphenylmethyl dyes may also absorb in the region 352-396nm (Brown, 1971).

The apparent extinction coefficient of a particular commercial dye will vary considerably from batch to batch (Fisher, et al, 1967). The position of the absorption peaks are little affected by solvent but the intensity of absorption and shape of the peaks depend somewhat on the solvent (Brown, 1971, page 314). The cyanide anion, which is typically present in solution with the dye, does not absorb in the visible or uv region discussed above (Brown, 1971, page 311).

The structure of triphenylmethyl dyes and triaryl compounds in general has been investigated and debated for more than thirty years. There are two reasonable and popular models for their structure. The first is a model proposed by Lewis, and the other is a more recent model pro-

posed by Newman and Deno. Lewis, et al, (1942) proposed that triphenylmethyl dyes normally exist in a "windmill" structure. The molecule is almost planar, but each phenyl group is rotated slightly in the same direction. The three phenyl groups share the positive charge equally. Complete coplanarity is impossible because of the repulsion of the hydrogen atoms ortho to the methane carbon. Martin and Smith (1964) calculate the rotation of the phenyls as 50-60° based on the probable distances of separation of the hydrogens and the forces of repulsion involved.

Lewis, et al, (1942) also noticed that there was a shoulder on the short wavelength side of the visible absorption peak of some triphenylmethyl dyes. This they attributed to a second windmill-like isomer, but this time with one of the "blades" (phenyl groups) turned in the opposite sense of the other two. This isomer is thought to have more energy than the symmetrical one.

The other popular structural model for triphenylmethyl dyes is a "distorted" one with two of the rings involved in the resonance interaction at a given time. The stability of triphenylmethyl dyes could be attributed to the large number of contributing resonance structures that are possible when all three rings are coplanar, but the propeller model destroys this coplanarity. Newman and Deno (1951) suggested that an alternative way of achieving this stabilization is by having one or two of the rings sharing

the positive charge at any given time. The rings not contributing to the resonance are essentially perpendicular to the plane of the central carbon atom. This model is supported by paramagnetic resonance studies (de Groot, et al, 1966) and studies of ionization and dissociation equilibria in liquid sulfur dioxide (Lichtin, et al, 1957).

Triphenylmethyl dyes are not normally fluorescent. However, in rigid solvents they display appreciable fluorescence (Lewis, et al, 1942). Studies of the effect of viscosity of the medium on this fluorescence show that it increases with viscosity (Oster and Nishijima, 1956). Their explanation depends on the fact that one way that these molecules in the excited state can return to the ground state is by energy dissipation via rotation of the phenyl groups. In a medium of high viscosity this process would be restricted and a higher proportion of the excited molecules would undergo de-excitation by fluorescence. By way of comparison, di- and triphenyl compounds with a "bridge" between the phenyl groups to prevent rotation (e.g., xanthene dyes) do fluoresce strongly even in non-rigid solutions (Venkataraman, II, 1952, page 744). Oster and Nishijima (1956) proposed the degree of fluorescence of triphenylmethane dyes as a practical measure of viscosity of a medium.

Fluorescence of triphenylmethyl dyes in non-rigid media is observed when the dye is bound to a high mole-

cular weight polymer (Oster and Oster, 1962). The binding apparently also inhibits rotation of the phenyl groups and thus increases the probability of fluorescence.

The fluorescence emission spectrum of triphenylmethyl dyes which lack trigonal symmetry is found to depend on the wavelength of the exciting light. These green dyes have two absorption peaks associated with two independent electronic systems. These two absorption peaks were called x and y bands by Lewis and his coworkers (Lewis and Bigeleisen, 1943b, 1943a; Lewis, et al, 1944). Absorption of the two different wavelengths of light amounts to exciting two perpendicular independent electronic systems. The fluorescences produced are different in color and polarized in perpendicular orientations.

Lewis and Bigeleisen (1943b) also produced photochemically asymmetrical dyes from leucocyanides in rigid media. They found that the dye molecules could be produced in specific orientation by using polarized light. The absorption spectrum of the dye then depended upon the polarization of the light used to determine absorption.

Triphenylmethyl dyes have notoriously poor lightfastness in practical application. The photofading of triphenylmethyl dyes has been attributed to oxidation, reduction, and decomposition. The products of the bleaching were found by Iwamoto (1935) to depend on the presence or absence of air. In the presence of air, he found solid

malachite green and crystal violet were converted into p-dimethylaminobenzophenone and Michler's ketone respectively.

Malachite green ⟶ 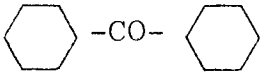 --- $N(CH_3)_2$

p-dimethylaminobenzophenone

Crystal violet ⟶ $(CH_3)_2N$ 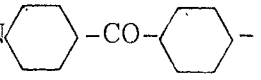 - $N(CH_3)_2$

Michler's ketone

These reactions are interpreted as being due to oxidation because when crystal violet was exposed to sunlight in the absence of air only the leuco compound was produced.

Crystal violet ⟶ $[(CH_3)_2NC_6H_4-]_3CH$

Leuco crystal violet

Hillson and Rideal (1953) studied the electrical potentials created on electrodes submerged in a triphenylmethyl dye solution as it was exposed to light. They concluded that the excited dye molecules may undergo either oxidation or reduction. The reduction process yielded the leuco base as shown below.

$$\text{Dye} + H_2 + e^- \longrightarrow \text{leuco base}$$

The photooxidation process had to involve either hydroxyl ions or water molecules. They found the rate of oxidation to be independent of the concentration of hydroxyl ions and hence concluded that the reaction must be with water.

Leaver (1972) studied photobleaching of crystal violet in solutions of dimethylformamide, ethanol, and water and in poly (vinyl alcohol) films. He used electron spin

resonance, absorption, and fluorescence spectroscopy to identify the photoproducts. He determined that in both solution and film, the semireduced tri-(p-dimethylamino-phenyl)methyl was the chief product. This radical is a likely precursor of the fully reduced leuco crystal violet and thus Leaver's work seems to indicate that except in pure solid state, photoreduction is the dominant method of bleaching for triphenylmethyl dyes.

Oster and his associates (Oster, et al, 1956, 1957, 1959; Oster and Oster, 1962) have made an extensive study of photoreduction of triphenylmethyl dyes. They have noticed that the dyes do not normally undergo photoreduction in solution in the presence of mild reducing agents. However, some of the dyes are readily photoreduced under the conditions in which they display fluorescence, namely in a rigid medium or when bound to high molecular weight polymers. They claim that this photoreduction proceeds via a long-lived intermediate state. The existence of this intermediate state is suggested by the kinetics of the reactions. Specifically, addition of a reductant does not significantly quench the fluorescence of bound dye. This must mean that the normal excited state of the dye does not directly react with a reductant to give the reduced dye, for this reaction would compete with fluorescence. If the first electronically excited state does not react with the reductant, another excited species must be involved. Oster

and Bellin (1957) claim that this intermediate species is produced via:

Dye in first electronically excited state + ground state dye ⟶ intermediate state dye + ground state dye

The production of intermediate state dye is thought to proceed in this manner rather than directly from the normal excited state because the quantum yield for photoreduction is proportional to the dye concentration.

The intermediate state is assumed to be long-lived because of its intimate relationship with phosphorescence of the dyes. The appearance of phosphorescence is a necessary criterion for photoreduction of a triphenylmethyl dye. As a result, the intermediate state and the phosphorescent state are assumed to be the same.

The intermediate state involved in the photoreduction of triphenylmethyl dyes is now thought to be the triplet state. Flash spectroscopy studies on closely related compounds have given proof that reductive photobleaching passes through the triplet state (Venkataraman, IV, 1971, page 436). The lifetime of this intermediate state in water is estimated at $10^{-4}$ seconds. This compares with the lifetime of the first electronically excited singlet state in water of $10^{-9}$ seconds (Oster and Oster, 1962).

The photoreduction process then is assumed to involve reaction of the intermediate excited triplet state of the dye with a reductant. The rate of photoreduction then

depends on the number of dye molecules in the triplet state. By increasing the viscosity of the medium or binding the dye to high molecular weight polymers, conversion from the singlet excited state to the ground state by internal rotation of the phenyl groups is inhibited and the number of transitions to the intermediate state increases. This would then imply increased photoreduction. However, photoreduction involves binary encounters between the intermediate state and an electron donor. Such encounters are diffusion-controlled and their frequency is inversely related to the viscosity of the medium. Increasing viscosity then has two opposing effects on the rate of photoreduction (Oster, et al, 1959).

Most of the discussion here has been on the photofading of triphenylmethyl dyes by reduction. Oxidation and other processes are also involved, especially under certain conditions. The probable photochemical reactions of triphenylmethyl dyes are summarized in the following diagram:

D = dye molecule (with net positive charge)
D* = dye molecule in singlet excited state
D' = dye molecule in long-lived intermediate (triplet) state
R = reductant

$D \xrightarrow{h\nu} D^*$ light absorption

$D^* \longrightarrow D$ fluorescence

$D^* \longrightarrow D$ via internal rotation

$D^* + D \longrightarrow D' + D$ production of the long-lived intermediate state

$D' \longrightarrow D$ phosphorescence

$D' + RH \longrightarrow DH + R$ reduction

$D^* + HOH \rightarrow DOH + H$ oxidation

The lightfastness of triphenylmethyl dyes can be improved by introduction of suitable substituents (e.g., p-anisidino or p-phenelidino groups or an indolyl nucleus) or by reacting them with a complex acid (Egerton and Morgan, 1970). As is the case with most dyes, the lightfastness depends as heavily upon the physical state of the dye as upon its chemical reactivity.

The Aims of the Present Study

Triphenylmethyl dye cyanides in various media are presently produced commercially for use in dosimetry of ionizing radiation. One popular method of utilizing the dye derivatives is in homogeneous solid solution in a thin film of nylon. Films of this type are produced by Far West Technology. The films are inexpensive and possess several characteristics which make them useful for measurement of high doses of radiation ($10^3$ - $10^7$ rads) (Humpherys, 1973):

- linear response over a wide range of doses
- dose-rate independence up to $10^{15}$ rad/sec
- energy independence down to a few kev
- equivalent response to X rays, gamma rays and electrons
- small temperature dependence
- long shelf life
- low atomic number constituents
- simple readout

These films are of course sensitive to ultraviolet radiation as well as ionizing radiation. The aim of the present study was to investigate the response of a particular triamino-triphenylmethyl dye cyanide, hexahydroxyethyl pararosaniline cyanide, in a solid nylon medium to ultraviolet radiation. A second goal was to explore the potential of the dye cyanide in nylon as a practical actinometer for ultraviolet light.

# EXPERIMENTAL METHODS

## Materials

The films used in these experiments were supplied by Kent C. Humpherys of Far West Technology and were prepared especially for this study using the same materials and manufacturing procedures used for the production of radiochromic films sold by Far West Technology for use in dosimetry of ionizing radiation. The films used are a homogeneous solid solution of hexahydroxyethyl pararosaniline cyanide in nylon (DuPont Elvamide 8061). Most experiments were performed with films containing 0.1% or 1.0% concentrations of dye cyanide, although films containing 10% dye cyanide and various concentrations of the uv absorber Tinuvin were available. Films of nylon with no dye cyanide added were also used. The thickness of a 6" x 6" sample of each type of film was measured with a micrometer in 20 random locations. The results are shown in the table below:

| FILM | THICKNESS | | | |
|---|---|---|---|---|
| | Maximum | Minimum | Mean | Std. Dev. |
| 0% dye | $7.2\times10^{-2}$mm | $5.5\times10^{-2}$mm | $6.38\times10^{-2}$mm | $.507\times10^{-2}$mm |
| 0.1% dye | $7.6\times10^{-2}$ | $5.8\times10^{-2}$ | $6.17\times10^{-2}$ | $.43\times10^{-2}$ |
| 1.0% dye | $7.2\times10^{-2}$ | $5.8\times10^{-2}$ | $6.10\times10^{-2}$ | $.535\times10^{-2}$ |

A sample of hexahydroxyethyl pararosaniline cyanide in powder form was also obtained from Far West Technology. The purity of this sample was checked using a specific ion

electrode (Chemtrix C 800 CN). This electrode, when placed in a solution containing cyanide ions, can produce a potential proportional to the $CN^-$ concentration. A Radiometer type PHM 26 pH-millivolt meter was used to monitor the potential produced between the selective ion electrode and a reference electrode (a Radiometer type K401 calomel electrode). A calibration curve was first determined using solutions of known concentration of sodium cyanide. This curve is shown in Figure 3. The NaCN solutions were made up using triply distilled water and reagent grade sodium cyanide. These solutions were also made 0.1 M in sodium perchlorate to ensure uniform ionic strength.

Since the photolysis of hexahydroxyethyl pararosaniline cyanide produces $CN^-$ ions, the concentration of $CN^-$ in a completely photolysed sample of the dye cyanide provided a check of the concentration of dye cyanide in the original solution. The purity of the dye cyanide sample was checked in this manner. A solution nominally $2.5 \times 10^{-6}$M in hexahydroxyethyl pararosaniline cyanide was prepared using triply distilled water, 0.1 M in sodium perchlorate. This solution was then exposed to sunlight in stages with the $CN^-$ concentration checked after each exposure using the specific ion electrode. The maximum potential produced by this solution was -273 mv and -276 mv in two independent experiments. Using the calibration curve of Figure 3, these potentials correspond to a $CN^-$ concentration of

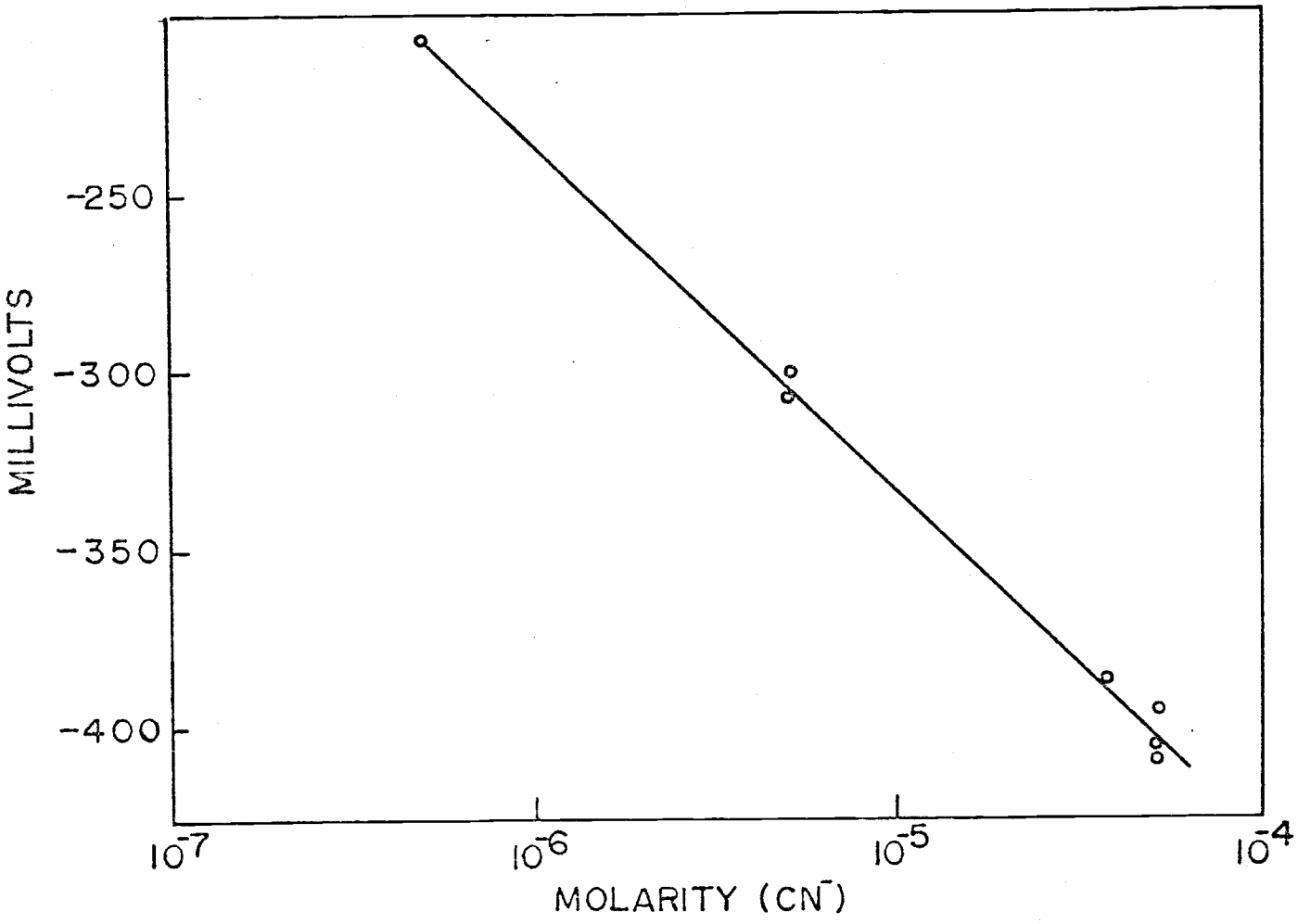


Figure 3. Potential produced between cyanide selective ion electrode and reference electrode as a function of $CN^-$ concentration.

$2.5 \times 10^{-6}$ M and $2.8 \times 10^{-6}$ M. This compares to $2.5 \times 10^{-6}$M if 100% sample purity is assumed. However, due to the logarithmic nature of the calibration curve and uncertainty in the potential reading, the estimated $CN^-$ concentration has a fairly large uncertainty associated with it.

For use in determining extinction coefficients, this sample of hexahydroxyethyl pararosaniline cyanide was assumed 100% pure.

Determination of Reflection Losses

Experimental apparatus used for determination of reflection losses is diagramed in Figure 4. The light source was a 100 watt tungsten-halogen lamp with a quartz bulb (Sylvania 6.6 A/T2½-Q/CL-100). Both monochromators were Bausch and Lomb monochromators with uv gratings (33-86-01). The monochromatic beam was made nearly parallel using an achromatic condenser lens (Bausch and Lomb 33-86-53) and then was split into two components by partial reflection from a plate of Spectrosil fused silica. Both detectors were RCA 1P28 photomultipliers. They were both connected to voltage-frequency converters (Dymec model 2210) producing a voltage across the converter's $10^6$ ohm input resistor. The output signal from the voltage-frequency converters was fed into two Harshaw scalers. The count rate on each scaler should then be proportional to the photomultiplier's output. The linearity of the count rate vs. light intensity was periodically checked using neutral

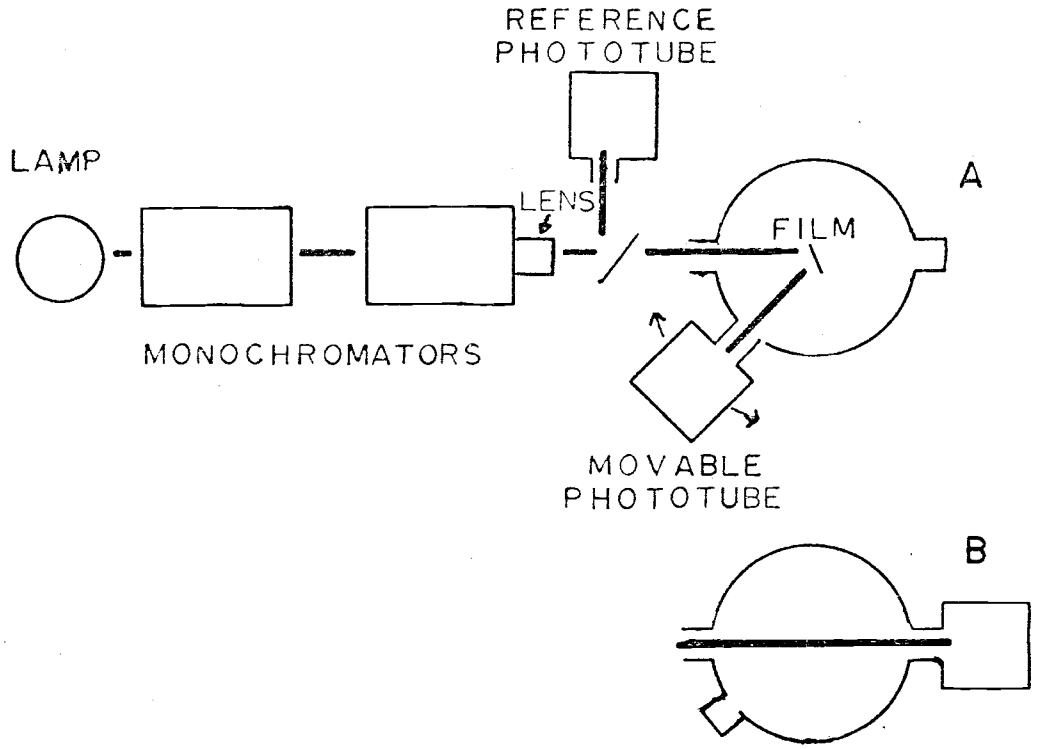


Figure 4. Apparatus used to determine reflection losses from films. (A) Movable photomultiplier and film positioned so that specular reflection from the film is monitored. (B) Movable photomultiplier rotated to monitor incident light intensity with film removed.

density filters of known transmittance in the light path.

The reference photomultiplier and its readout system served as a concurrent check on the consistency of the light source. The movable photomultiplier could be used to monitor the reflected light at any of several angles as shown in Part A of Figure 4. It could also be used to determine the intensity of the incident light by moving it to Position B (Figure 4) and removing the reflector (film). The ratio of the count rates from the movable photomultiplier in these two positions was the fraction of the light reflected.

The apparatus and procedure for reflection measurements was checked before use with the film by measuring reflection from a Spectrosil fused silica plate. The optical constants of the fused silica plate are available from the manufacturer (American Therma Fused Quartz Co.). Using Fresnel's laws of reflection on this data, the theoretical reflectivity at normal incidence from an air-fused silica interface can be calculated. For non-zero angles of incidence the polarization of the incident light must be considered. This was experimentally determined by measuring the relative transmittance of a uv linear polarizer (Polaroid HNP'B) in vertical and horizontal orientations in the incident light path. This data was then used to calculate the theoretical reflectivity at various angles of incidence and various wavelengths of an air-fused silica

interface. The calculations were done using the equation:

$$R = \tfrac{1}{2}\left(\frac{\tan (i-r)}{\tan (i+r)} (1+\bar{p}) + \frac{\sin (i-r)}{\sin (i+r)} (1-\bar{p})\right)$$

R = reflectivity
i = angle of incidence
$\bar{p}$ = polarization of incident light
r = angle of refraction = $\sin^{-1}$ (sin i/r)

The total fraction of the incident light that should be reflected from the two air-fused silica interfaces was calculated following Hunt and Hill (1947):

$$\frac{I_r}{I_o} = R\left(1 + \frac{1-R}{1+R}\right)$$

The calculated theoretical fractions reflected for several angles of incidence and several wavelengths were then compared with experimentally determined reflection data for the fused silica plate. A typical result is shown in Figure 5 for reflections at 320 nm. For all wavelengths investigated there was good agreement between experimental and theoretical results.

The fractional reflection at normal incidence from films was determined by graphical extrapolation of experimentally determined fractional reflection data at non-zero angles of incidence. Data for reflection with angles of incidence of 20°, 22.5°, 25°, 30°, 35° and 40° was plotted as in Figure 6.

The fractional reflection from films containing 0% and 1% dye cyanide was also determined using a Beckman DK2 ratio recording spectrophotometer equipped with an integrating sphere. The film tested was placed on a black

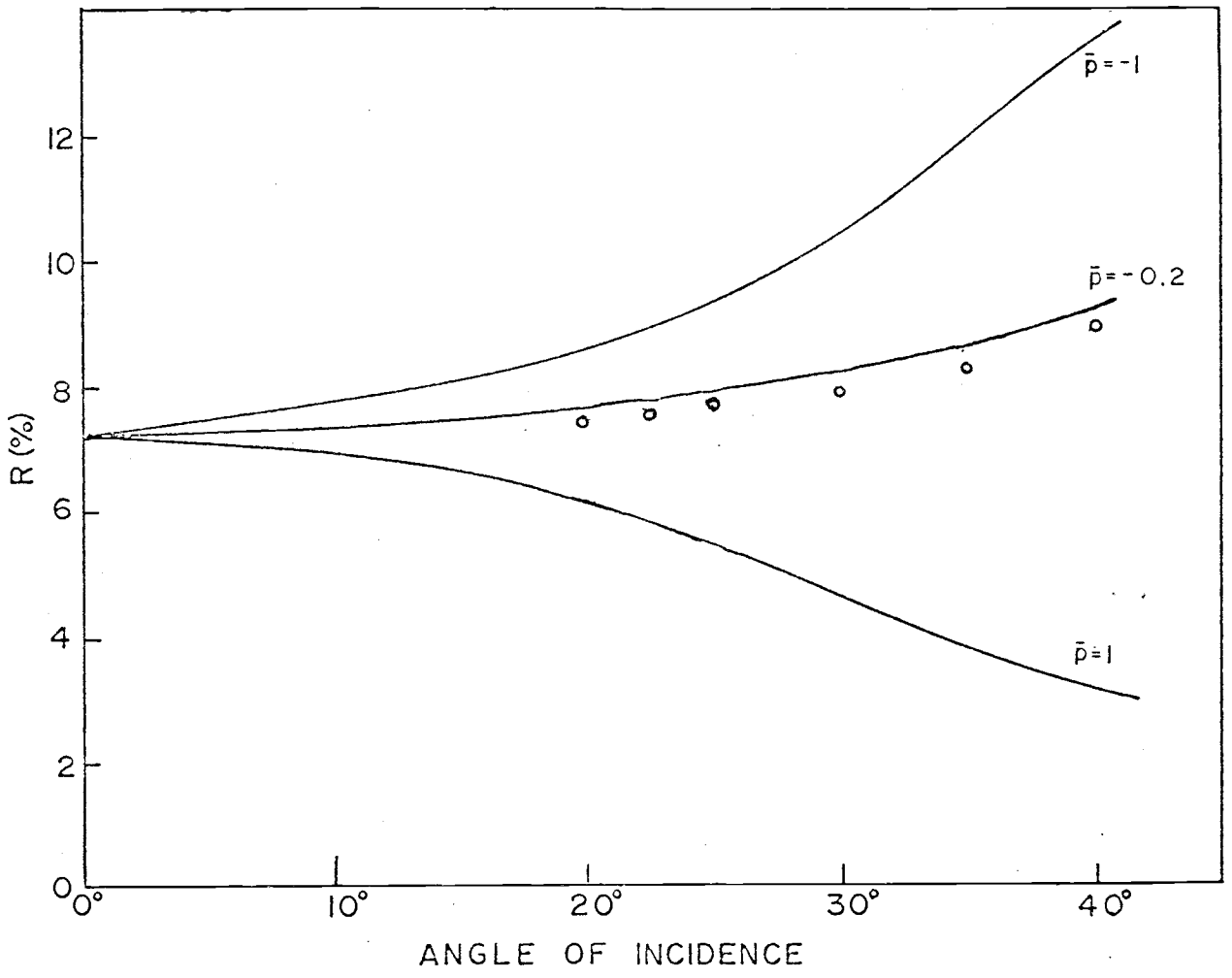


Figure 5. Theoretical and experimental per cent reflection at 320 nm from a fused silica plate. The solid lines are the theoretical values for polarizations of incident light of 1, -1, and -0.2, the polarization of the incident light actually used. The circles represent experimental values.

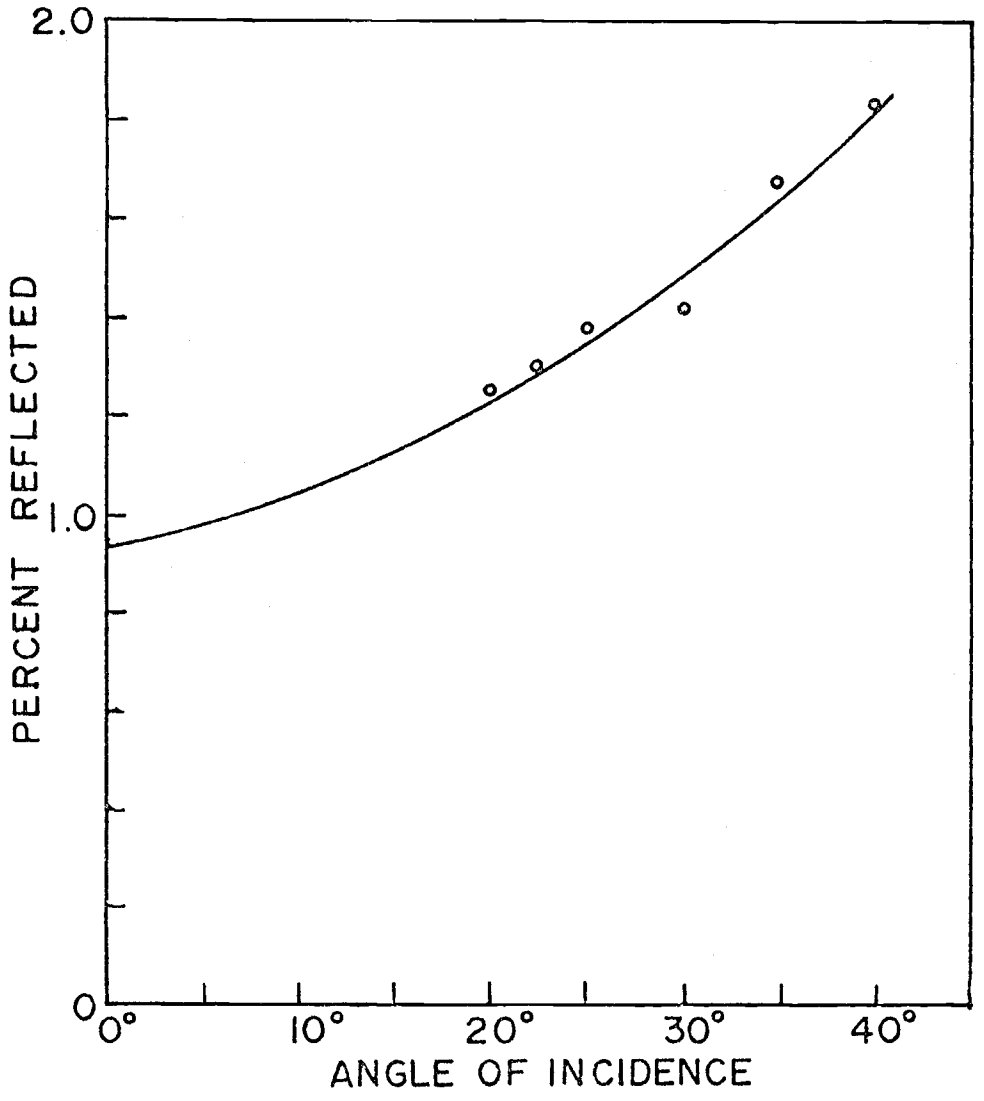


Figure 6. A typical plot of per cent of incident light reflected from a film (1% dye cyanide) vs. angle of incidence. The wavelength of light used in this case was 340 nm. The per cent reflected at normal incidence was extrapolated using graphs of this type.

background and the instrument was set up for determining total (specular plus diffuse) reflection. Correction was made for light reflected from the black background as follows:

$$R_{cor}^{\lambda} = R_{uncorrected}^{\lambda} - (T^{\lambda})^2 R_b^{\lambda}$$

where $T^{\lambda}$ is the fractional transmission of the film and $R_b$ is the fractional reflection from the "black" background itself.

Absorption Spectra

All absorbance measurements in the uv and visible regions were done in a Cary 1501 spectrophotometer equipped with a digital data recording system. Infrared absorption spectra of the films were determined using a Shimadzu MPS-50L recording spectrophotometer.

The absorption spectra of all liquids were determined using 1 cm path length fused silica cells. The spectra of solutes in liquid solution was determined from the absorption of the solution compared to the absorption of the solvent itself. This was determined directly by using a 1 cm path length fused silica cell filled with solvent in the reference beam of the spectrophotometer.

The absorption spectrum of dye cyanide and/or dye in a nylon film was determined by placing the film in the sample chamber of the spectrophotometer with a film of pure nylon of the same thickness in the reference chamber. The thicknesses were matched by comparing absorbances in a wave-

length region where neither the dye nor the dye cyanide absorb. A small correction was then made for the difference in reflection losses from the two films as determined using the integrating sphere. The absorption spectrum of the film as a whole was determined from the absorbance observed with only air in the reference chamber of the spectrophotometer. For determination of fractional absorption for quantum yield calculations, the spectra were corrected for the light lost by reflection.

Determination of the Extinction Coefficient of the Dye and the Dye Cyanide in the Nylon Film

The extinction coefficients of the dye cyanide in dimethyl sulfoxide (DMSO) were determined using Beer's law from the absorption spectrum of a $1.98 \times 10^{-5}$ M solution of hexahydroxyethyl pararosaniline, giving the value $6.25 \times 10^4$ liter $mole^{-1}$ $cm^{-1}$ at the absorption maximum 277 nm and at 20° C. Similar values for $\varepsilon$ were obtained using different concentrations. The solutions used in these determinations of $\varepsilon$ were made up using the dye cyanide in powder form obtained from Far West Technology with the assumption of 100% purity.

The extinction coefficient of the dye cyanide in the film was determined by comparison of dye cyanide absorption in the film and in DMSO. The absorbance at 277 nm due to dye cyanide in a film was determined and the volume of the same film was calculated from micrometer measurements. The dye cyanide was then leached from the film by a small volume of DMSO. Twice a day for three days the DMSO was

poured off into a volumetric flask and new DMSO was poured onto the film. At the conclusion of this process the film's absorption spectrum was determined and found to show no remaining absorption peak in the region of dye cyanide absorption. The DMSO containing the dye cyanide was diluted to 10 ml and the absorption of the dye cyanide in the solution was determined. Using Beer's law, the path lengths, volumes, and absorbances determined, the ratio of the extinction coefficients of the dye cyanide in nylon film and in DMSO was obtained as shown below:

$$A_{film} = \varepsilon_{film}\, c_{film}\, l_{film}$$

$$A_{DMSO} = \varepsilon_{DMSO}\, c_{DMSO}\, l_{DMSO} = \varepsilon_{DMSO}\, c_{film}\left(\frac{V_{film}}{V_{DMSO}}\right) l_{DMSO}$$

dividing one equation by the other =

$$\frac{\varepsilon_{film}}{\varepsilon_{DMSO}} = \frac{A_{film}\, l_{DMSO}\, V_{film}}{A_{DMSO}\, l_{film}\, V_{DMSO}}$$

This analysis was carried out at the wavelength of maximum dye cyanide absorption (277 nm). The results on two independent experiments were:

$$\frac{\varepsilon^{277\text{ nm}}_{film}}{\varepsilon^{277\text{ nm}}_{DMSO}} = .98 \quad \text{and} \quad \frac{\varepsilon^{277\text{ nm}}_{film}}{\varepsilon^{277\text{ nm}}_{DMSO}} = .96$$

Because these ratios are essentially one (within experimental error limits), the extinction coefficient of the dye cyanide at 277 nm was assumed to be the same in the film as in the DMSO. The value of $\varepsilon = 6.25 \times 10^4$ liters mole$^{-1}$ cm$^{-1}$ at 277 nm was thus adopted.

The extinction coefficient of the dye in nylon was obtained by comparison of dye cyanide absorption before photolysis and dye absorption after photolysis in the same film. The absorption due to dye cyanide in a film was measured at 277 nm. The film was then exposed to uv under conditions most favorable to dye formation (335 nm and 80° C, see discussion section). The absorbance at the dye peak was checked frequently during photolysis and photolysis continued until the maximum dye absorption was obtained. At this point all of the dye cyanide was assumed to be converted to dye. The ratio of the absorbance of the dye to the absorbance of dye cyanide was then used to calculate the extinction coefficient of the dye in the film.

$$\frac{A_{d}^{608\ nm}}{A_{d-c}^{277\ nm}} = \frac{\varepsilon_{d}^{608\ nm}}{\varepsilon_{d-c}^{277\ nm}} = 1.12$$

using the value of $\varepsilon_{dc}^{277\ nm}$ obtained above:

$$\varepsilon_{d}^{608\ nm} = 7.0 \times 10^{4} \text{ liter mole}^{-1} \text{ cm}^{-1}$$

The value of the maximum extinction coefficient for the dye in DMSO was found to be $9.3 \times 10^{4}$ liter $\text{mole}^{-1}$ $\text{cm}^{-1}$. The shape of the absorption spectrum used in determining the dye $\varepsilon_{max}$ in the film is very similar to the absorption spectrum of a solution of dye cyanide in DMSO after exposure to maximum dye concentration (compare Figures 14 and 20).

Actinometry

The intensity of uv at 302 nm was determined using differential oxalate actinometry (Pitts, et al, 1955). The actinometry solution (0.005 M $H_2C_2O_4$ and 0.001 M $UO_2C_2O_4$) was prepared using reagent grade oxalic acid and uranyl oxalate prepared by Robert Satcher (Ph.D. Thesis, 1971). The 1.35 x $10^{-2}$ M $Ce^{+4}$ solution was prepared using reagent grade ceric ammonium sulfate. The $Ce^{+4}$ solution was made 0.8 N with $H_2SO_4$ to improve the stability of the solution. All solutions were made with triply distilled water and stored in the dark.

Three ml of actinometry solution (0.005 M $H_2C_2O_4$ and o.001 M $U_2C_2O_4$) were saturated with oxygen by bubbling $O_2$ through the solution for five minutes and then irradiated in a 1 cm fused silica cell. Two ml of this irradiated solution was then placed in a 25 ml volumetric flask along with two ml of $Ce^{+4}$ solution. The flask and its contents were heated for 15 minutes in a water bath at 70° C and then cooled to room temperature. The contents were then diluted to 25 ml using 0.88 N $H_2SO_4$. The resulting final solution was about 0.8 N $H_2SO_4$and ready for readout.

The use of the actinometer depends on the following reactions:

$$UO_2^{++} + h\nu \longrightarrow (UO_2^{++})^*$$

$$(UO_2^{++})^* + H_2C_2O_4 \longrightarrow UO_2^{++} + CO_2 + CO + H_2O$$

The overall result is that oxalate is consumed by the

photochemical reaction. The quantum yield for oxalate consumption is well known. The value of 0.57 at 302 nm was used (Calvert and Pitts, 1966, page 787). The oxalate remaining after photolysis is oxidized by the $Ce^{+4}$ added.

$$C_2O_4^{-2} + 2\ Ce^{+4} \longrightarrow 2\ CO_2 + 2\ Ce^{+3}$$

The solution was heated to ensure that this reaction goes to completion.

$Ce^{+4}$ has a broad absorption band in the near uv with a maximum at 320 nm where the extinction coefficient in 0.8 N $H_2SO_4$ is 5609 liter $mole^{-1}$ $cm^{-1}$ (Boyle, 1962). The absorbance of the final solution at 320 nm was used to determine the $Ce^{+4}$ remaining after the $Ce^{+4}$ had reacted with the oxalate.

The procedure described above was carried out after photolysis at 302 nm for various time intervals. In each case a control actinometry solution was treated exactly as the irradiated actinometry solution except that it was not exposed to uv. The difference in absorbance of 1 cm path lengths of final control and irradiated solutions was measured and plotted in Figure 7. The slope of the line was determined by linear regression analysis to be $4.05 \times 10^{-3}$ $min^{-1}$. Since

$$\Delta A = \varepsilon\ \Delta c_{Ce} l \quad \text{(Beer's law)}$$

this corresponds to a rate of change in $Ce^{+4}$ concentration of:

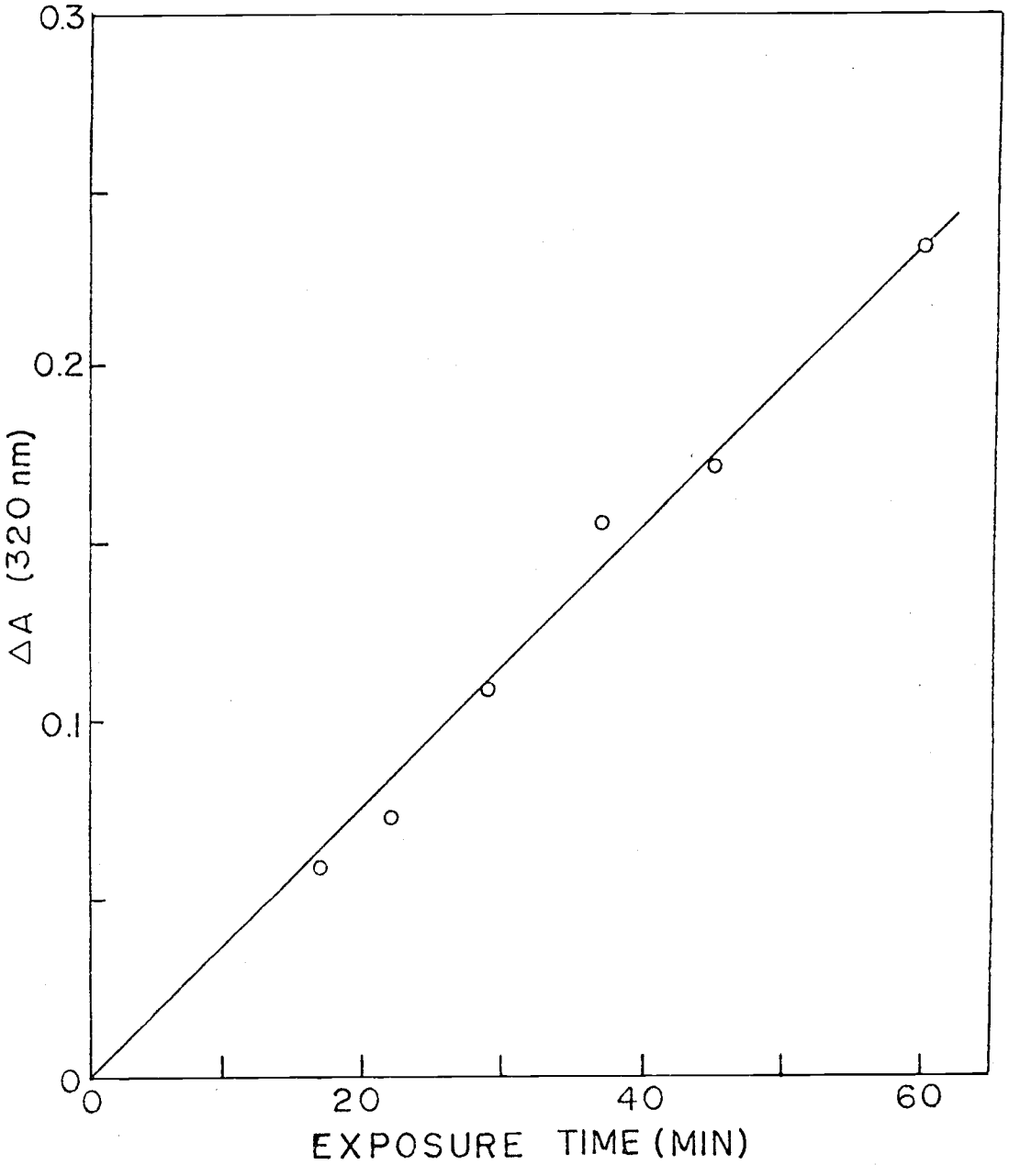


Figure 7. Difference in absorbance between control and irradiated final actinometry solutions as a function of exposure time.

$$\frac{\Delta c_{Ce}}{\Delta t} = \frac{\Delta A/\Delta t}{\varepsilon l} = \frac{4.05 \times 10^{-3} \text{ min}^{-1}}{5609 \text{ l mole}^{-1} \text{ cm}^{-1} \times 1 \text{ cm}} =$$

$7.22 \times 10^{-7}$ mole liter$^{-1}$ min$^{-1}$

Allowing for the fact that two $Ce^{+4}$ ions are reduced by one $C_2O_4^{-2}$ ion and dilution of the actinometry solution, the rate of change of concentration of oxalate in the original actinometry solution was:

$$\frac{\Delta c_{ox}}{\Delta t} = \frac{1}{2} \cdot \frac{25 \text{ ml}}{2 \text{ ml}} \cdot \frac{\Delta c_{Ce^{+4}}}{\Delta t} =$$

$4.51 \times 10^{-6}$ mole liter$^{-1}$ min$^{-1}$

Since the volume of the actinometry solution was 3 ml, this corresponds to $1.35 \times 10^{-8}$ moles of oxalate consumed per minute. Using the quantum yield:

$$\Phi = \frac{\text{moles of oxalate consumed/min}}{\text{einsteins absorbed/min}} = 0.57$$

$2.37 \times 10^{-8}$ einsteins were absorbed per minute. The irradiated area of the actinometry solution was 0.92 cm$^2$, so that the intensity of absorbed light ($I_a$) was $2.59 \times 10^{-8}$ einstein cm$^{-2}$ min$^{-1}$ .

The intensity of light incident at the front surface of the fused silica photolysis cell was calculated from the result above using the method of Hunt and Hill (1947). This method corrects for reflection from the cell and for transmission.

$$\frac{I_a}{I_o} = \left[T_o - T\right] \left[ \frac{T_o^{\frac{1}{2}}}{T_o - R\left[1 + \frac{T_o}{(1-R)^2}\right] T} \right]$$

$I_o$ = intensity at front surface of cell

$T_o$ = fraction transmitted by empty cell
$T$ = fraction transmitted by cell filled with actinometry solution
$R$ = reflectivity of fused silica-air interface

$T_o$ and $T$ were determined experimentally and $R$ was calculated using Fresnel's laws of reflection assuming normal incidence with the index of refraction at 302 nm provided by the American Thermal Fused Quartz Company. The resulting intensity of uv at the front of the cell was $3.5 \times 10^{-8}$ einstein $cm^{-2}$ $min^{-1}$.

The experimental apparatus used for actinometry and determination of quantum yield at 302 nm is shown in Figure 8. The light source was a 500 watt high pressure mercury lamp (PEK Model 912). Most of the infrared light emitted by the lamp was absorbed by water in two 1 cm quartz photolysis cells. The monochromator was the same type used in the reflection experiments. The reference photomultiplier and its readout system was also the same as that used in the reflection experiments. The count rate from the reference photomultiplier was constantly monitored during exposure and later compared with count rates during film exposures for quantum yield determinations.

Determination of Quantum Yield at 302 nm

The quantum yields at 302 nm were determined using the experimental apparatus in Figure 8. The actinometry solution was replaced by a small piece of film containing 0.1%

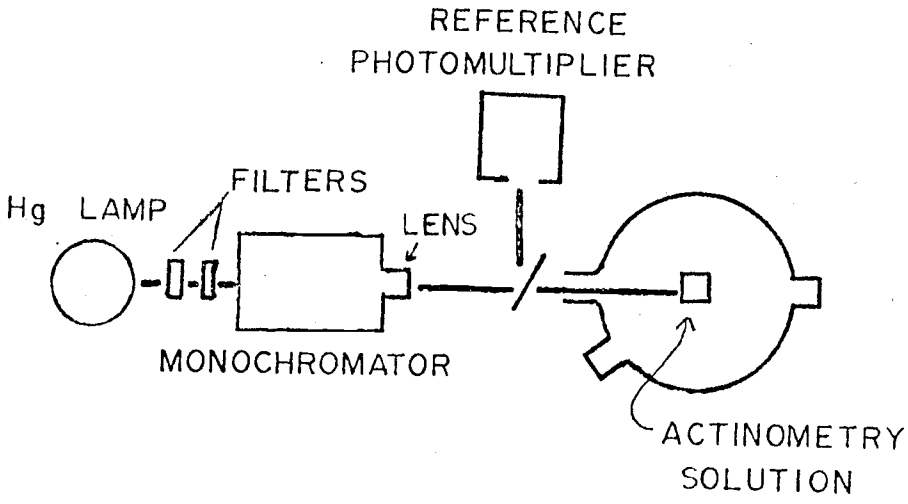


Figure 8. The experimental apparatus used for actinometry and determination of the quantum yield at 302 nm.

dye cyanide behind a plate of fused silica. The irradiation of the film was done just after the actinometer exposures. The count rate from the reference photomultiplier was also monitored during film exposures to assure that the intensity of the light in the exposure chamber was the same as it was during exposure of the actinometry solutions.

The film was exposed to 302 nm uv for short intervals and immediately transferred to the Cary 1501 spectrophotometer for absorbance measurement. The absorbances at 769, 608, and 277 nm were measured after each of 14 consecutive exposures. The absorbance at 769 nm (where neither the dye cyanide nor the dye absorb) was used as a check to compensate for any small changes in absorbance reading due to spectrophotometer sensitivity changes, position of the film holder, etc. The change in absorbance at the other two wavelengths was calculated from:

$$\Delta A_{608} = (A_{608} - A^{o}_{608}) + (A^{o}_{769} - A_{769})$$

$$\Delta A_{277} = (A_{277} - A^{o}_{277}) + (A^{o}_{769} - A_{769})$$

where the superscripts on the A's indicate the absorbance readings of the unexposed film. The graphs of change in absorbance vs. exposure time for these two wavelengths are shown in Figure 9. The initial slopes of these curves were determined by fitting the data with $\Delta A < .25$ to a curve of the form:

$$\Delta A = A_{max} (1-e^{KT})$$

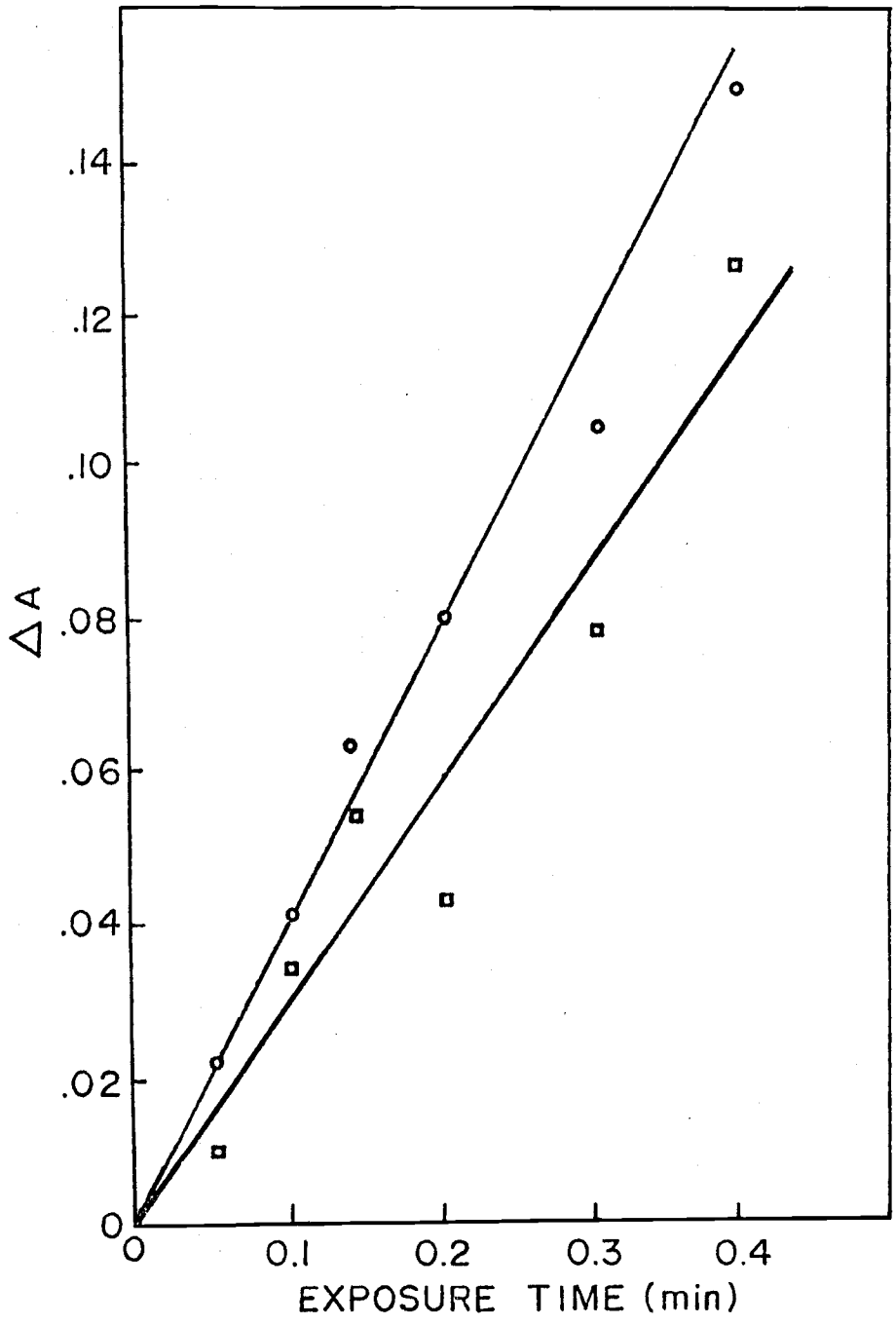


Figure 9. The change in absorbance at the dye absorption peak, 608 nm (circles), and at the dye cyanide absorption peak, 277 nm (squares), vs. exposure time. The top line shows the initial rate of change in absorption at the dye peak. The bottom line shows the initial rate of dye cyanide loss.

where T is exposure time. The value of 1.2 was used for $A_{max}$ since this was a typical value for the maximum absorption obtained under these conditions. The value of the constant K was determined by regression analysis using a Hewlett-Packard 9100A calculator. The initial slope of the curve was then calculated:

$$\text{initial slope} = 1.2\ Ke^{K \cdot 0} = 1.2\ K$$

This elaborate procedure was used instead of simply fitting the data to a straight line because in some cases the curvature was greater than in Figure 9.

The initial rate of change of absorbance was transformed to an initial rate of change in dye concentration using Beer's law:

$$\frac{dc_D}{dt} = \frac{\frac{dA^{608}}{dt}}{\varepsilon_D l}$$

The initial rate of dye formation per square cm is then:

$$\frac{dD}{dt} = \frac{dc}{dt} \times \frac{\text{vol (liters)}}{\text{area (cm}^2\text{)}} = \frac{dA^{608}/dt}{\varepsilon_D^{608}} =$$

$$5.4 \times 10^{-9} \text{ mole cm}^{-2} \text{ min}^{-1}$$

Similarly, the initial rate of dye cyanide loss was:

$$\frac{dDC}{dt} = \frac{dA^{277}/dt}{\varepsilon_E^{277}} = 5.8 \times 10^{-9} \text{ mole cm}^{-2} \text{ min}^{-1}$$

where the effective $\varepsilon$ at 277 = $\varepsilon_{DC}^{277} - \varepsilon_D^{277} = \varepsilon_E^{277} =$

$$5.0 \times 10^{4} \text{ l mole}^{-1} \text{ cm}^{-1}$$

Before the quantum yields can be calculated, the fraction of the incident light which is absorbed by the film (f) is needed. This was determined from the absorption spectrum of the film after correction was made for reflection losses. At 302 nm this fraction was 0.63. The rate of photon absorption by the film was then:

$$I_A = I_o(f) = (3.5 \times 10^{-8} \text{ einstein cm}^{-2}\text{min}^{-1})(.63)$$

The quantum yields for dye formation and dye cyanide loss based on rate of photon absorption by the total film are then found by:

$$\Phi_{dye} = \frac{\text{rate of dye formation}}{\text{rate of photon absorption by film}} =$$

$$\frac{5.4 \times 10^{-9} \text{ mole cm}^{-2} \text{ min}^{-1}}{2.4 \times 10^{-8} \text{ einstein cm}^{-2} \text{ min}^{-1}} = .23$$

$$\Phi_{DC} = \frac{\text{rate of dye cyanide loss}}{\text{rate of photon absorption by film}} =$$

$$\frac{5.8 \times 10^{-9} \text{ mole cm}^{-2} \text{ min}^{-1}}{2.4 \times 10^{-8} \text{ einstein cm}^{-2} \text{ min}^{-1}} = .24$$

Determination of Action Spectrum and Quantum Yield at Various Wavelengths

The apparatus used for studying the photochemical response of the film at various wavelengths is shown in Figure 10. A 150 watt xenon lamp (Bausch and Lomb 33-86-20-01) and one monochromator (Bausch and Lomb 33-86-01) were used as the source of monochromatic uv. The monochromator slit widths were set to allow a band width at

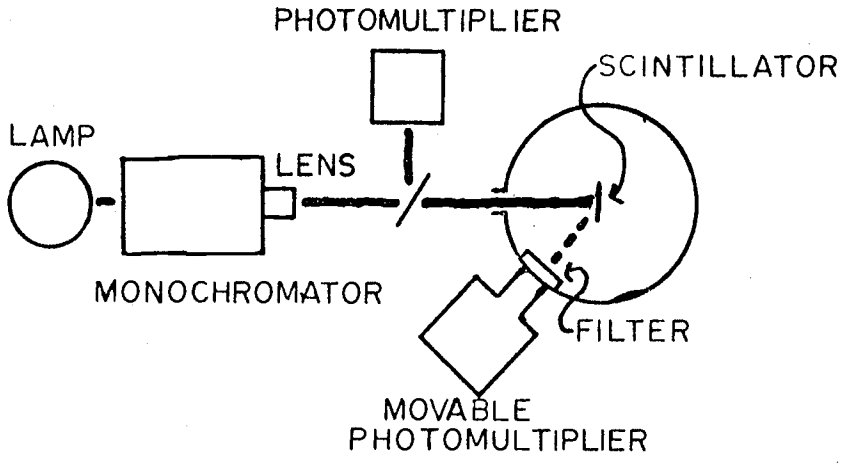


Figure 10. Experimental apparatus used for study of action spectrum and relative quantum yield.

one-half maximum of 10 nm for the output beam, which was collimated with an achromatic condenser lens (Bausch and Lomb 33-86-53). A fused silica plate coated on the front surface with sodium salicylate was placed at the center of the exposure chamber. The sodium salicylate coating was formed by spraying a solution of sodium salicylate in methanol on the plate using an atomizer and drying with a warm air flow. The entrance to the movable photomultiplier was covered with a Corning 3-73 filter. This sharp cutoff filter has 10% transmission at 410 nm and is opaque to uv. The photomultipliers and their readout systems were identical to those described in the reflection determination section and the linearity of the count rate from these photomultipliers vs. light intensity was checked periodically using neutral density filters of known transmittance.

Sodium salicylate is strongly fluorescent with a quantum yield for fluorescence which is nearly constant for excitation in the wavelength region 160 - 350 nm (Sampson, 1967). The emission from the sodium salicylate has a peak at about 420 nm. The 3-73 filter allows a constant fraction of the fluorescence emitted by the sodium salicylate to reach the movable photomultiplier but prevents reflected or scattered uv from reaching the detector. The light incident on the movable photomultiplier should then be proportional to the intensity of uv striking the sodium salicylate (in photons $min^{-1}$), independent of the wavelength of

the exciting light.

The sodium salicylate plate was excited with uv of 11 different wavelengths and the count rates from both photomultipliers were recorded over a period of one minute. The ratio of the count rate from the reference photomultiplier to the count rate from the movable photomultiplier is a measure of the relative sensitivity of the reference photomultiplier to uv of that wavelength. The results are shown in Table 1.

Films containing 0.1% dye cyanide were then placed in the exposure chamber in the position of the scintillator in Figure 10. A film was exposed to a series of short exposures at each of 11 wavelengths. The absorbance at 769, 608, and 277 nm was determined before and after each exposure. All exposures were done at 20° C. At each wavelength a graph of change in absorbance at both 277 and 608 nm vs. cumulative exposure in counts measured from the reference photomultiplier was completed. The initial slope of each of these curves was determined in the same manner as described in the section on quantum yield at 302 nm determination. A typical graph and its calculated slope are shown in Figure 11.

The initial slope is related to the initial rate of dye formation, but correction must be made for the relative sensitivity of the reference photomultiplier before comparisons among wavelengths can be made. This was done

Table 1. Count rates from movable and reference photomultipliers and the relative sensitivity of the reference photomultiplier at various wavelengths.

| λ | Count Rate Movable Phototube | Count Rate Reference Phototube | Relative Sensitivity |
|---|---|---|---|
| 240 nm | 30120 ct/min | 110160 ct/min | 3.66∝count/photon |
| 250 | 37880 | 139600 | 3.69 |
| 260 | 53700 | 191940 | 3.57 |
| 270 | 66280 | 220380 | 3.32 |
| 280 | 83730 | 250610 | 2.99 |
| 290 | 106840 | 289120 | 2.71 |
| 302 | 135930 | 341620 | 2.51 |
| 310 | 159190 | 391810 | 2.46 |
| 320 | 215790 | 519280 | 2.41 |
| 330 | 245400 | 577740 | 2.35 |
| 340 | 279100 | 698120 | 2.50 |

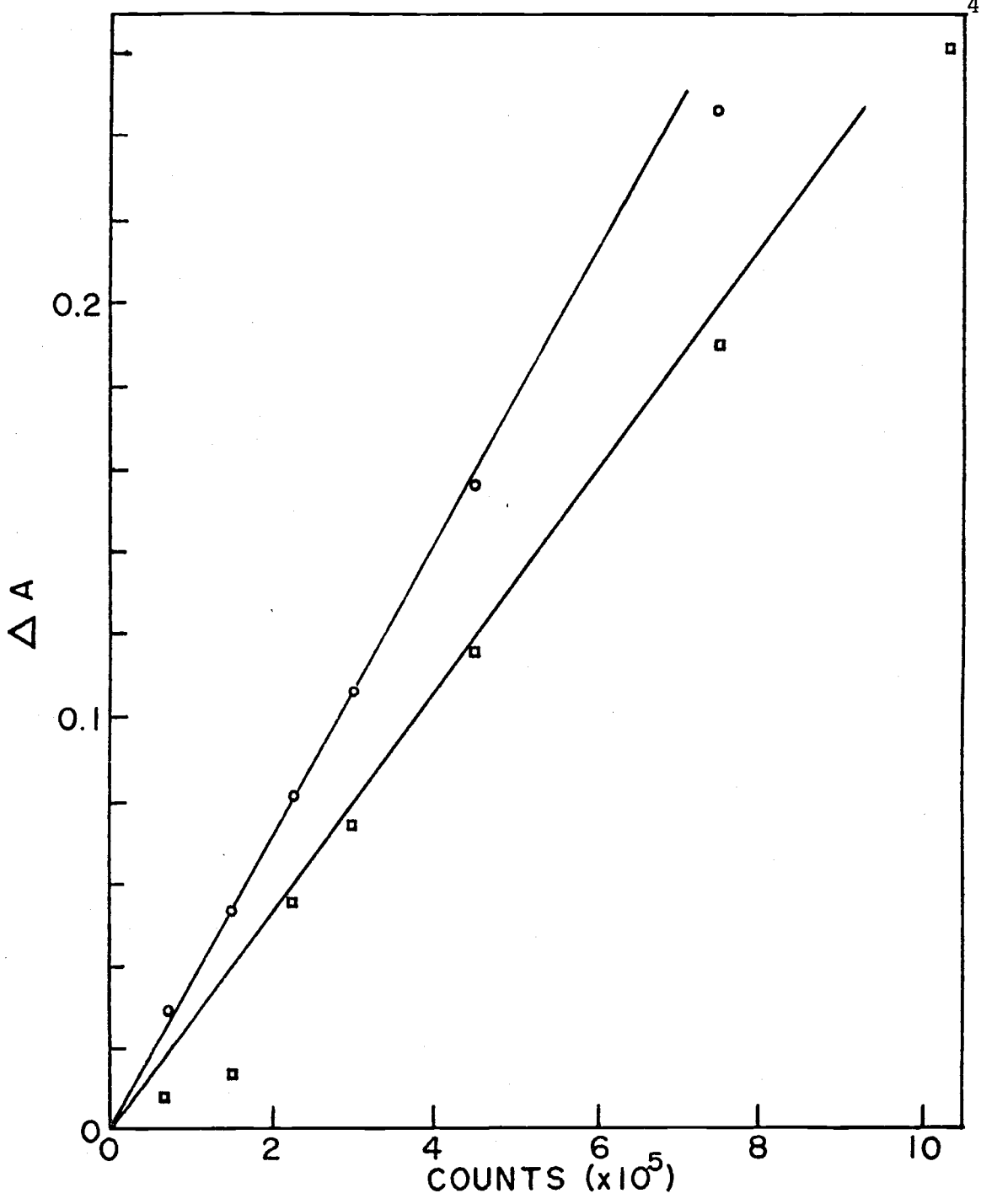


Figure 11. A typical graph of change in absorbance at 608 nm (circles) and 277 nm (squares) vs. exposure in counts. The wavelength of uv used in this case was 270 nm. The initial slopes determined by curve fitting are shown as the straight lines.

using the data in Table 1. The relative sensitivity of the film per photon incident (action spectrum) was calculated as:

relative sensitivity = initial slope x relative sensitivity of reference photomultiplier

For quantum yield calculations, the fraction of the incident light which is absorbed was necessary. Since fairly wide slits were used on the monochromator and the xenon lamp emits a continuous spectrum, light of many wavelengths is actually incident on the film at any monochromator setting. As a result, the integrated fraction absorbed by the film over the range of incident wavelengths was needed. These integrated fractional absorptions were approximated by numerical integration using a Hewlett-Packard 9100A calculator.

$$\frac{I_A}{I_o} = \frac{1}{I_o} \int \left(\frac{I_A}{I_o}\right)_\lambda I_\lambda \, d\lambda$$

where $\left(\frac{I_A}{I_o}\right)_\lambda$ is the fractional absorption by the film at $\lambda$. $I_\lambda$ is the monochromator's output intensity at $\lambda$. $I_o$ was the total monochromator output intensity. The integration was carried out by dividing the wavelength region around the monochromator setting into ten 2 nm wide bands. The fractional absorption at the center of each of these bands was determined from corrected absorption spectra. The mom-

chromator output in each of these bands was approximated by placing a second monochromator with very narrow slits ($\frac{1}{2}$ width = 0.48 nm) behind the original monochromator. The second monochromator was assumed to transmit only one wavelength. The second monochromator was set at various wavelengths and the intensity of the light transmitted by the two monochromators in tandem was determined by the count rate from the reference photomultiplier. In this way the spectral output from the original monochromator was obtained. The intensity within each 2 nm wide wavelength band was calculated from this data.

The relative quantum yields were calculated by using:

$$\text{relative quantum yield} = \frac{\text{relative sensitivity}}{\text{fractional absorption of film}}$$

Temperature Effects

The effect of changes in film temperature during photolysis was studied by irradiating films using the same experimental setup used in determination of the quantum yield at 302 nm. The wavelength was, however, changed to 315 nm. The temperature of the film was taken by measuring the air temperature inside the exposure chamber near the film holder with a mercury thermometer. Films were heated to above room temperature with a stream of warm dry air from a heat gun (Master Appliances Model H G 301 LD). The temperature and velocity of the air flow were controlled with

a voltage adjuster on the heat gun. Temperatures below room temperature were obtained by allowing the cool nitrogen boiling off a flask of liquid nitrogen to flow into the exposure chamber. Precise control of film temperature was difficult by these methods and temperature variations were frequent. However, every effort was made to keep the temperature reading within $3^{o}$ C of the desired temperature.

In all cases, the absorbance of a film at 608 nm was measured before irradiation and the film was then placed in the exposure chamber for three minutes to allow it to reach the desired temperature. The film was then exposed for a short time, the absorbance at 608 was rechecked, and the film was returned to the exposure chamber for temperature equilibration. Several exposureswere made at each wavelength. At each wavelength, exposures were continued until the absorbance at 608 nm began to decline.

Intensity Effect

The dependence of film response on the intensity of ultraviolet radiation was tested in two separate but similar experiments. The intensity dependence over a range of low intensities with monochromatic uv was studied using the apparatus shown in Figure 10. All components and their arrangement were the same as used in determination of the action spectrum except the monochromator slits were narrow-

ed to emit a 2 nm half-width beam. All exposures were with the monochromator set at 310 nm. Commercial filters of various transmittance were placed between the xenon lamp and the monochromator to vary the intensity of the beam. As before, the count rate from the reference photomultiplier was assumed to be proportional to the intensity of the beam in the exposure chamber. The validity of this assumption was checked periodically using neutral density filters of known transmittance.

Film containing 1.0% dye cyanide was placed in the exposure chamber and given a series of exposures. The absorbance at 608 nm was checked before and after each exposure. The length of the exposure was dictated by the cumulative number of counts recorded from the reference photomultiplier while the film was being exposed. All films were exposed to 10, 30, 60, 100, 100, 400, 800, 1600 x $10^4$ cumulative counts regardless of how long it took for the counts to accumulate. This series of exposures was carried out with three different light intensities. The highest intensity used in this series of tests produced an absorbance of 1.0 at 608 nm after 50 minutes of exposure.

In the second series of tests of the effect of changes in intensity, much more intense polychromatic light was used. The experimental apparatus was the same except that the xenon lamp and monochromator were replaced by a 500

watt high pressure mercury lamp (PEK Model 912). No monochromator was used, but two 1 cm fused silica cells filled with water were placed between the lamp and the beam splitter to filter out most of the infrared emitted by the lamp. The intensity of the beam in the exposure chamber was varied by placing fine metal grids in the beam path between the water filters and the beam splitter.

Exposures were made using a procedure similar to that described in the first series of tests. 0.1% dye cyanide film was used in this case for all exposures. A series of exposures to 5, 10, 20 x $10^4$ counts were made at six different intensities. The highest intensity used produced an absorbance of 1.0 at 608 nm in 0.6 min.

Fluorescence

Studies of the fluorescence properties of the films were carried out in three ways. The fluorescence of both the dye and the dye cyanide in nylon film were studied using a Baird-Atomic fluorescence spectrophotometer (Model SF-100). The films were placed on an aluminum foil backing and placed in the cell compartment with the film at a 45$^o$ angle with respect to both the exciting beam and the fluorescence detector. No attempt was made to make quantitative measurements of the shapes or intensities of the emission spectra by this method. The general wavelength

region of fluorescence emission from both the dye and the dye cyanide was determined by this method. The general wavelength region of fluorescence emission from both the dye and the dye cyanide was determined by this method.

The fluorescence of the dye in the film was also studied by exciting the film containing dye with a helium-neon laser (Spectra-Physics Model 133). The apparatus was arranged as shown in Figure 12a. The monochromator was a Bausch and Lomb (Model 33-86-01) uv grating monochromator. The slits were adjusted to emit a 2 nm band width at $\frac{1}{2}$ maximum. The detector used was a EMI 9558 Q1B photomultiplier. This photo tube was used instead of the 1P 28 because of its greater red sensitivity. The photomultiplier was connected to a voltage-frequency converter and a scaler as in the experiments described above. The count rate from the photomultiplier was found to be proportional to the light intensity entering the photomultiplier by varying the beam intensity with neutral density filters of known transmittance.

With the laser light (633 nm) incident on the film, the monochromator was set at various wavelengths and the count rate from the photomultiplier was recorded. In this way, the general shape of the emission spectrum of the dye fluorescence could be obtained except in the 630-635 nm region where reflected and scattered laser light was transmitted by the monochromator. Detection of laser light was

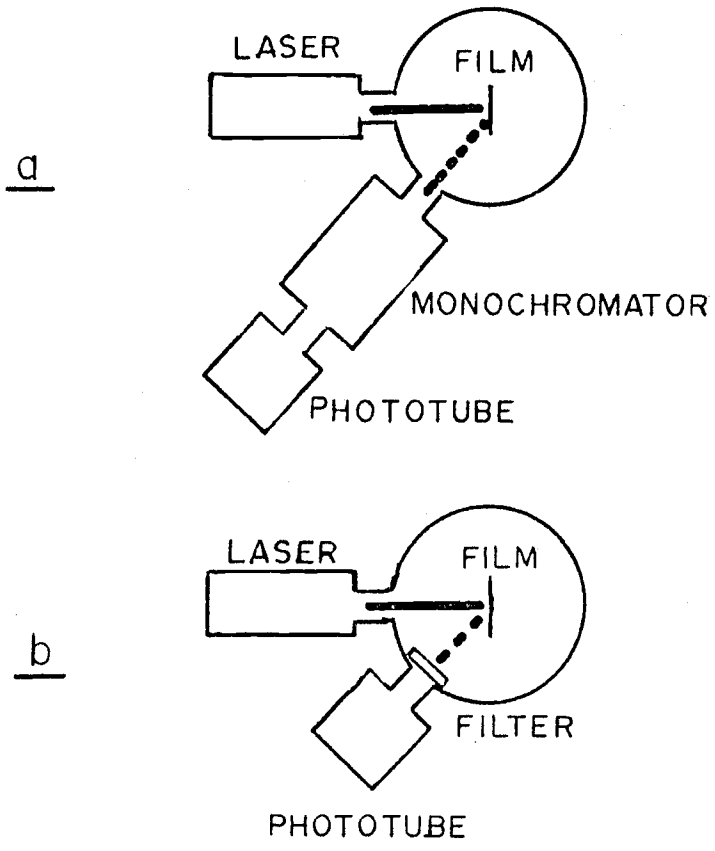


Figure 12. Apparatus used to study fluorescence of the dye in the film. Arrangement a allows study of the emission at various wavelengths. Arrangement b was used to compare overall fluorescence intensity in various films.

shown not to be a problem at other wavelengths by putting a piece of highly reflecting aluminum foil in place of the film and checking the count rate for various wavelength settings of the monochromator. The spectrum obtained is, however, uncorrected for variation in spectral sensitivity of the photomultiplier over the wavelength range.

The overall intensity of the dye fluorescence from various films was also studied using the apparatus shown in Figure 12b. The only change from the apparatus shown in Figure 12a is the replacement of the monochromator by a red filter (Corning 2-64). This filter is nearly opaque to the laser light (633 nm), but transmits much of the fluorescence emission from the dye ($\lambda$>650 nm). Various films were placed in the exposure chamber and excited with the laser. The count rate from the photomultiplier was assumed to be proportional to the intensity of the fluorescence.

Fading of the Dye

The light induced fading (photobleaching) of the dye in the nylon films was studied using films originally containing 0.1% dye cyanide which were irradiated to near maximum dye concentration. The films were then exposed to monochromatic uv or visible light to determine which absorption band of the dye was more responsible for the photobleaching. The source of visible monochromatic light was a helium-neon laser (Spectra-Physics Model 133). This

laser emits red light of wavelength 633 nm. The monochromatic uv was supplied by the 500 watt high pressure mercury lamp and monochromator used for determination of the quantum yield at 302 nm. The monochromator was set on 302 nm with slit widths set for a 10 nm spectra peak width at $\frac{1}{2}$ maximum. The relative intensity of these two sources was estimated by comparing their effect on a RCA 1 P 28 photomultiplier, with correction made for the very different photomultiplier sensitivities at the two wavelengths. The laser was estimated to produce the intenser beam at the film (in quanta per unit area per unit time) by a factor of ten. Films were checked for their absorbance at 608 nm and placed in the exposure chamber for exposure to either uv or visible light. The films were periodically removed from the chamber and checked for changes in absorbance due to dye destruction.

Fading of the dye in the absence of light was also studied using films originally containing 0.1% dye cyanide. These films were irradiated to produce a near maximum dye concentration. The absorbance of the films at 608 nm was determined and the films were placed in light tight paper envelopes. Films were stored at room temperature (20$^{o}$ C), in a freezer compartment (-17$^{o}$ C), and in a refrigerator (2.2$^{o}$ C). The films were later allowed to reach room temperature, removed from the envelopes, and checked for change in the absorbance at 608 nm.

# RESULTS

## Absorption Spectra

The absorption spectra of films originally containing 0.1% dye cyanide are shown in Figures 13 and 14. The spectra show absorption by an unexposed film and a film containing a maximum dye concentration. These spectra are not corrected for reflection losses. Dye formation leads to absorption increases in four wavelength regions: 460-710 nm, 350-400 nm, 290-340 nm, and 240-280 nm. These absorption bands correspond well with the typical absorption bands of triphenylmethyl dyes given by Brown (1971).

The near infrared absorption spectrum of an unexposed film containing 0.1% dye cyanide is shown in Figure 15. There is little infrared absorption by the dye cyanide.

Figure 16 shows the uncorrected absorption of a film of nylon containing no dye cyanide or dye. The absorption of nylon extends to longer wavelengths than would be expected based on the absorption of the amide groups. Amide absorption spectra show strong absorption at wavelengths shorter than 200 nm with absorption becoming negligible at 260 nm (Calvert and Pitts, 1966, page 452). The absorption by nylon at longer wavelengths may be due to hydrogen bonding between the amide groups. The fact that nylon absorption extends into the region where the dye cyanide absorbs brings about the possibility of energy transfer. Conceiv-

ably, the nylon may absorb photons of wavelength 240-340 nm and transfer the energy received from these photons to dye cyanide molecules. This could lead to dye formation and increase the quantum yield for dye formation.

Figure 17 shows the extinction coefficient of the dye cyanide and the dye vs. wavelength. The shapes of the curves were obtained from comparison of absorption spectra of films containing dye or dye cyanide with the absorption spectrum of a film of nylon of the same thickness with correction made for the different reflectivity of the films. The extinction coefficient scale was based on the value of $\varepsilon=7.0 \times 10^{4}$ liter $mole^{-1}$ $cm^{-1}$ at 608 nm.

Figure 18 shows the absorption due to dye cyanide and dye in a solution with DMSO. The general shapes of both curves resemble the comparable spectra in Figure 17.

Figure 19 shows the build up of the principle dye absorption peak in a film originally containing 0.1% dye cyanide. The absorption, uncorrected for reflection losses, is shown after 0, 10, 80, 320, and 2700 seconds in the sun. With extensive exposure to sunlight the dye peak begins to diminish and shift to slightly shorter wavelengths. This is probably due to photobleaching of the dye by solar uv. The shoulder on the short wavelength side of the absorption peak which was attributed to a dye isomer by Lewis et al (1942) is visible in this figure.

Figure 20 is a graph showing typical results obtained when the uncorrected absorbance at 608 nm of the film is determined after a series of exposures to sunlight. The log-log plot is nearly linear initially.

Reflection from Films

The fractional reflections from films obtained using the apparatus shown in Figure 4 were surprisingly small. The reflection from the film containing dye cyanide was smaller than the reflection from films of pure nylon even in regions where the dye cyanide does not absorb (360-400 nm). Close inspection of the films reveals that the surface of films containing dye cyanide are irregular. The result is probably considerable diffuse reflection from these films. Some of this diffuse reflection is not detected in the experimental apparatus used for reflection measurements since it was designed to measure specular reflections. The fractional reflection data for the film containing 1% dye cyanide is as a result probably erroneously low.

Because these values were in question, the fractional reflection was also determined using a spectrophotometer with an integrating sphere. These results are shown in Figure 21. The values represent specular plus diffuse fractional reflection. All absorbance data needed for quantum yield calculations were corrected for reflection losses using this data.

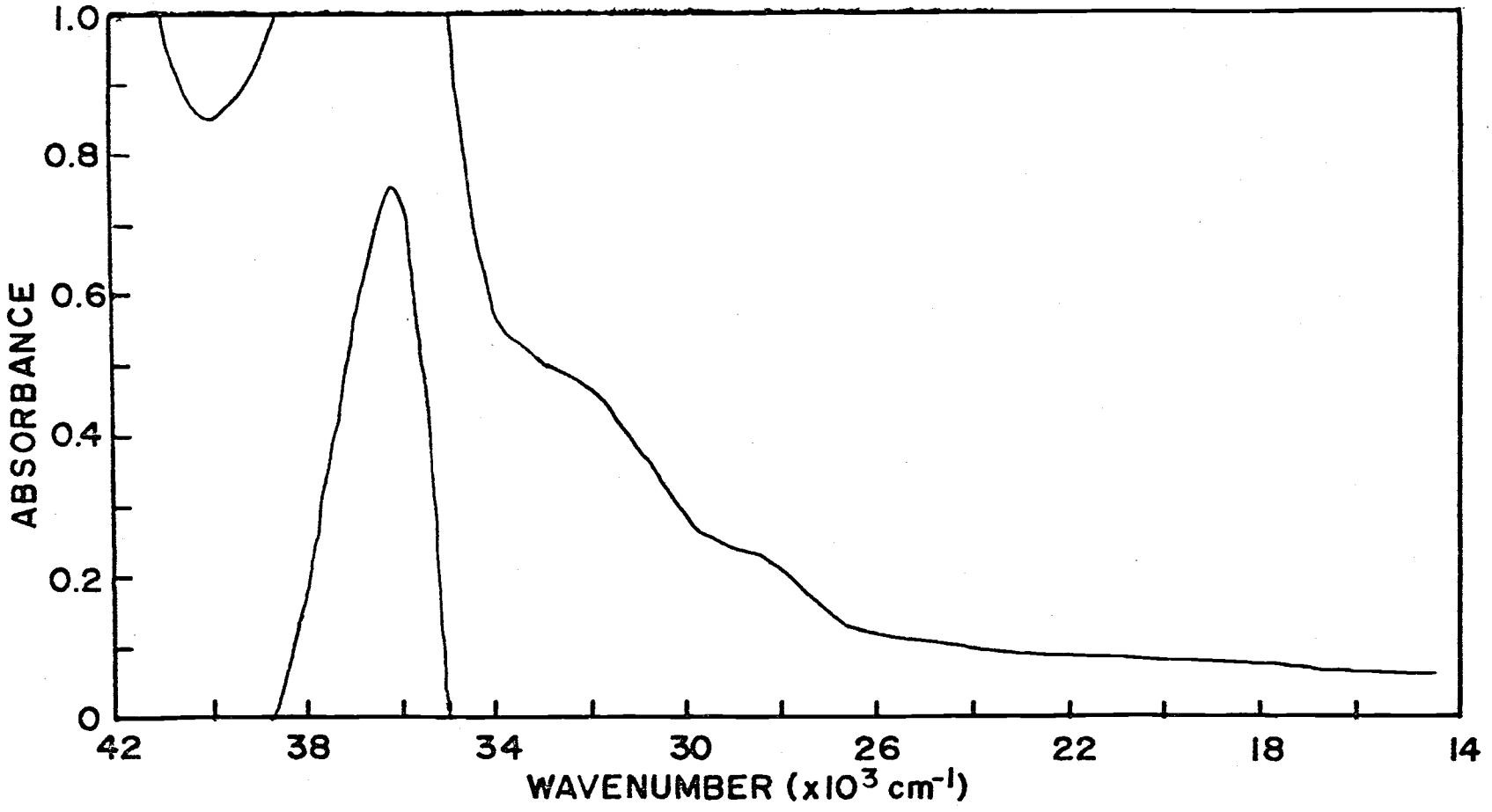


Figure 13. The uncorrected absorption spectrum of a film containing 0.1% dye cyanide.

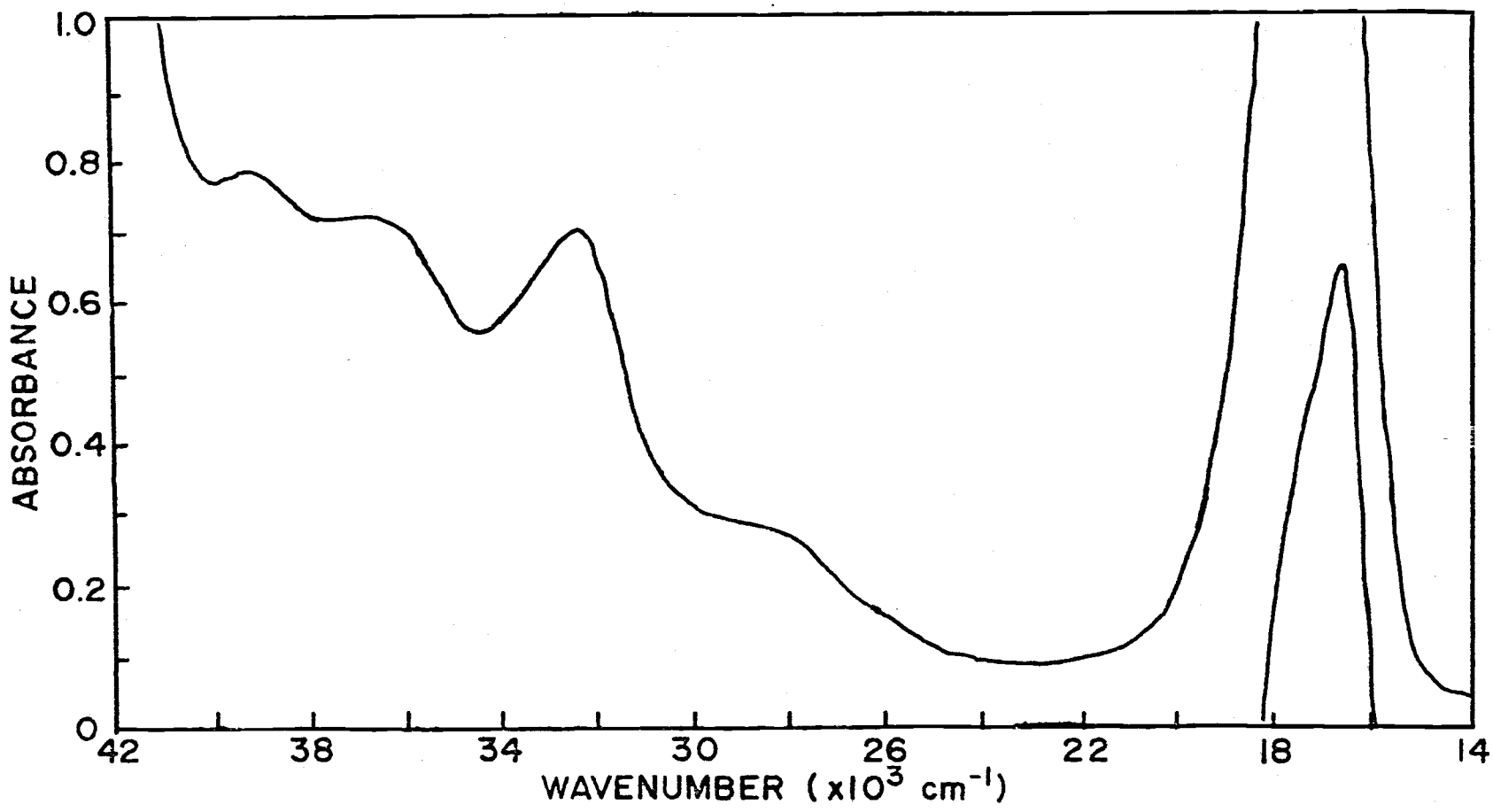


Figure 14. The uncorrected absorption spectrum of a film originally containing 0.1% dye cyanide. The spectrum shown was taken when the absorbance at 608 nm was at a maximum and complete conversion to the dye was assumed.

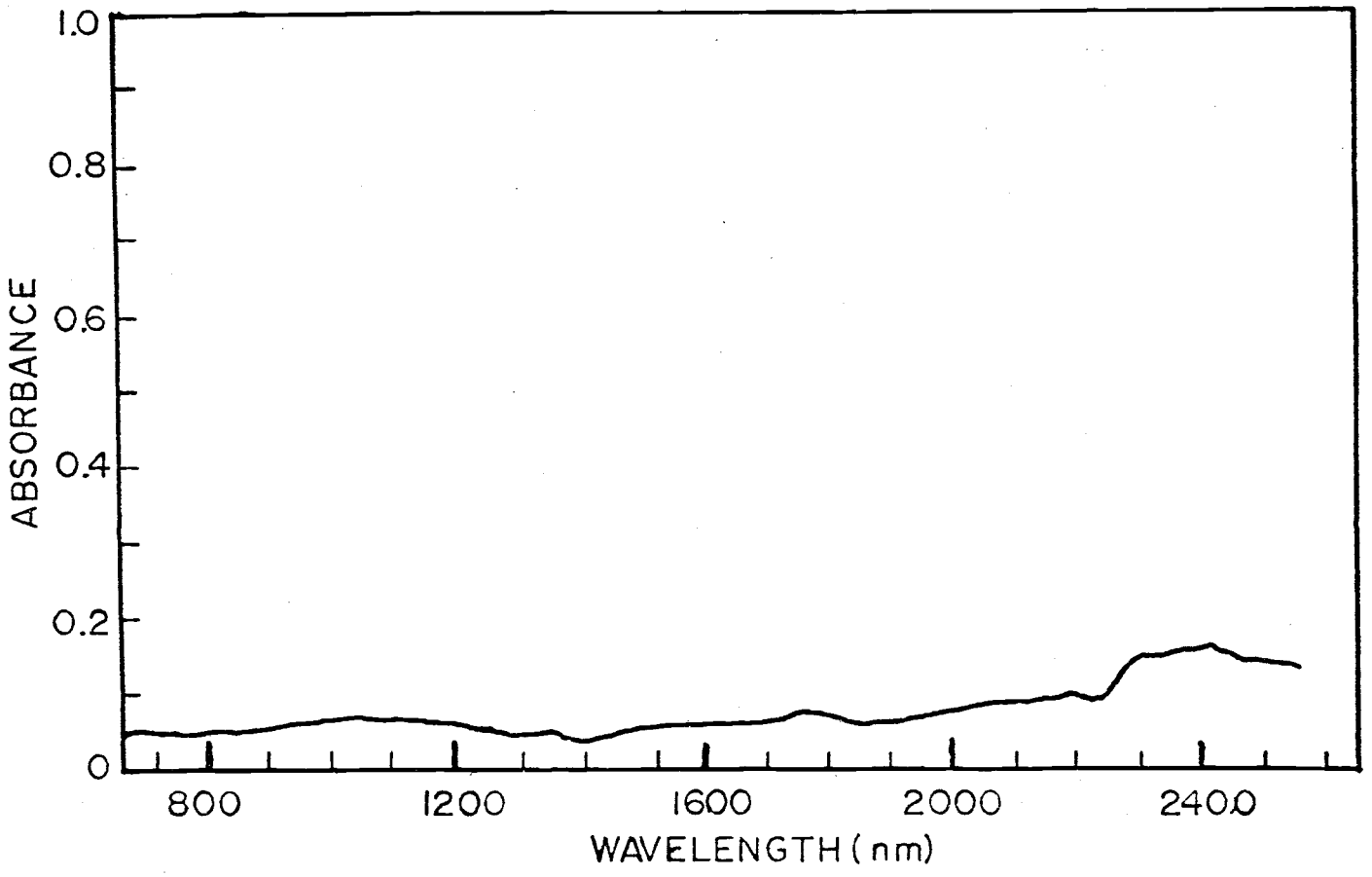


Figure 15. The near infrared absorption spectrum (uncorrected) for a film containing 0.1% dye cyanide.

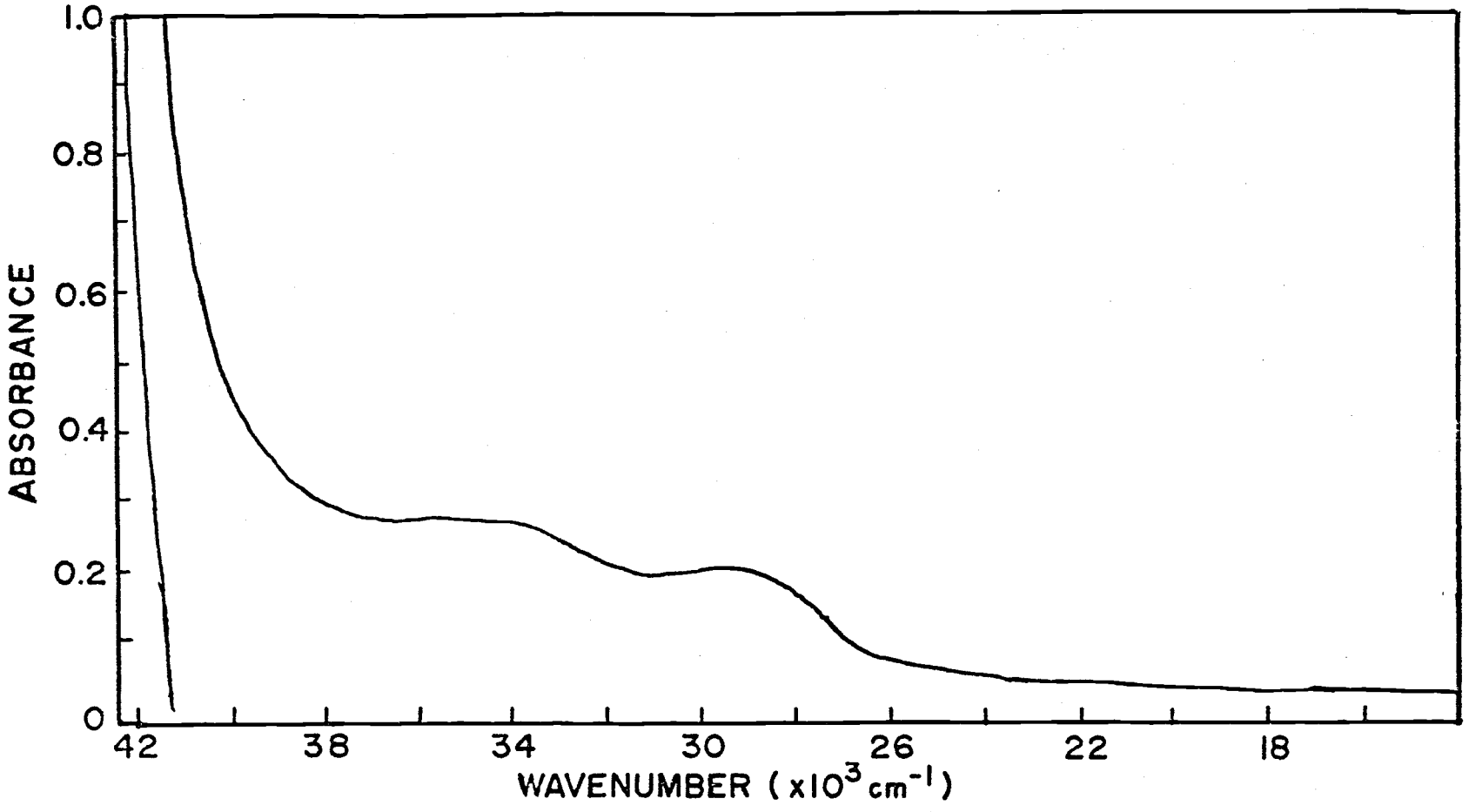


Figure 16. The uncorrected absorption spectrum of a film of nylon containing no dye or dye cyanide.

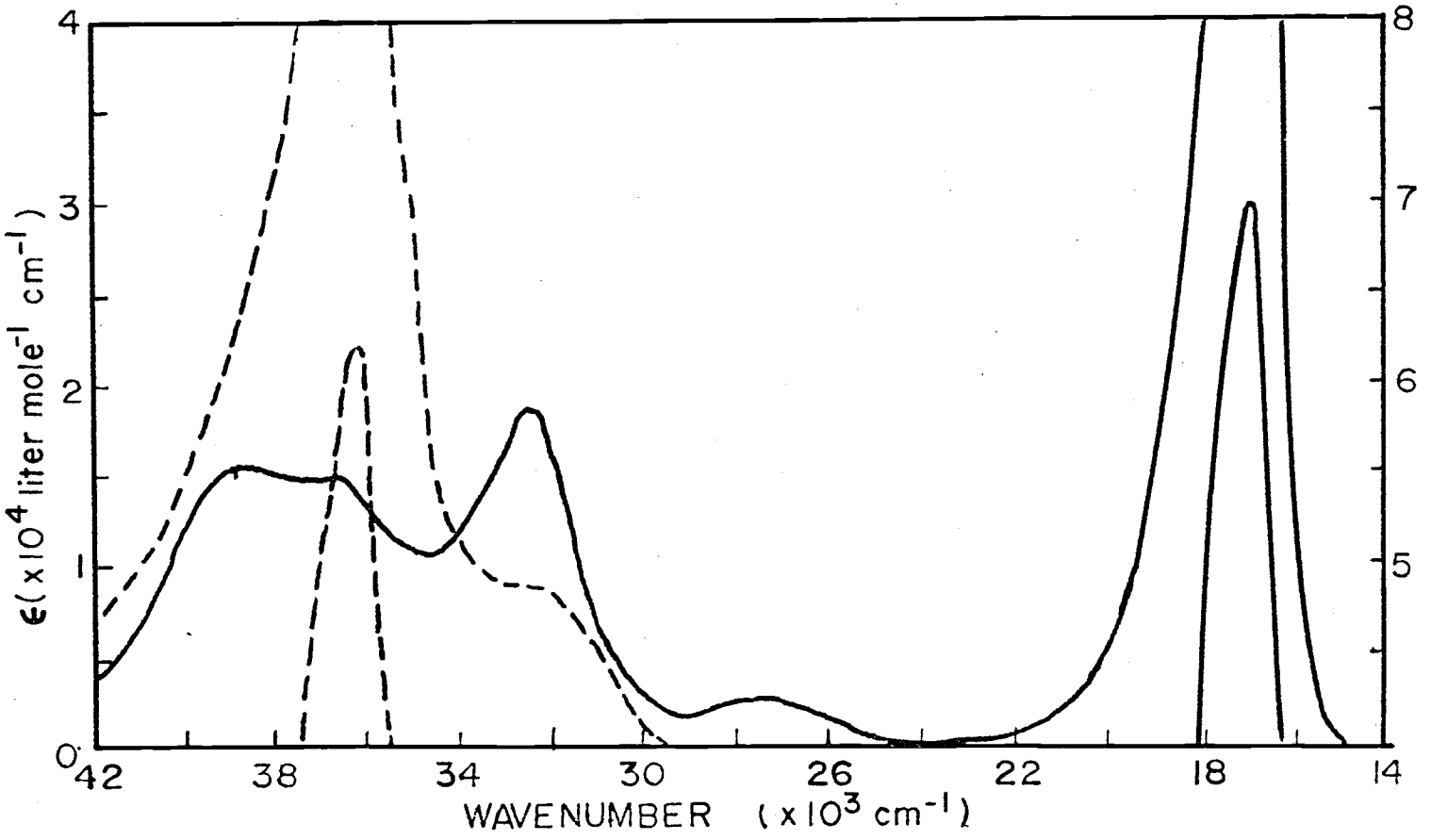


Figure 17. The extinction coefficients of the dye (solid line) and the dye cyanide (broken line) in the film.

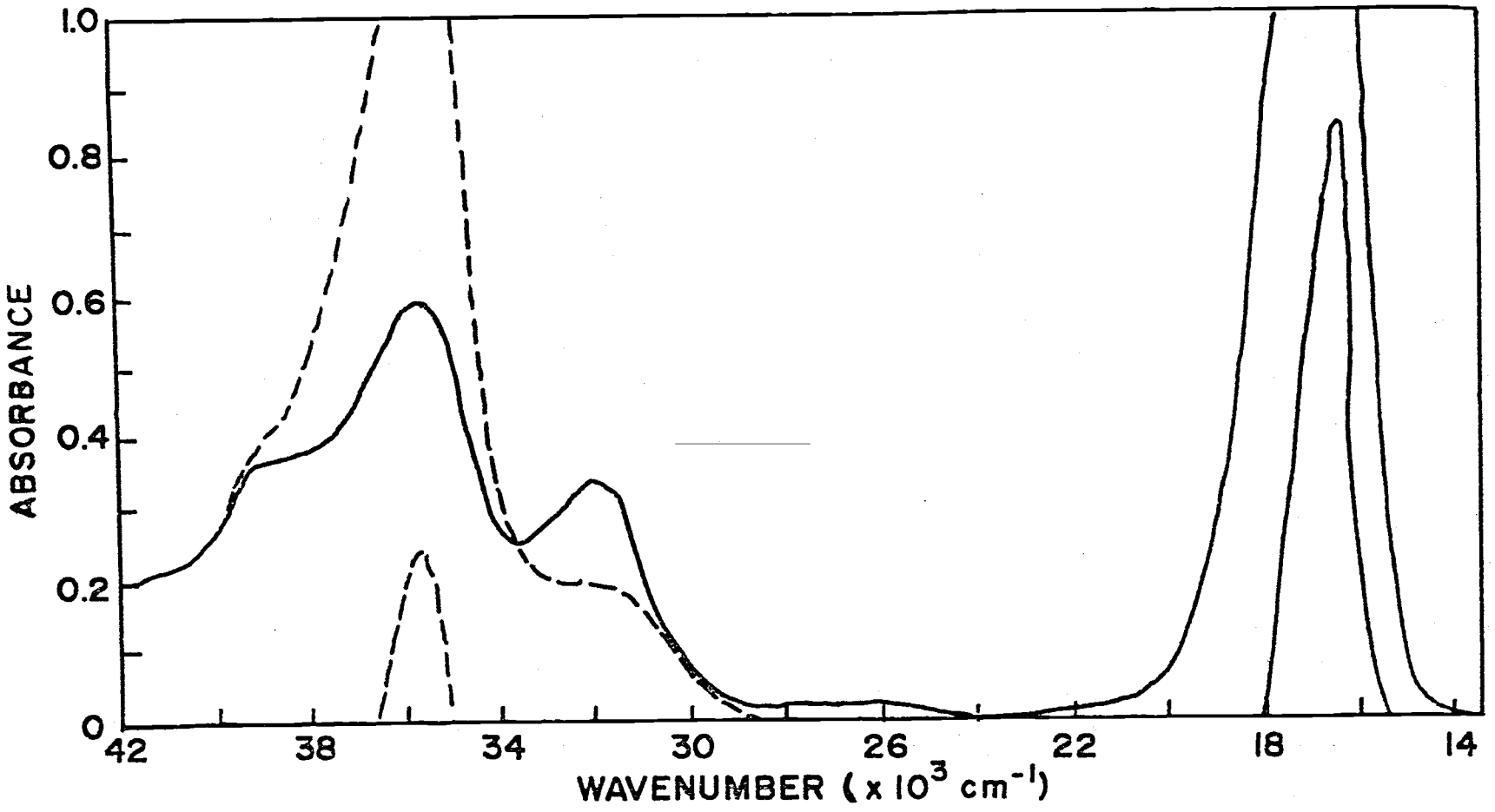


Figure 18. The absorption spectra of 1.98 x $10^{-5}$ M solutions of dye (solid line) and dye cyanide (broken line) in DMSO.

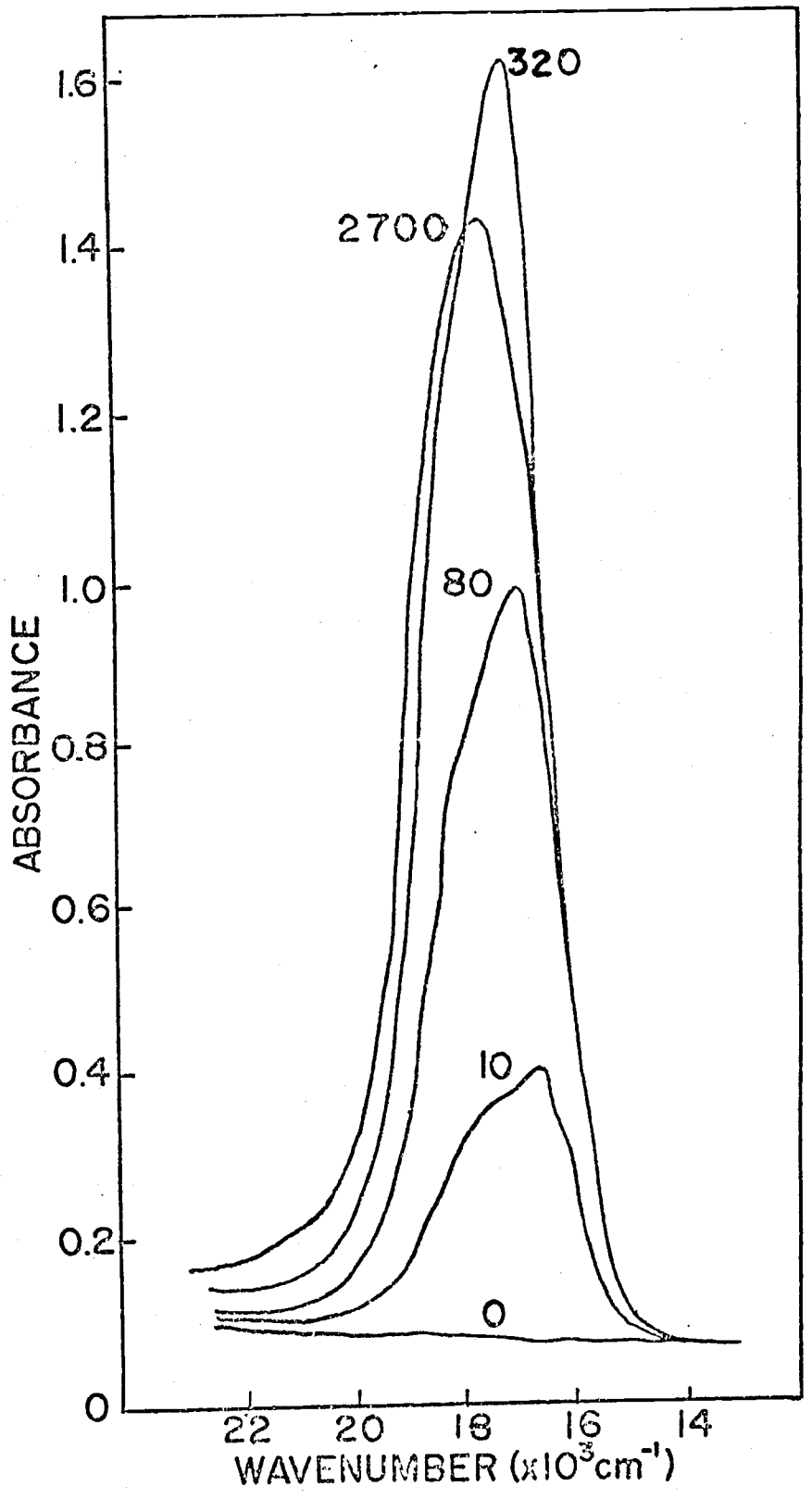


Figure 19. The uncorrected absorption spectrum of a film originally containing 0.1% dye cyanide after various exposures to sunlight. The numbers indicate the cumulative exposure time in secs.

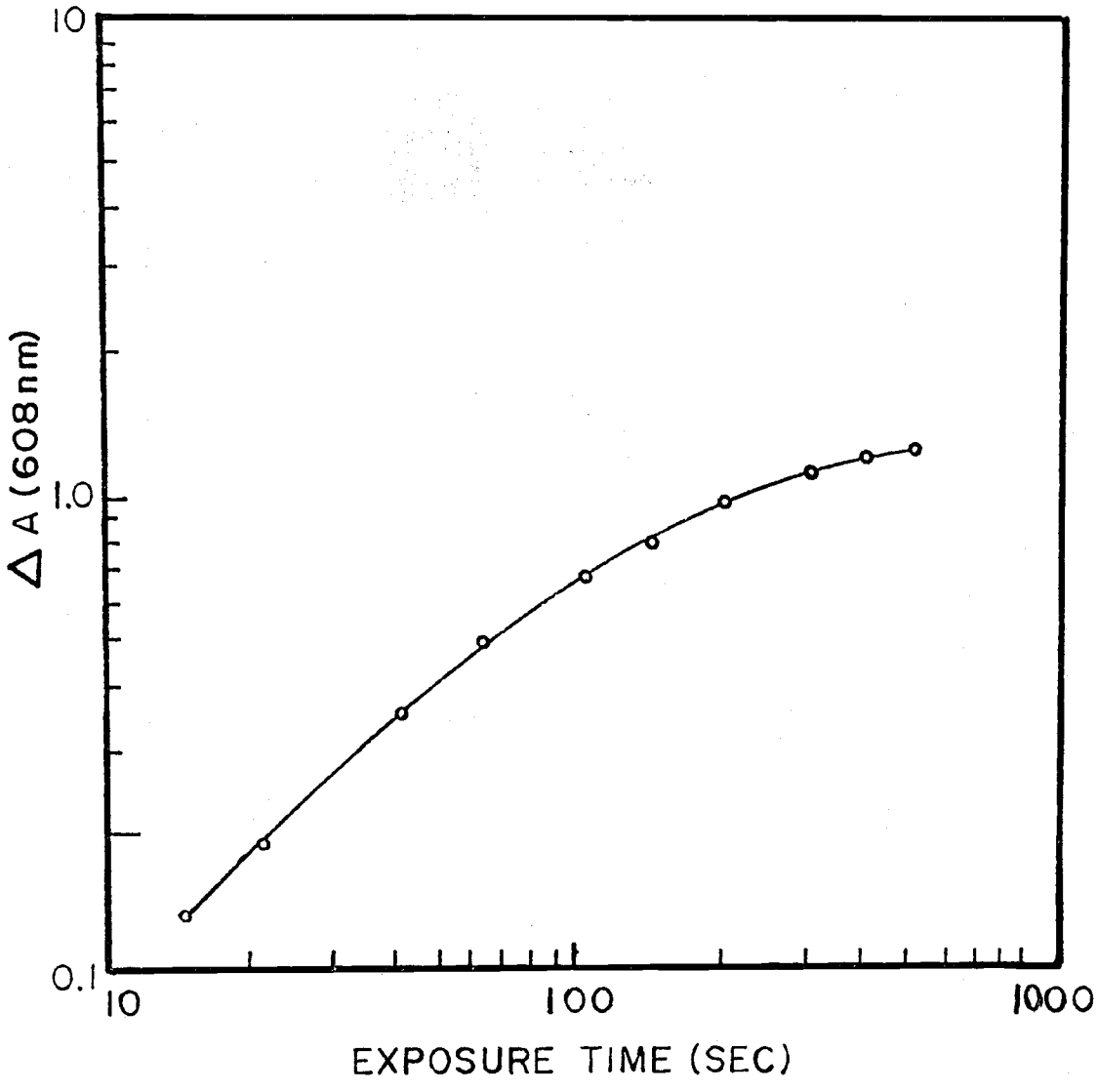


Figure 20. Change in absorbance at 608 nm vs. cumulative exposure time in the sun. The film used originally contained 0.1% dye cyanide.

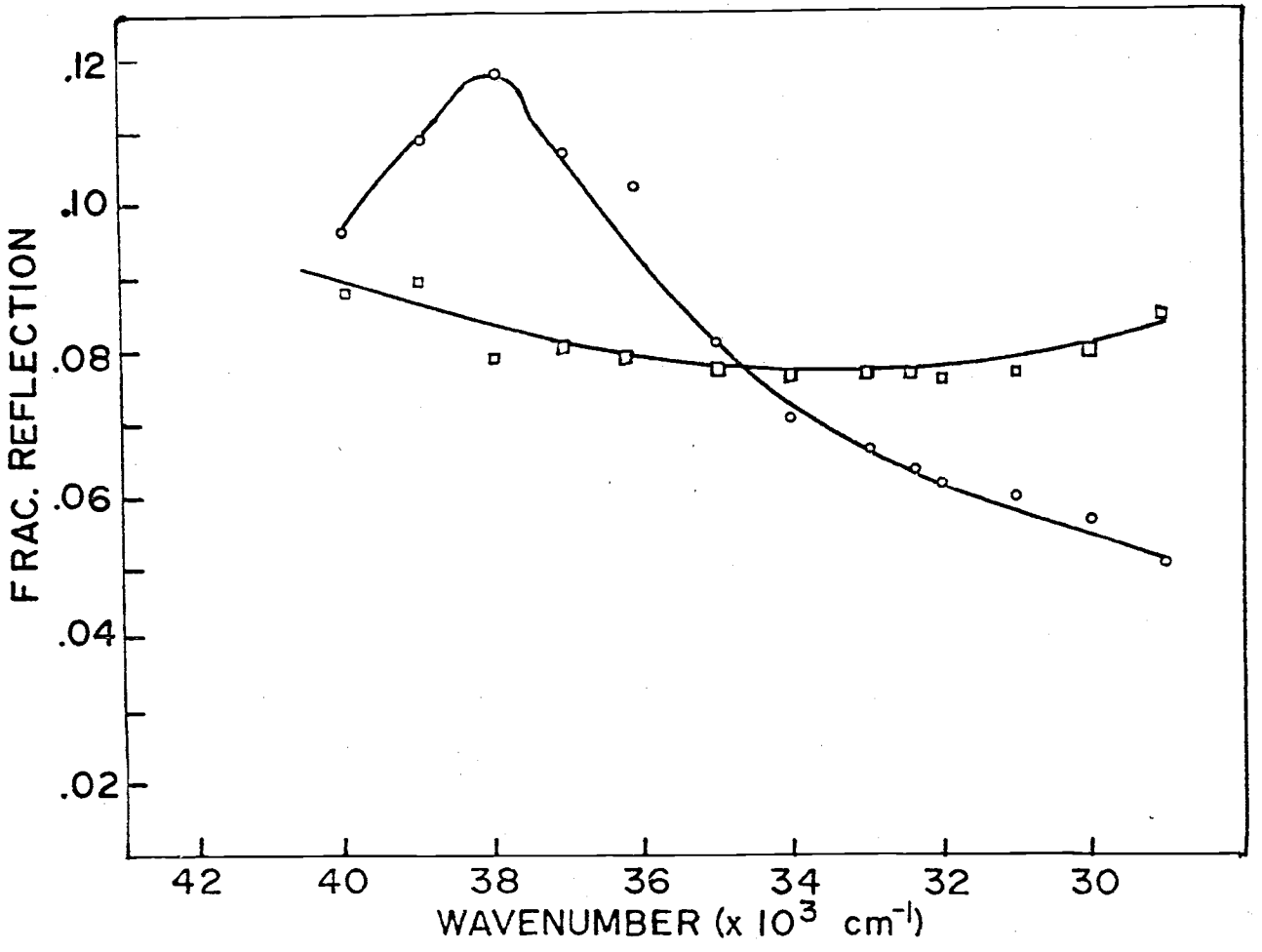


Figure 21. Fractional reflection (diffuse plus specular) vs. wavenumber for films containing 0% (circles) and 0.1% (squares) dye cyanide.

Action Spectrum

The action spectrum (relative response per photon incident) of film containing 0.1% dye cyanide is shown in Figure 22. The curve shows the relative sensitivity of the film per incident photon. The curve roughly resembles the shape of the absorption spectrum of the dye cyanide.

Film containing dye cyanide was shown to be unaffected by light of wavelengths longer than 350 nm by exposing films to sunlight between two Corning 0-52 filters which are opaque to $\lambda < 350$. The films were unaffected by even 20 minutes in the sun under these conditions.

Quantum Yields

The quantum yield for dye formation per photon absorbed by the film at room temperature is shown in Figure 23 as a function of wavelength of incident light. The shape of the curve was obtained from the results of the relative quantum yield experiments. The absolute numerical scale was added based on the quantum yield for dye formation found at 302 nm. The quantum yield depends strongly on the wavelength of the incident light, as would be expected if light absorbed by the dye cyanide was primarily responsible for dye formation.

Quantum yields for dye cyanide loss were not calculated at all wavelengths because the high noise level in the spectrophotometer readings at 277 nm ($A \simeq 1.7$) made

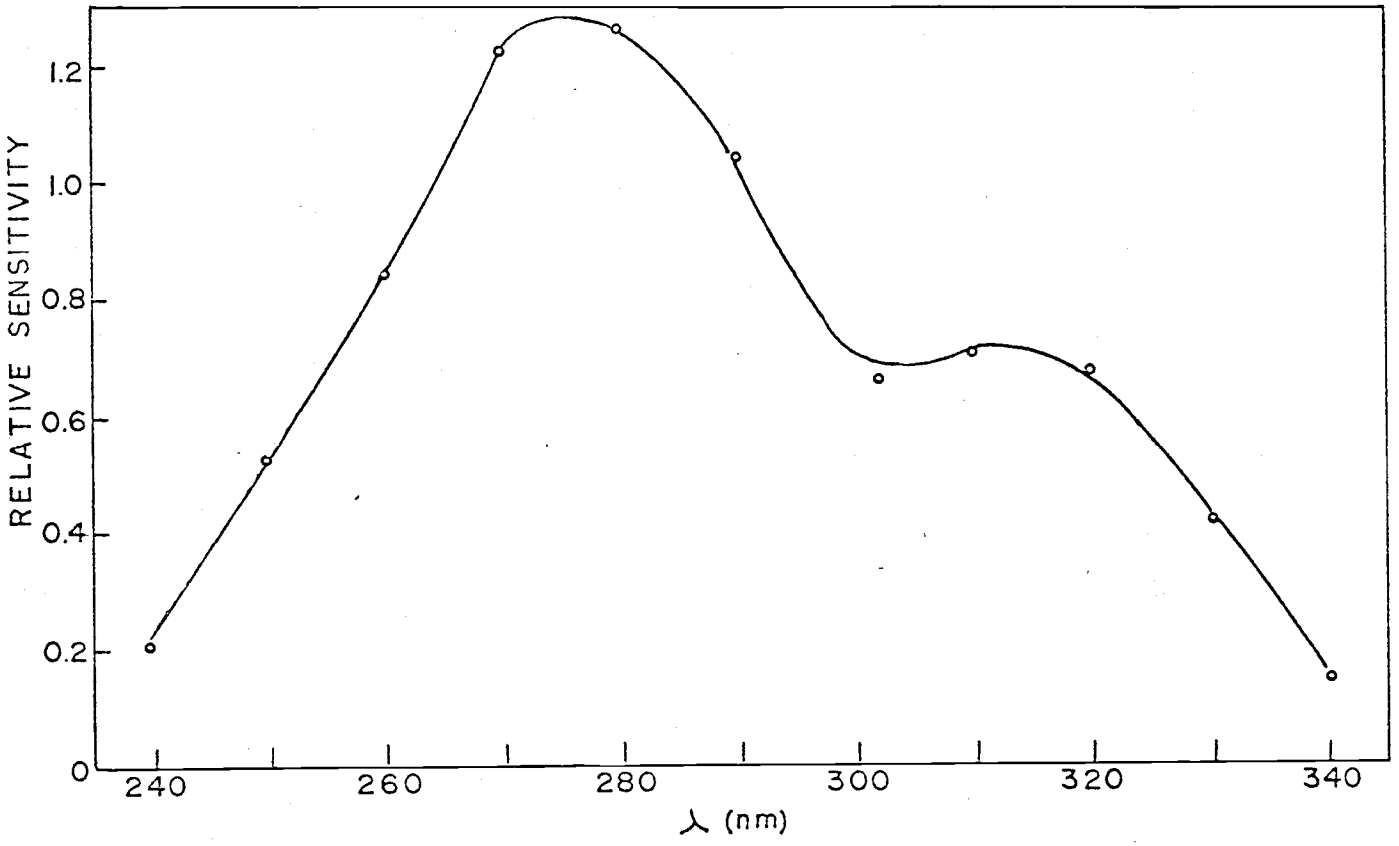


Figure 22. The action spectrum of film containing 0.1% dye cyanide. The relative sensitivity is proportional to the number of dye molecules formed per incident photon.

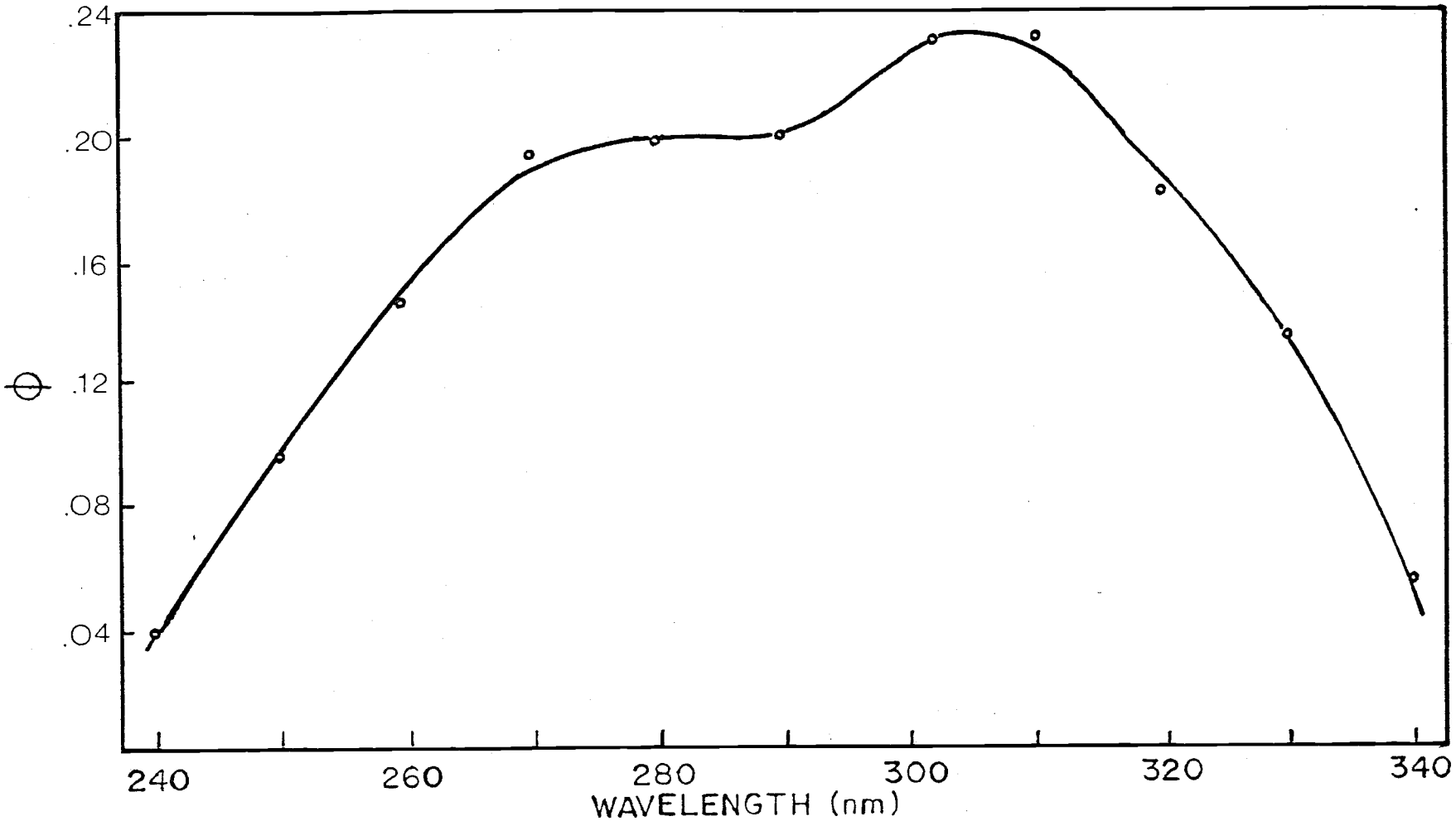


Figure 23. The overall quantum yield for dye formation vs. wavelength.

values of initial rate of change in dye cyanide concentration very uncertain.

A second quantum yield was calculated at each wavelength. This is the quantum yield for dye production per photon absorbed by the dye cyanide. This will be referred to as the partitioned quantum yield ($\phi_p$). The relative partitioned quantum yields were obtained by dividing the relative sensitivity of the film at each wavelength by the fraction of incident light that was absorbed by the dye cyanide. The fraction of light absorbed by the dye cyanide ($I_{dc}$) was calculated from

$$I_{dc} = I_{film} \times \frac{A_{dc}}{A_{film}}$$

where the absorbance values and the fraction of light absorbed by the film were obtained from absorption spectra corrected for reflection losses. Table 2 gives the value of $I_{dc}$ for the 11 wavelengths used for excitation.

The absolute partitioned quantum yield at 302 nm was obtained from the known light intensity and fractional absortion by the dye cyanide at this wavelength.

The absolute partitioned quantum yield at other wavelengths was obtained by normalizing the relative partitioned quantum yields to the value of $\phi_p = .44$ at 302 nm. The results are shown in Figure 24. The partitioned quantum yield is nearly unity at the longest wavelengths of dye cyanide absorption but is considerably smaller at shorter

Table 2. Per cent absorption by a film containing 0.1% dye cyanide as a whole and per cent absorption by the dye cyanide at various wavelengths. The values were determined from absorption spectra corrected for reflection losses.

| λ | Per cent Absorption Of Film | Fraction Absorbed By Dye Cyanide | Per cent Absorption By Dye Cyanide |
|---|---|---|---|
| 240 nm | 76% | .16 | 12% |
| 250 | 78 | .46 | 36 |
| 260 | 84 | .72 | 60 |
| 270 | 90 | .80 | 72 |
| 280 | 91 | .81 | 74 |
| 290 | 74 | .61 | 45 |
| 302 | 62 | .52 | 33 |
| 310 | 59 | .55 | 32 |
| 320 | 53 | .52 | 28 |
| 330 | 44 | .31 | 14 |
| 340 | 37 | .09 | 3 |

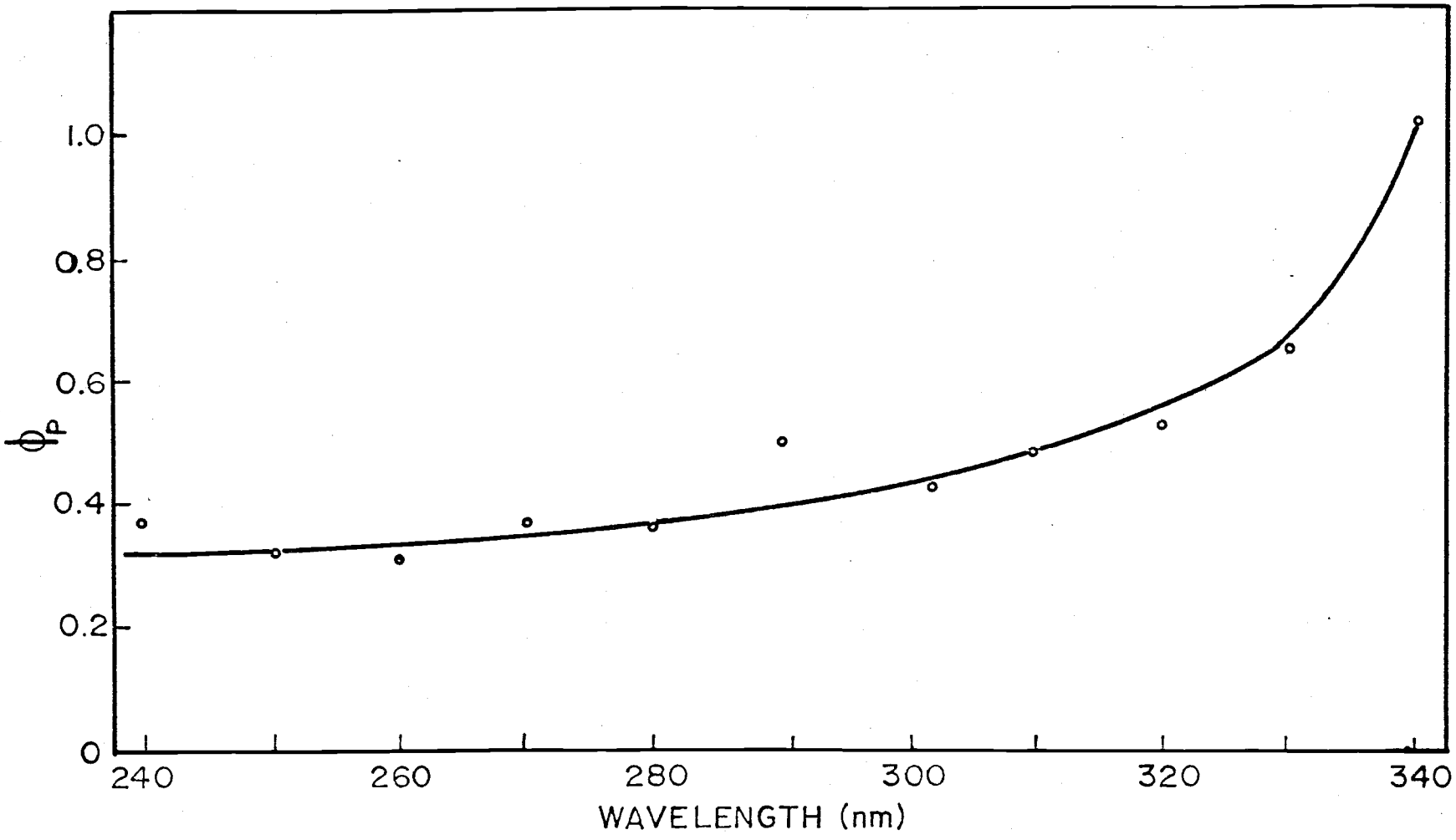


Figure 24. The partitioned quantum yield for dye formation of the dye cyanide in nylon film vs. wavelength.

wavelengths. This result would seem to indicate that energy transfer from the nylon to the dye cyanide is not important as a cause of photoionization. If it were important, the partitioned quantum yield for dye formation would be expected to be largest at wavelengths where the nylon absorbs strongly ($\lambda$ < 255 nm).

Temperature Dependence

The results of photolysis of films originally containing 0.1% dye cyanide at various temperatures is shown in Figures 25 and 26. Figure 25 shows the maximum absorbance obtained at 608 nm as a function of temperature. The films used were all exposed to 315 nm uv until maximun absorption in the dye peak was obtained. The height of this peak and apparently the maximum amount of dye that can be produced depends strongly on the temperature of the film during photolysis.

During the same series of exposures, the change in absorbance of each film after exactly two minutes of photolysis was recorded. Since the intensity of the light source and the fractional absorption by the dye cyanide probably did not vary appreciably from one exposure to the next, the change in absorbance after two minutes was assumed proportional to the relative partitioned quantum yield for dye formation. The absolute partitioned quantum yield for each temperature was calculated by normalization to the value of $\Phi_p$ = .50 for excitation at 315 nm at 20° C (from Figure 24).

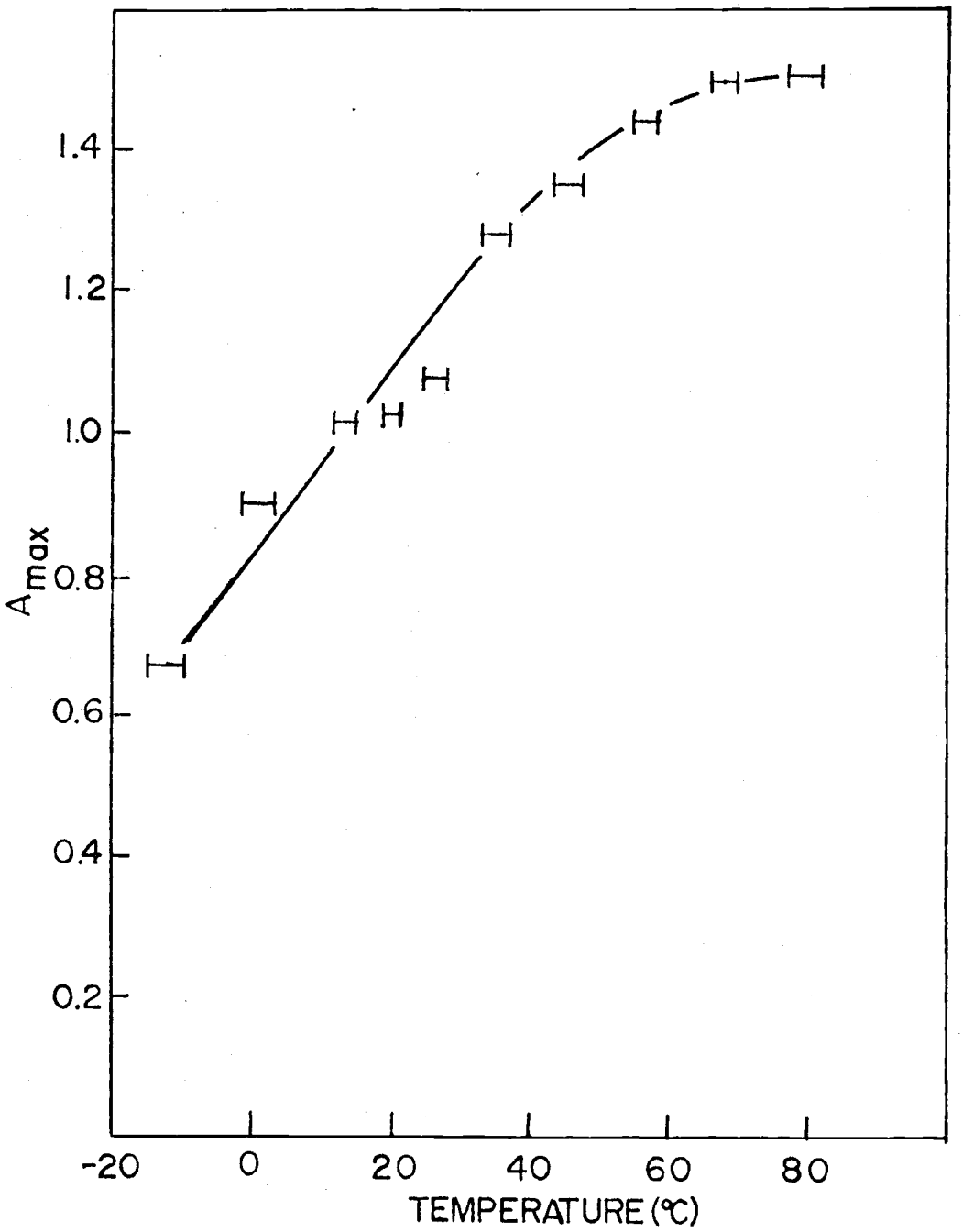


Figure 25. The maximum obtainable uncorrected absorbance at 608 nm vs. the film temperature during photolysis. 0.1% dye cyanide film was used and the exposures were all at 315 nm.

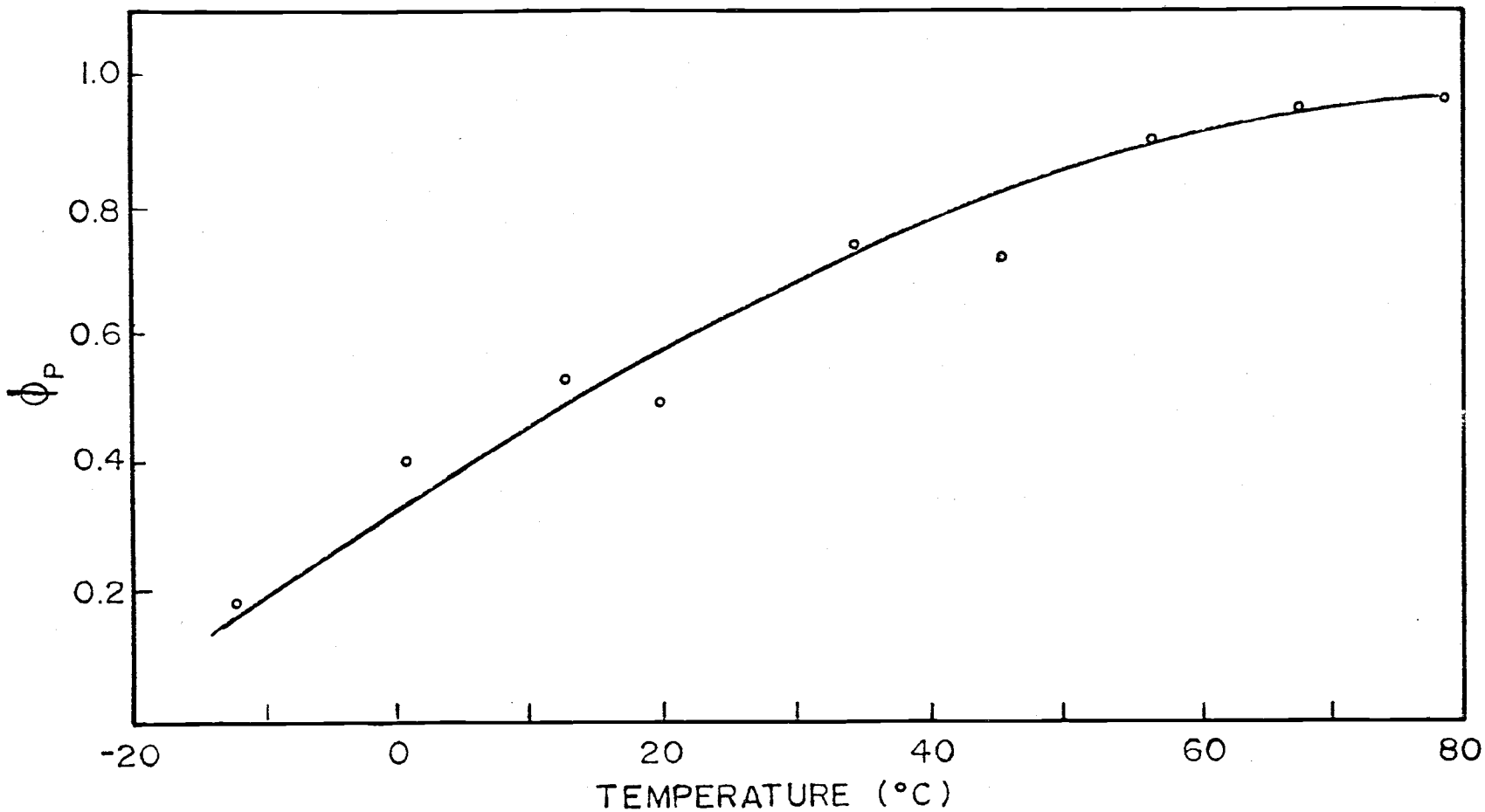


Figure 26. The partitioned quantum yield for dye formation at 315 nm vs. temperature during irradiation.

The results are shown in Figure 26.

The partitioned quantum yields for dye formation thus determined seem to increase with temperature and approach a limiting value of nearly unity.

Intensity Dependence

The results of the experiments aimed at testing for an intensity dependence (dose-rate dependence) for film response are shown in Figures 27 and 28. In both graphs the change in absorbance at 608 nm after two fixed exposures (as determined by the accumulated counts from the reference photomultiplier) are plotted vs. relative intensity of the photolysis beam.

The intensities used in experiments leading to Figure 27 are several hundred times smaller than the intensities leading to the graph in Figure 28. Thus the graphs cover two very different ranges of intensity. There seems to be little evidence for failure of the reciprocity law.

Fluorescence

Both the dye cyanide and the dye were found to be fluorescent in the rigid nylon medium. Experimentation with the fluorescence spectrophotometer showed that the dye cyanide fluoresces when excited at wavelengths shorter than 350 nm. The emission seems to peak at about 390 nm. The fluorescence emission spectra of both the dye cyanide and

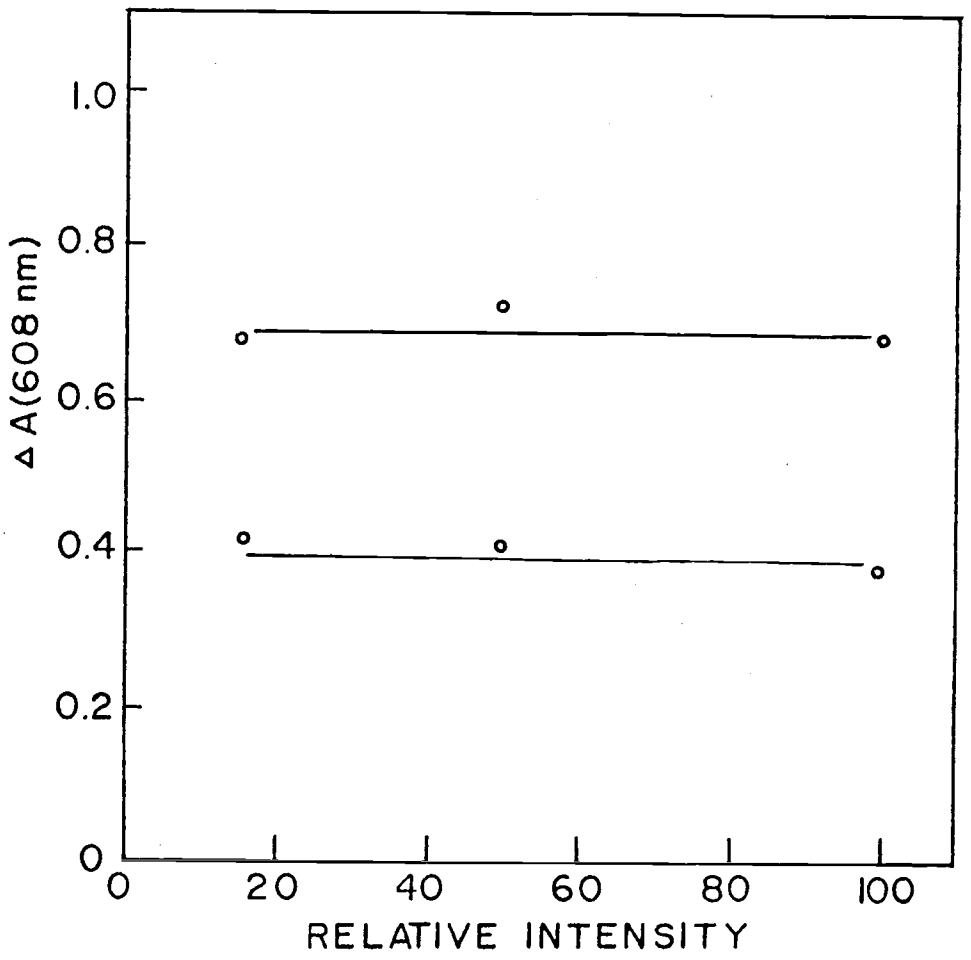


Figure 27. Change in absorbance at 608 nm after $8 \times 10^6$ counts (lower points) and $1.6 \times 10^7$ counts (upper points) vs. relative intensity of the uv used. The source of uv was a 150 watt xenon lamp and monochromator set at 310 nm.

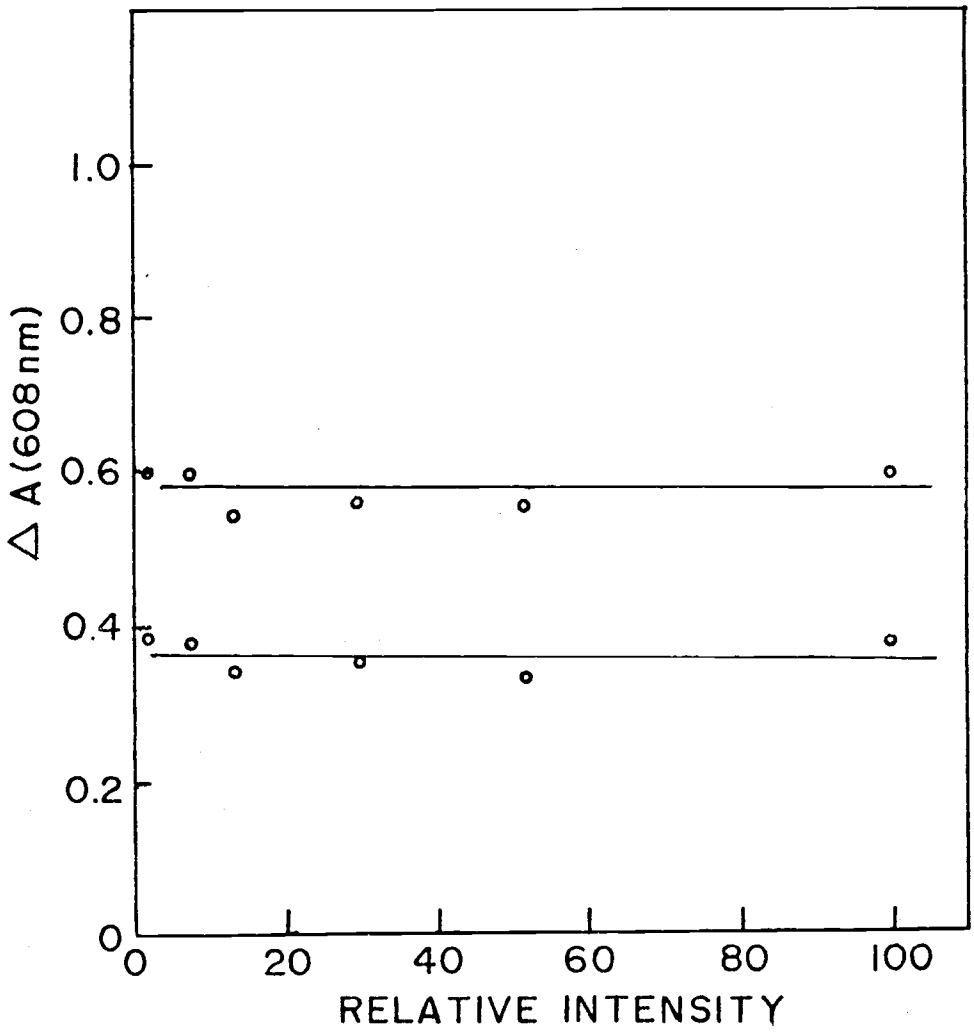


Figure 28. Change in absorbance at 608 nm after $5 \times 10^4$ counts (lower points) and $1 \times 10^5$ counts (upper points) vs. the relative intensity of the uv source. The source of uv was a 500 watt high pressure mercury lamp. No monochromator was used.

the dye as determined in the fluorescence spectrophotometer are shown in Figure 29. These spectra are not corrected for the spectral sensitivity of the spectrophotometer and hence only give an approximation of the shape of the fluorescence emission spectrum of the dye and the dye cyanide. Furthermore, no correction is made for the different intensities used to excite the two fluorescent substances. Hence no comparison of relative fluorescence efficiency between the two should be made.

The fluorescence from the dye was studied in more detail using excitation with a helium-neon laser. The emission spectrum obtained in this manner is shown in Figure 30. Some of the emitted fluorescence is of shorter wavelength than the 633 nm exciting light (anti-stokes radiation).

The use of the intensity of fluorescence from a film when excited by the laser as a means of determining dye concentration was also investigated. This was done by comparing fluorescence intensity with the absorbance of a film at the dye absorption peak (608 nm). Both of these should increase as dye concentration increases. A film was exposed to a low pressure mercury lamp (Mineralight R51) in 11 stages. The fluorescence intensity and the absorbance at 608 nm were checked after each exposure. The results are shown in Figure 31. The fluorescence intensity does increase with increasing dye concentration. The rate of

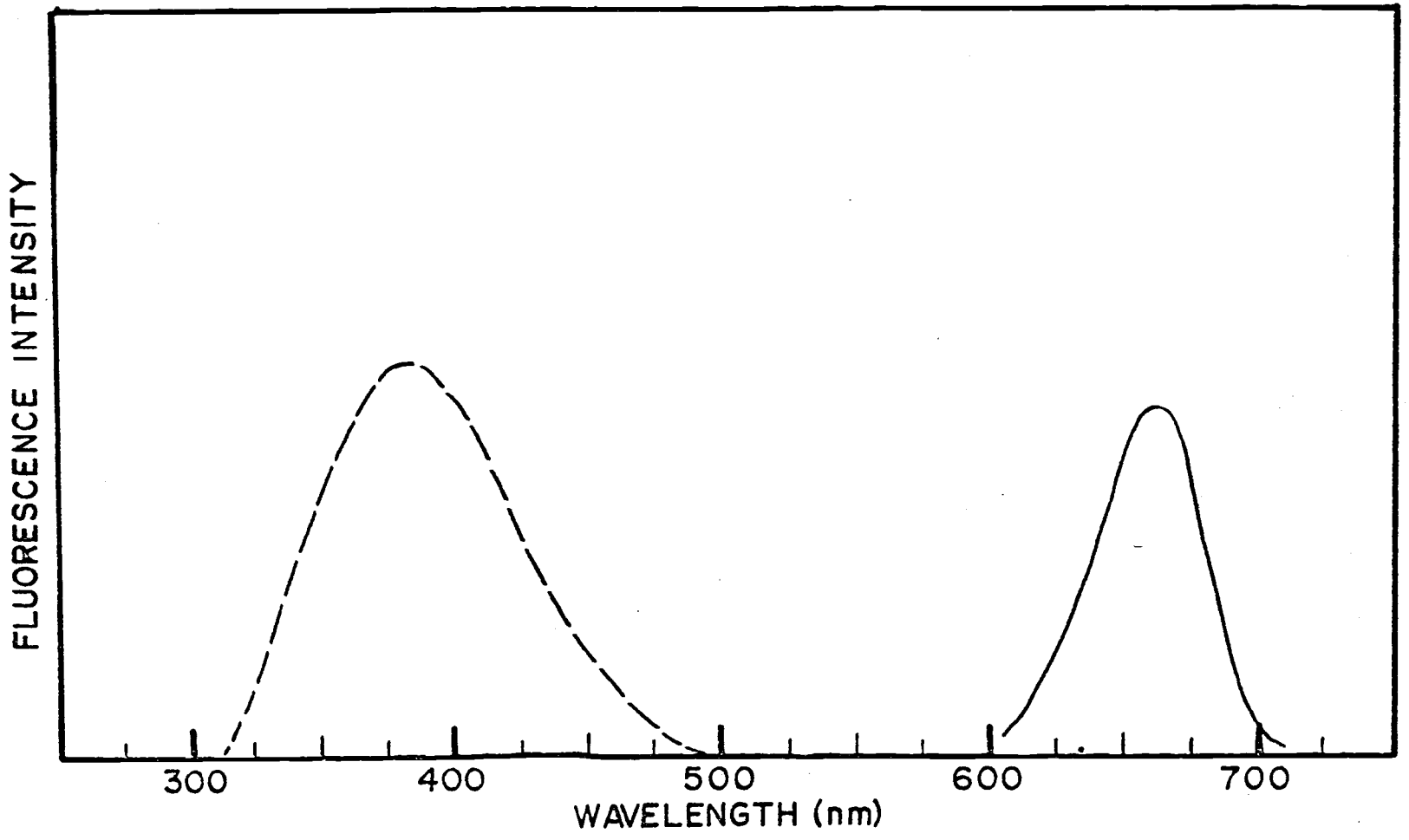


Figure 29. The approximate emission spectra of the dye cyanide (broken line) and the dye (solid line) in nylon film.

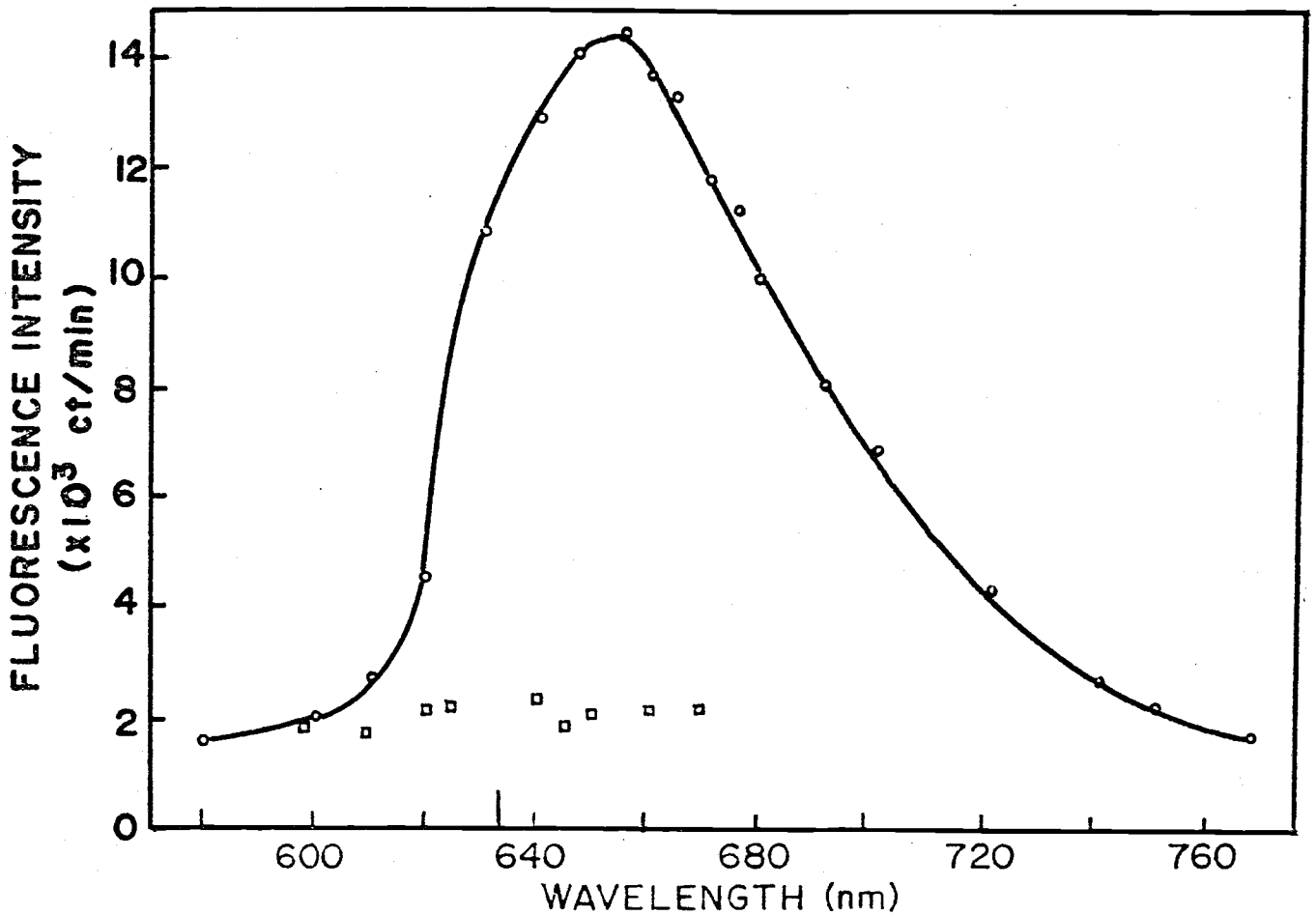


Figure 30. The emission spectrum of the dye in a film originally containing 0.1% dye cyanide. The spectrum is not corrected for the variation in detector sensitivity over this wavelength range. The squares correspond to intensity observed when the film was replaced by aluminum foil.

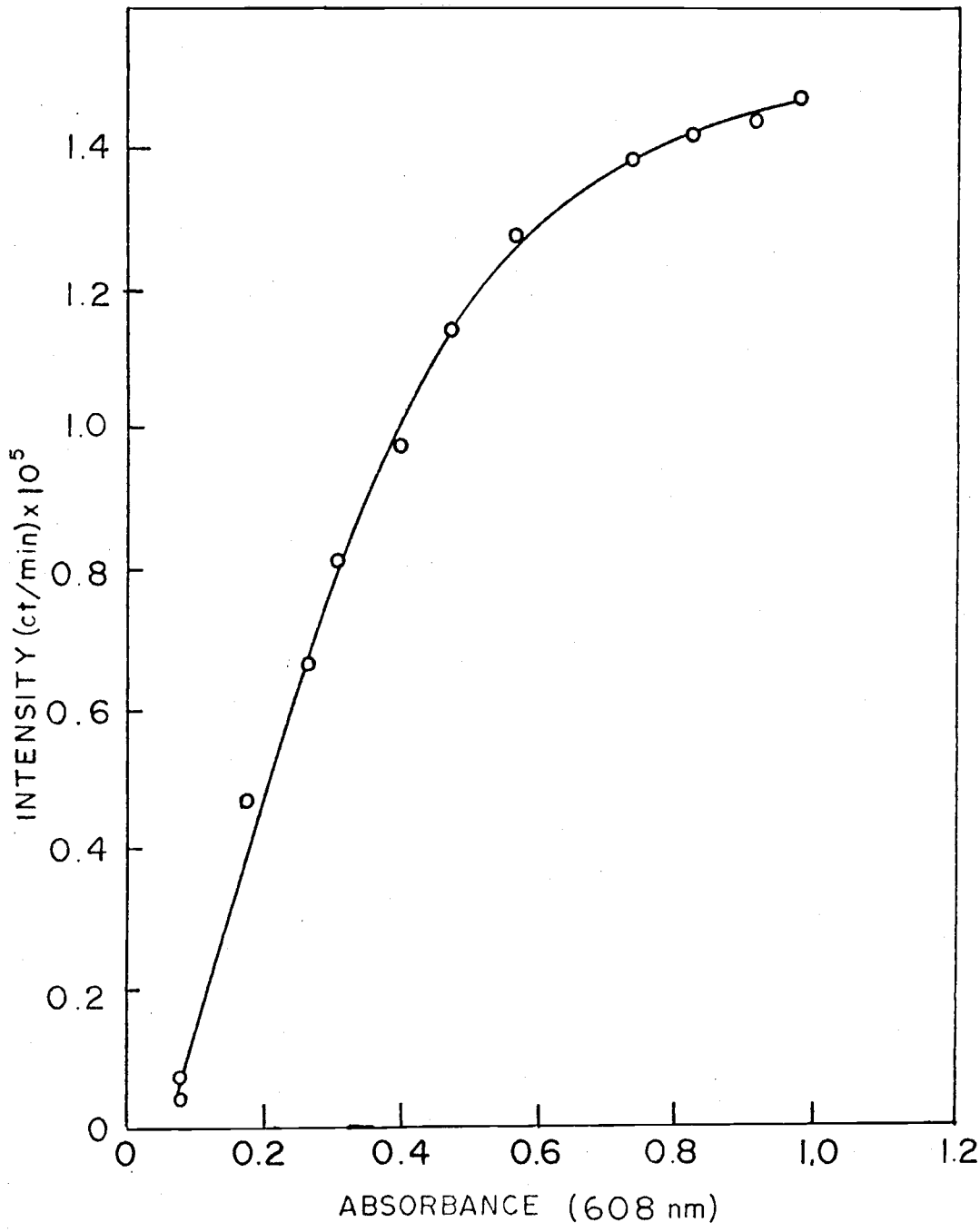


Figure 31. Intensity of fluorescence from a film originally containing 0.1% dye cyanide when excited by a helium-neon laser compared with absorbance at 608 nm for the same film. The film was exposed to uv in 11 stages.

increase decreases at high dye concentrations, probably due to internal filtering of the emitted light by the dye molecules.

Fading of the Dye

Ultraviolet light was shown to be much more effective than visible light in producing bleaching of the dye in films. The gradual fading of the dye is shown in Figure 32. The absorbance at the dye absorption maximum (608 nm) can be seen to decrease at a faster rate under irradiation by uv. This is true even though the visible (laser) light is estimated to be about ten times more intense. Using this estimate, the rate of fading per photon incident is about 35 times greater using uv light.

Even using uv, the rate of photobleaching is much smaller than the initial rate of dye formation. Figure 33 follows the photolysis of a film originally containing 0.1% dye cyanide as the dye is rapidly formed and gradually destroyed by uv. The initial rate of dye formation was about 500 times greater than the rate of fading of the dye during the photolysis of this film.

The fading of films kept in the dark is very slow. The table below shows the absorbance change at the dye peak over a period of 298 days for films stored in the dark at various temperatures

| Approximate Temperature | $A_{608}$ 8/23/74 | $A_{608}$ 6/17/75 | $\Delta A_{608}$ |
|---|---|---|---|
| 20° C | 0.556 | 0.509 | -.047 |
| 2° C | 0.781 | 0.756 | -.025 |
| -17° C | 0.725 | 0.745 | +.020 |

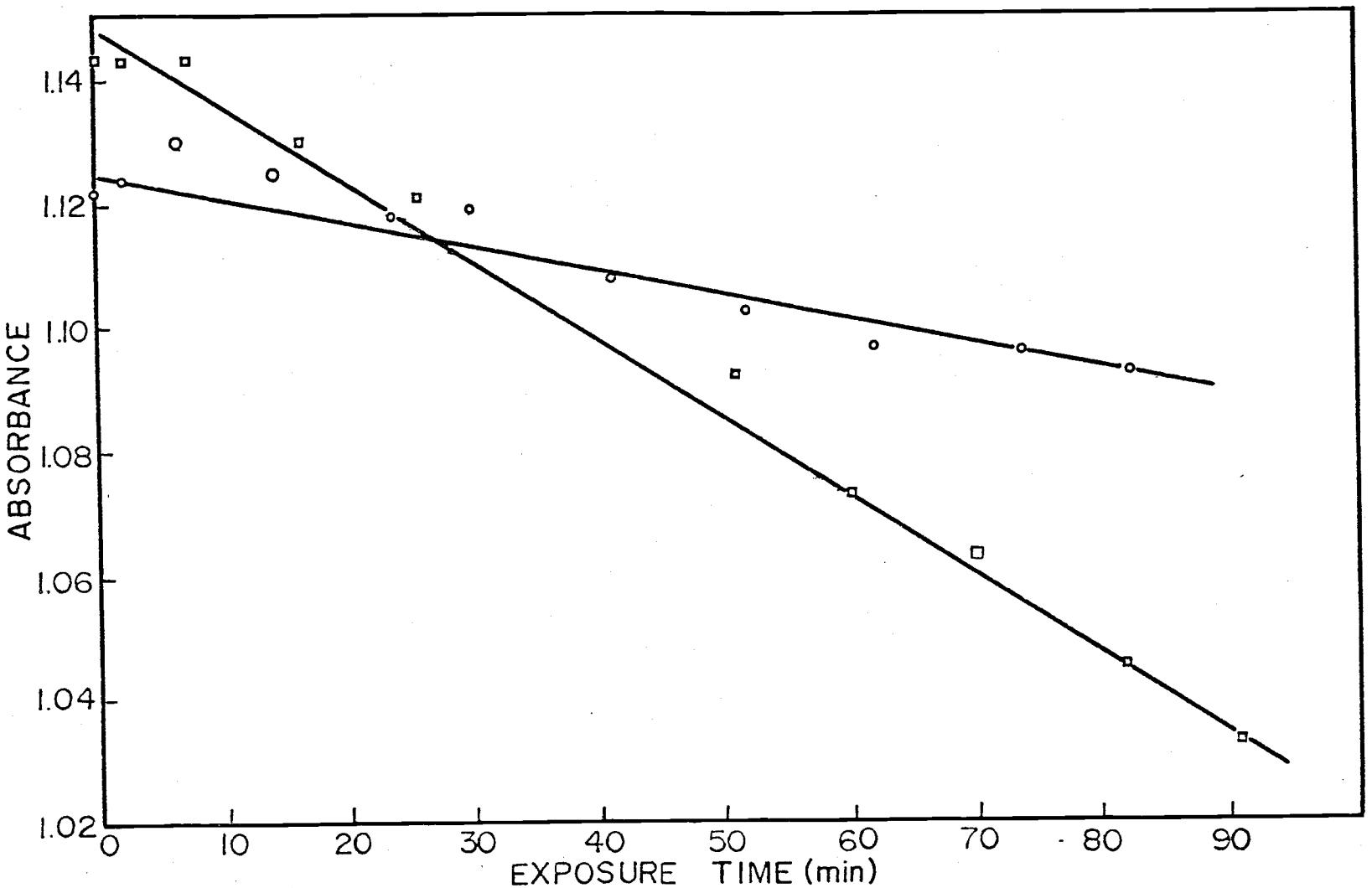


Figure 32. The absorbance at 608 nm vs. time during exposure to monochromatic uv of $\lambda$ = 302 nm (squares) and laser light of $\lambda$ = 633 nm (circles).

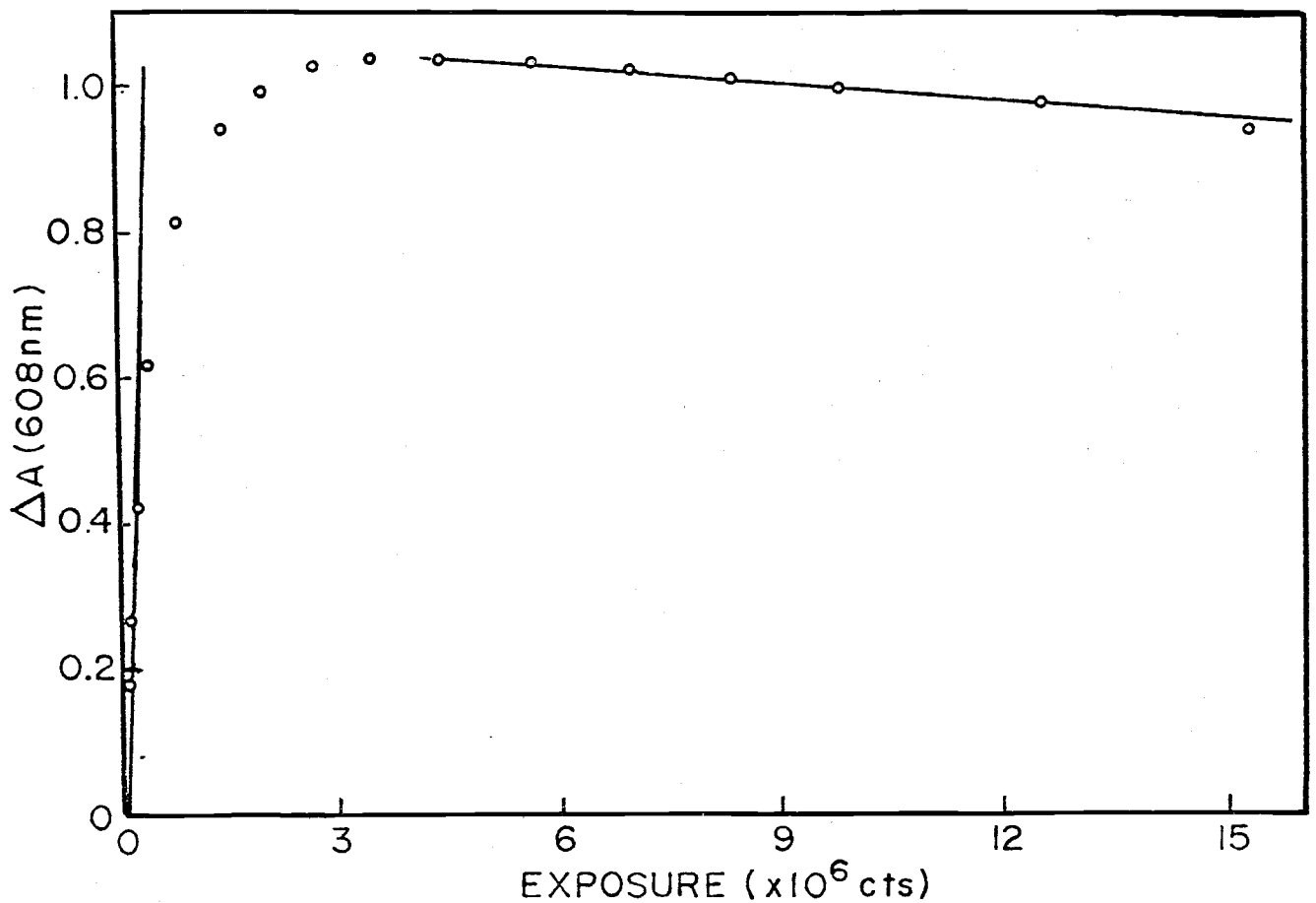


Figure 33. The change in absorbance at 608 nm for a film originally containing 0.1% dye cyanide vs. the exposure. The exposure is in terms of counts on the reference photomultiplier during photolysis. The exposure was at 302 nm. The straight lines indicate the initial rate of dye formation and the rate of photobleaching of the dye.

# DISCUSSION

## Variations in the Quantum Yield

The variation of the partitioned quantum yield for dye formation with temperature and wavelength of excitation was somewhat unexpected. Alcoholic solutions of triphenylmethyl dye cyanides have been reported to show no change in quantum yield over the range of uv absorption (Harris and Kaminsky, 1935b and Calvert and Rechen, 1952).[3] In addition, Harris and Kaminsky found that the temperature coefficient for their actinometer was essentially 1.

The temperature coefficients for response to ionizing radiation of liquid and solid solutions of triphenylmethyl dye derivatives are, however, apparently larger than unity. Although Humpherys and Wilcox (1973) claim the temperature dependence of film of the type used in this study is < 10% over the range 0-100° C, other studies with similar films indicate a greater temperature dependence. Over the temperature range -20° to 80° C, both Bishop et al (1973) and Hussman and McLaughlin (1970) observed a variation in response to cobalt 60 gamma rays of nearly 50%. Liquid solutions of triphenylmethyl dye cyanides have been reported

---

[3]The distinction between total quantum yield and partitioned quantum yield is less important in the case of alcoholic solutions since the alcohol does not absorb appreciably. Virtually all absorption is due to the dye cyanide and the two quantum yields are essentially the same.

to have similar temperature response when used with ionizing radiation (McLaughlin and Kosanic, 1974).

Examination of the absorption spectra of various films exposed to maximum absorption at the dye peak, lead to an interesting discovery. Films exposed at short wavelengths or at low temperatures showed considerable absorption in regions where neither the dye cyanide nor the dye absorb appreciably. This absorption must be attributed to the formation of an alternative photo product (X). Using the spectrum of a film exposed with 245 nm uv at 20° C to maximum dye concentration, the absorption spectrum of this photoproduct was determined. The spectral separation was done using the previously determined extinction coefficients for the dye in the film, with the assumptions that the absorption due to X at 608 nm was negligible and that no dye cyanide remained in the film. The resulting spectrum is shown in Figure 34. This broad absorption band in the near and middle uv shows up in spectra of all films exposed at low temperatures and short wavelengths.

Mechanism

The mechanism shown in Figure 35 is proposed to explain the observed variations in the quantum yield.

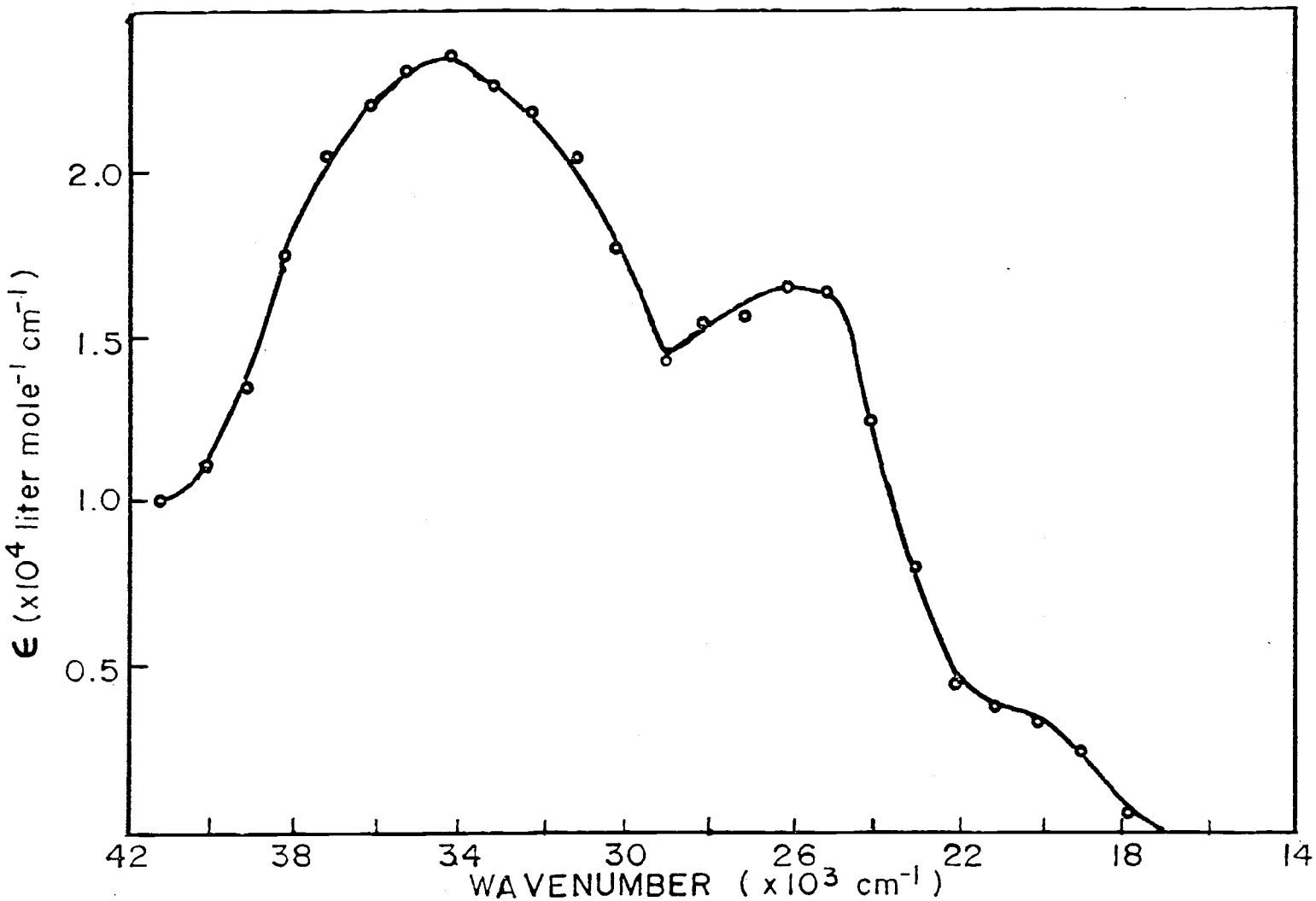


Figure 34. The absorption spectrum of the alternative photoproduct "X".

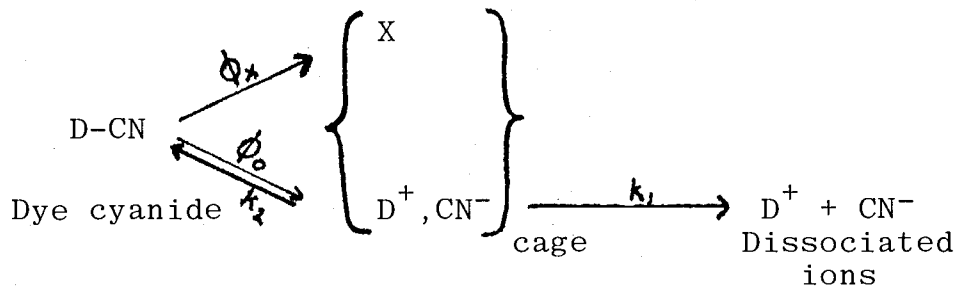


Figure 35.

In this scheme the absorption of a photon by a dye cyanide molecule can lead to either formation of ions or the alternative photoproduct X. Whichever photoproduct is formed, it is trapped in a "cage" of nylon. If ions are formed, they can dissociate only if one of the pair can escape from the cage. Otherwise they will eventually recombine and form the dye cyanide.

The fact that more X is formed at short wavelengths and the partitioned quantum yield for dye formation is dependent on wavelengths indicates that the relative amount of each of these formed depends on the wavelength of absorbed light. One explanation of this is that absorption of light by the two absorption oscillators in the dye cyanide lead to different photochemical results. Absorption of a photon by the lower energy oscillator may generally lead to photoionization. Absorption of a photon to excite the higher energy oscillator may be more likely to lead to a different chemical change and the formation of X. The two absorption oscillators correspond to the 277 nm and

the 315 nm peaks in the dye cyanide absorption spectrum. No direct evidence for this explanation is claimed. It is, however, a simple possible explanation for the wavelength dependence of the partitioned quantum yield for dye formation.

The quantum yield variation with temperature during photolysis is explained in the proposed scheme by relating the quantum yield to the rate of escape of ions from the cage of nylon. For small particles trapped in a cage like this, mathematical approximation of the rate of escape and its dependence on temperature is possible. The solvent (nylon) is assumed to consist of molecules each occupying volume v at temperature T. This volume v will consist partly of free space since the molecules are vibrating about an equilibrium position and consequently excluding other molecules from taking up positions too close to them. There is the possibility that in this situation some of the molecules will move apart and leave a "hole" in the solvent. The probability that a particle trapped in the cage will escape is proportional to the probability that a hole of sufficient size will be found adjacent to the cage. Bueche (1962) used this simple model to calculate that the probability of a hole of sufficient size (radius $\geq b^*$) being next to the cage is:

$$\text{Probability} = (\pi\varepsilon^*/kT)^{\frac{1}{2}} \exp(-\varepsilon^*/kT)$$

where:

k = Boltzman constant

$\varepsilon^* = 4\pi\varepsilon b^{*2}$ = activation energy

$\varepsilon$ = surface energy per unit area

In the calculations leading to this result the additional assumption that the activation energy is much greater than kT was made.

The probability of escape will thus be approximately proportional to $\exp(-\varepsilon^* kT)$ since the exponential is much more temperature sensitive than the pre-exponential factor. The rate of diffusion of ions out of the cage ($k_1$ in Figure 35) is then:

$$k_1 = \Theta \exp(-\varepsilon^*/kT)$$

where $\Theta$ depends only slightly on temperature and will be assumed constant. If the rate of recombination of dye cyanide ($k_2$ in Figure 35) is assumed temperature independent, the fraction of the caged ions which dissociate to form dye will be:

$$\text{fraction dissociated} = \frac{\Theta \exp(-\varepsilon^*/kT)}{\Theta \exp(-\varepsilon^*/kT) + k_2}$$

The observed partitioned quantum yield for dye production should then be:

$$\Phi_p = \Phi_o \left(\frac{\Theta \exp(-\varepsilon^*/kT)}{\Theta \exp(-\varepsilon^*/kT) + k_2}\right)$$

where $\Phi_o$ is the quantum yield for production of ions in the cage.

If the mechanism described above fits the data, a plot of $\ln(\frac{1}{\Phi p} - \frac{1}{\Phi o})$ vs. $\frac{1}{T}$ based on experimentally determined partitioned quantum yields for dye production at various temperatures should be linear. Such a graph is shown in Figure 36. The value of $\Phi_o = 0.99$ was assumed in this case. This value was adopted because this was the limit which the partitioned quantum yield for dye formation at 315 nm approached at high temperatures. At this limit every pair of ions formed would dissociate and $\Phi_p = \Phi_o$. The slope of the best straight line fit (determined by regression analysis) is $4.9 \times 10^{-3}$ °K. This is equal to:

$$\frac{\varepsilon^*}{k} = 4.9 \times 10^{-3} \text{ °K}$$

which gives an activation energy:

$$\varepsilon^* = 6.8 \times 10^{-20} \text{ joules/molecule} =$$

$$9.8 \text{ kcal/mole}$$

This value is within the range of typical values of $\varepsilon^*$ given by Bueche (1962). It is also of the same magnitude as the activation energy given by Crank and Park (1968) for diffusion of simple gasses (which should be similar in size to the cyanide ion) through various polymers.

The fact that the plot of $\ln(\frac{1}{\Phi_p} - \frac{1}{\Phi_o})$ vs. $\frac{1}{T}$ is reasonably linear and the value of $\varepsilon^*$ obtained in this way is of a reasonable size is evidence that the mechanism proposed above is a possible explanation of the observed variation in quantum yield with temperature during excitation.

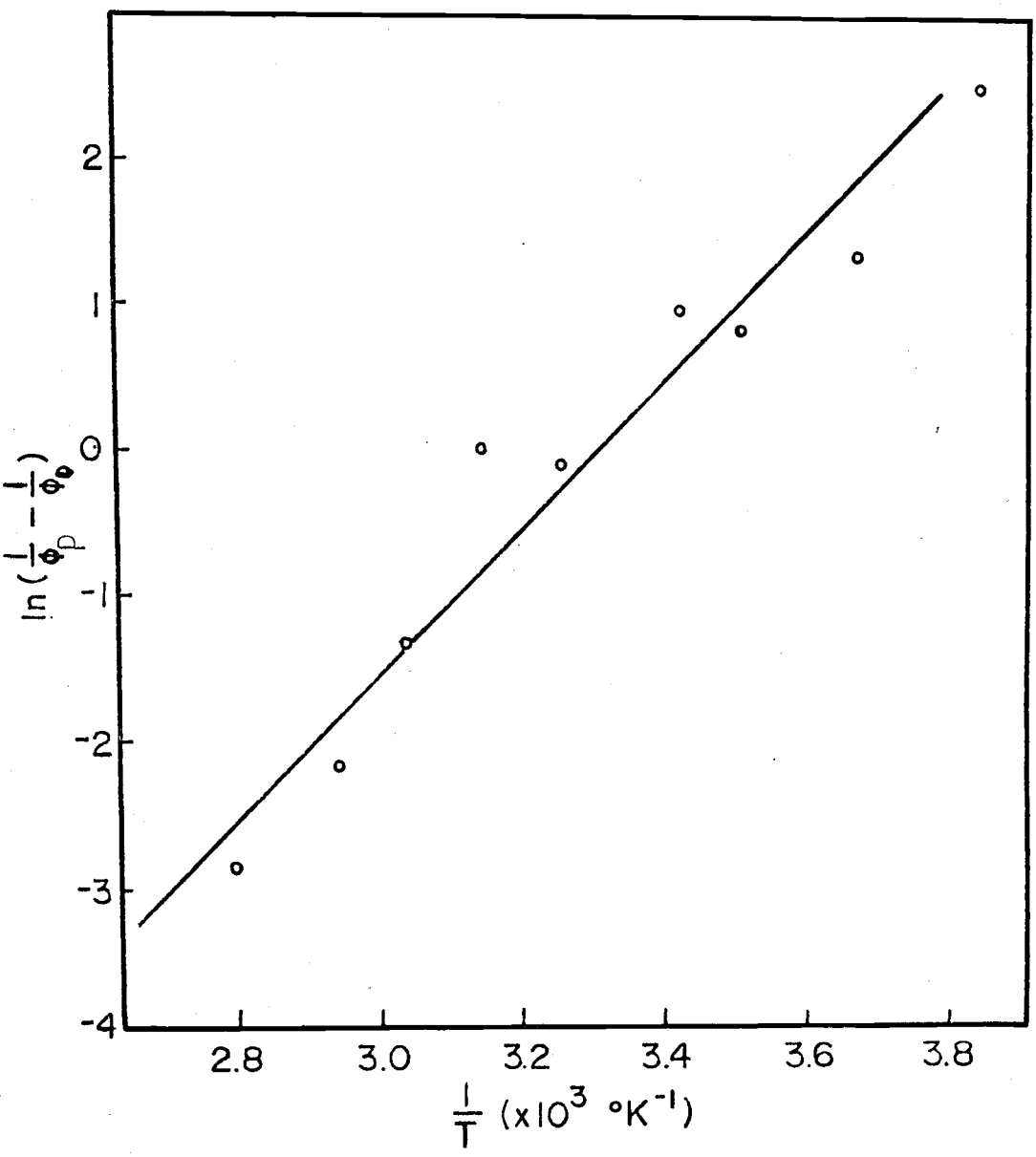


Figure 36. The natural logarithm of $\left(\frac{1}{\Phi_p} - \frac{1}{\Phi_0}\right)$ vs. inverse temperature. The approximate linearity of this data indicates that the model proposed to explain the temperature dependence of $\phi_p$ fits the data.

In summary, then, the proposed mechanism is as follows: absorption of uv may lead to formation of ions or X, either of which will be trapped in a cage within the solid nylon matrix. The formation of X is more likely when the high energy absorption oscillator is excited. When ions are formed they may dissociate to form dye or they may recombine. Dissociation requires that one of the ions escape from the cage. The probability of escape from the cage is shown using the model discussed above to increase with temperature. Hence $\Phi_p$ increases with temperature.

Potential as a uv Actinometer

The potential of the films as actinometers of ultraviolet radiation is limited to some extent by the variability of the quantum yield and other factors. The strong temperature dependence of the quantum yields requires that for actinometry the film temperature during irradiation be determined. The change in quantum yield with wavelength limits the use of the film for actinometry to monochromatic light of known wavelength. Even when used with monochromatic light with a known film temperature, a complicated table or formula of $\Phi$ vs. $\lambda$ and temperature would be required before absolute uv intensity could be determined. The variability of the film from batch to batch may require calibration of each batch individually to allow for differences in dye cyanide concentration, film thickness, and reflectivity.

One of the original reasons for our interest in the film was to investigate its potential as an actinometer of solar erythemal uv in various locations. This application is limited by two additional considerations. Both unexposed and exposed films are affected by water. The dye or dye cyanide in the film is to some extent transferred to the water whenever the film gets wet. If the film is soaked in water for several days, virtually all of the dye and dye cyanide will be removed. In many biological applications, care would have to be exercised to avoid getting the film wet to avoid erroneous apparent response.

The spectral response of the particular film used does not match the normal spectral erythema response curves as well as it would in the ideal situation. For example, human skin has an erythemal action spectrum which indicates there is little response to uv of wavelength >315 nm (Koller, 1952). The spectral sensitivity of the film extends to somewhat longer wavelengths ($\lambda \simeq 345$ nm), as was shown in Figure 22. In fact, when exposed to sunlight, the film responds primarily to uv of wavelength 315 to 345 nm, which is much more intense than the shorter wavelength uv. Experimental evidence of this was obtained by exposing films to sunlight between mylar filters which are opaque to light of wavelength < 310 nm. The response of the film is not significantly reduced in this situation compared to films exposed to unfiltered sunlight. The film used in this

study will thus not directly monitor the solar erythemal uv.

For use with monochromatic light in the laboratory or for determination of relative uv intensity, several characteristics of the film make it desirable for actinometry. As shown in Figures 27 and 28, the response of the film is not dependent on the intensity of exciting light. This dose-rate independence is essential for a useful actinometry system. The films studied were very sensitive to uv and the sensitivity can be increased or decreased at the manufacturing stage by altering the concentration of dye cyanide in the film. In addition, many of the characteristics of the film which have lead to its use as a dosimeter of ionizing radiation are positive features for uv actinometry. These include: long shelf life, high resolution images, and no need for ultra-pure, ultra-clean handling (Humpherys, 1973). The fading of the film has been found to be very slow both by our own experiments and by studies by Humpherys and Wilcox (1972).

The optical read-out procedure is simple and may be carried out with nearly any absorption spectrometer or densitometer. The fluorescence of the dye in the solid nylon medium provides an alternative read-out system. The intensity of the fluorescence from a film increases with dye concentration as shown in Figure 31. This fluorescence can be fairly intense if excited by a helium-neon laser and very small changes in dye concentration may be detected. The

equipment needed for this read-out procedure is a small laser, appropriate filter, photomultiplier, and a micro-ammeter or some other device indicating the photomultiplier's output signal. Most of this equipment is inexpensive and the fluorescence read-out system may be a desirable alternative because of its sensitivity to low dye concentrations.

The uv response of nylon films containing triphenylmethyl dye cyanide may be put to use in other applications in addition to actinometry. The film provides a convenient method of determining the shape and uniformity of a uv light beam. In this way it may be useful for alignment of optical apparatus when uv is used. Other proposed uses involving the uv sensitivity of films containing dye cyanides include uv photography and holography and data storage (Humpherys and Wilcox, 1973).

Armstrong, W.A. and G.A. Grant. 1958. Use of leuco triarylmethane compounds for chemical dosimetry. Radiation Research, 8:375.

Bennett, H.E. and W.F. Koehler. 1960. Precision measurement of absolute specular reflectance with minimized systematic errors. Journal of the Optical Society of America, 50:1.

Bishop, W.P., K.C. Humpherys, and P.T. Randtke. 1973. Poly(halo)styrene thin-film dosimeters for high doses. Review of Scientific Instruments, 44:443.

Boyle, J.W. 1962. The decomposition of aqueous sulfuric acid solutions by cobalt gamma-rays. Radiation Research, 17:427.

Brown, G.H. and W.G. Shaw. 1961. Phototropism. Review of Pure and Applied Chemistry, 11:2.

Brown, G.H. et al. 1962. Kinetic studies of phototropic reactions. I-Evidence for an ion-pair intermediate in the reaction of methyl violet with cyanide ion. Journal of Physical Chemistry, 66:2426.

Brown, G.H., ed. 1971. Photochromism. Vol. III of Techniques of Chemistry. Edited by A. Weissberger. 3 vols. Wiley-Interscience, New York. 853 p.

Calvert, J.G. and J.N. Pitts. 1966. Photochemistry. John Wiley and Sons, Inc., New York. 899 p.

Calvert, J.G. and H.J.L. Rechen. 1952. Precision actinometry at low light intensities with malachite green leucocyanide. Journal of the American Chemical Society, 74:2101.

Chalkley, L. 1929. Phototropy. Chemical Reviews, 6:217.

_____. 1952. Photometric papers sensitive only to short save ultraviolet. Journal of the Optical Society of America, 42:387.

_____. 1955. Hydrophilic dye cyanides. I-Ethyl green and xylene blue cyanides. Journal of the American Chemical Society, 77:1848.

_____. 1959. Conditions for the projection copying on dye cyanide sensitized materials. Photographic Science and Engineering, 3:174.

_____. 1973. Precision Dosimetry of High Energy Radiation. U.S. Patent 3,710,109.

Clayton, R.K. 1970. The Physical Part. Vol. I of Light and Living Matter. 2 vols. McGraw-Hill, New York. 148 p.

Cox, A. and T.J. Kemp. 1971. Introductory Photochemistry. McGraw-Hill, New York. 193 p.

Crank, J. and G.S. Park. 1968. Diffusion in Polymers. Academic Press, New York. 452 p.

Cutchis, P. 1974. Stratospheric ozone depletion and solar ultraviolet radiation on earth. Science, 184:13.

Davies, J.A. and P.P. Manning. 1957. Photochemical techniques. Journal of the American Chemical Society, 79:5148.

deGroot, M.S., I.A.M. Hesselmann, and J.H. Vander Waals. 1966. Paramagnetic resonance in phosphorescent aromatic compounds. IV-Ions in orbitally degenerate states. Molecular Physics, 10:241.

Egerton, G.S. and A.G. Morgan. 1970. Photochemistry of dyes. I-Fundamental principles. Journal of the Society of Dyers and Colourists, 86:79.

Ellis, C. and A.A. Wells. 1925. The Chemical Action of Ultraviolet Rays. The Chemical Catalog Company, Inc., New York. 362 p.

Engstrom, R.W. 1947. Multiplier phototube characteristics; application to low light levels. Journal of the Optical Society of America, 37:420.

Feofilov, P.P. 1961. The Physical Basis of Polarized Emission. Consultant's Bureau, New York. 274 p.

Field, G.R. and E. Murphy. 1971. Method of using reflectance ratios of different angles of incidence for determination of optical constants. Applied Optics, 10:1402.

Fisher, G.J., J.C. LeBlanc, and H.E. Johns. 1967. A calorimetric determination of the quantum yield for the ionization of malachite green cyanide by ultraviolet. Photochemistry and Photobiology, 6:757.

Forbes, G.S. and L.J. Heidt. 1934. Optimum composition of uranyl oxalate solutions for actinometry. Journal of the American Chemical Society, 56:2363.

Harrah, L.A. 1970. Chemical dosimetry with doped poly (halo)styrene film. Radiation Research, 41:229.

Harris, L., J. Kaminsky, and R.G. Simard. 1935a. The absorption spectrum of malachite green leucocyanide and the mechanism of dark reaction after photolysis. Journal of the American Chemical Society, 57:1151.

_____. 1935b. A precision actinometer for the ultraviolet region (including an exact test of the Einstein Equivalence Law). Journal of the American Chemical Society, 57:1154.

Hillson, P.J. and E. Rideal. 1953. The Becquerel effect in the presence of dyestuffs and the action of light on dyes. Proceedings of the Royal Society. London. Series A. Mathematican and Physical Sciences, 216: 458.

Holmes, E.O. 1957. The phototropy of malachite green leucocyanide in ethyl alcohol, cyclohexane, ethylene dichloride and ethylidene dichloride, and some mixtures of them. Journal of Physical Chemistry, 61:434.

_____. 1966. The effect of the properties of solvents of various dielectric constants and structures on the photoionization of leucocarbinals and leucocyanides of MG, CV, sunset orange and related phenomena. Journal of Physical Chemistry, 70:1037.

Humpherys, K.C. and R.L. Wilcox. 1968. High dose range X-Ray and gamma-ray dosimetry. EG&G Report, Santa Barbara Division No. S-424-R. 33 p.

_____. 1968. Radiachromic materials dosimetry study. EG&G Report, Santa Barbara Division No. S-443-R. 6 p.

_____. 1969. Radiachromic dosimetry and rate effects. EG&G Report, Santa Barbara Division No. S-464-R. 10 p.

_____. 1970. Radiachromic dosimetry materials study. EG&G Report, Santa Barbara Division No. S-498-R. 4 p.

Humpherys. 1973. Radiachromic dosimetry materials. Radiachromic Note 1.

Hunt, R.E. and T.L. Hill. 1947. A simplified method of calculating absorbed intensity in photometric experiments. Journal of Chemical Physics, 15:111.

Hunter, W.R. 1965. Errors in using the reflectance vs. angle of incidence method of determining optical constants. Journal of the Optical Society of America, 55:1197.

Hussmann, E.K. and W.L. McLaughlin. 1970. Dye films and gels for megarad dosimetry. U.K. Panel on Gamma and Electron Irradiation, The National Physical Laboratory, Teddington, England.

Inove, E. et al. 1967. Photoreversible photographic system. Photographic Science and Engineering, 11:181.

Iwamoto, K. 1935. On the fading of dyestuffs. I-Photochemical decomposition of malachite green and crystal violet. Bulletin of the Chemical Society of Japan, 10:420.

Johns, H.E. 1968. Dosimetry in photochemistry. Photochemistry and Photobiology, 8:547-563.

Kaminow, I.P. et al. 1972. Photobleaching of organic laser dyes in solid matrices. Applied Optics, 11:1563.

Koller, Lewis R. 1952. Ultraviolet Radiation. John Wiley and Sons, Inc., New York. 270 p.

Küttner, H.G., H.L. Selzle, and E.W. Schlag. 1974. Messung absoluter Quantenausbeuten von Quantenwandlern. Z. Naurforsch, 29a:224.

Lampe, F.W. and R.M. Noyes. 1954. Absolute quantum yields for dissociation of iodine in inert solvents. Journal of the American Chemical Society, 76:2140.

Leaver, I.H. 1972. Photoreduction of crystal violet in solution and in poly (vinyl alcohol) films. Photochemistry and Photobiology, 16:189.

Lewis, G.N., T.T. Magel, and D. Lipkin. 1942. Isomers of crystal violet ion. Journal of the American Chemical Society, 64:1774.

Lewis, G.N. and J. Bigeleisen. 1943a. The orientation of molecules produced photochemically in rigid solvents. Journal of the American Chemical Society, 65:520.

_____. 1943b. The y-bands in absorption spectra. Journal of the American Chemical Society, 65:2102.

Lewis, G.N., D.Lipkin, and T.T. Magel. 1944. The light absorption and fluorescence of triarylmethyl free radicals. Journal of the American Chemical Society, 66:1579.

Lifschitz, J. and C.L. Joffe. 1920. Photochemical rearrangements in the triphenylmethane series. Chemical Abstracts, 14:1984.

Lifschitz, J. and G. Girbes. 1926. Photochemical rearrangements in the triphenylmethane, series III. Chemical Abstracts, 20:1231.

Luck, W. and H. Sand. 1964. Über Phototrophie. Angew. Chem., 76:463.

McLaughlin, W.L. and L. Chalkley. 1965a. Measurement of radiation dose distributions with photochromic materials. Radiology, 84:124-125.

_____. 1965b. Radiolytic image formation in dye cyanide. Photographic Science. Symposium, Paris. Edited by J. Pouradier. Focal Press, London. 447.

_____. 1965c. Low atomic number dye systems for ionizing radiation measurement. Photographic Science and Engineering, 9:159.

McLaughlin, W.L. 1966, Microscopic visualizations of dose distributions. International Journal of Applied Radiation and Isotopes, 17:85.

McLaughlin, W.L. and L. Chalkley. 1967. Versatile chemical dosimetry systems for radiation processing. Transactions of the American Nuclear Society, 10:52.

McLaughlin, W.L. 1968. Dye systems for dosimetry of intense radiation fields. The International Conference on the Constructive Uses of Atomic Energy. Washington, D.C.

McLaughlin, W.L. and E.K. Hussmann. 1969. The measurement of electron and gamma-ray dose distributions in various media. Proceedings of IAEA Symposium on Utilization of Large Radiation Sources and Accelerators in Industrial Processes, Munich.

McLaughlin, W.L. 1970a. Films, dyes and photographic systems. Manual on Radiation Dosimetry. Edited by N.W. Holm and R.J. Berry. Marcel Dekker, Inc., New York. 129-177.

_____. 1970b. Radiochromic dye cyanide dosimeters. Manual on Radiation Dosimetry. Edited by N.W. Holm and R.J. Berry. Marcel Dekker, Inc., New York. 377-385.

McLaughlin, W.L. et al. 1971. A chemical dosimeter for monitoring gamma-radiation doses of 1-100 krad. International Journal of Applied Radiation Isotopes, 22:135.

McLaughlin, W.L., M. Kosanic, and I. Draganic. 1972. Extending the linear gamma-ray response of pararosaniline cyanide solutions from 0.1 to 1 megarads. IAEA Symposium on Dosimetric Techniques in Agriculture, Industry, Biology, and Medicine, Vienna.

McLaughlin, W.L. and M. Kosanic. 1974. The gamma-ray response of pararosaniline cyanide dosimeter solutions. International Journal of Applied Radiation Isotopes, 25:249.

Macnair, R.N. 1967. Photochromism in triphenylmethanes. Photochemistry and Photobiology, 6:779.

Martin, J.C. and R.G. Smith. 1964. Factors influencing the basicities of triarylcarbinols. Journal of the American Chemical Society, 86:2252.

Maslowski, S. 1974. High density storage on ultraviolet sensitive tape. Applied Optics, 13:857.

Murrell, J.N. 1963. The Theory of the Electronic Spectra of Organic Molecules. Spottiswoode, Ballantyne & Co., Ltd., London. 328 p.

Newman, M.S. and N.C. Deno. 1951. Aryl carbonium ions in sulfuric acid. Journal of the American Chemical Society, 73:3644.

Noyes, R.M. 1961. Effects of diffusion rates on chemical kinetics. Progress in Reaction Kinetics. Vol. 1. Edited by G. Porter. Pergamon Press, New York. 129-161.

Noyes, R.M., W. Albert, Jr., and P. Albert. 1941. The Photochemistry of Gases. Dover Publications, Inc., New York. 475 p.

Oster, G., and A.H. Adelman. 1956. Long-lived states in photochemical reactions. Journal of the American Chemical Society, 78:913.

Oster, G. and Y. Nishijima. 1956. Fluorescence and internal rotation: Their dependence on viscosity of the medium. Journal of the American Chemical Society, 78:1581.

Oster, G., and J.S. Bellin. 1957. Photoreducation of triphenylmethane dyes in the bound state. Journal of the American Chemical Society, 79:294.

Oster, G., J. Joussot-Dubien, and B. Broyde. 1959. Photoreduction of dyes in rigid media. Journal of the American Chemical Society, 81:1869.

Oster, G. and G.K. Oster. 1962. Notes from interdependence of excited states of dichroic molecules. Luminescence of Organic and Inorganic Materials. Edited by H. Kallman and G. Spruch. John Wiley and Sons, Inc., New York. 186-195.

Pitts, J.N., F. Wilkinson, and G.S. Hammond. 1963. The "vocabulary" of photochemistry. Advances in Photochemistry. Vol. 1. Edited by W.A. Noyes, Jr., G.S. Hammond and J.N. Pitts. Wiley-Interscience Publishers, New York. 1-21.

Prokert, K. and W. Stolz. 1970. Dosimetrie ionisierende Strahlung mittels fester Farbstoffsysteme. Isotopenpraxis, 6:325.

Rechen, H.J.L. 1951. Malachite green leucocyanide excitation studies with ultraviolet light and highly ionizing radiation. Unpublished Ph.D. thesis, Ohio State University.

Samson, J.A.R. 1967. Techniques of Vacuum Ultraviolet Spectroscopy. John Wiley and Sons, Inc., New York. 348 p.

Satcher, R. L. 1971. A study of the photolysis of the acqueous thymine system at 214 nm, 229 nm and 254 nm. Unpublished Ph.D. thesis, Oregon State University.

Sheppard, S.E. and H.R. Brigham. 1944. Some effects of solvents upon the absorption spectra of dyes; temperature and organic solutions of cyanide dyes. Journal of the American Chemical Society, 66:380.

Sporer, A.H. 1961. Photoionization of transmethyl leuconitriles. Transactions of the Faraday Society, 57:983.

Strobel, Howard. 1960. Chemical Instrumentation. Addison-Wesley, Reading, Massachusetts. 653 p.

Thyrion, F.C. 1971. Photo-oxidation of leuco methyl crystal violet. Journal of Chemical Education, 48:766.

Venkataraman, K. 1952. The Chemistry of Synthetic Dyes. Vol. I. Academic Press, New York. 704 p.

_____. 1952. The Chemistry of Synthetic Dyes. Vol. II. Academic Press, New York. 737 p.

_____. 1971. The Chemistry of Synthetic Dyes. Vol. IV. Academic Press, New York. 485 p.

Weyde, E. and W. Frankenburger. 1931. The measurement of uv radiation, especially of the physiologically active uv (which produces erythema) by means of the photochemical formation of triphenylmethane dyestuffs from the leuco compounds. Transactions of the Faraday Society, 27:561.

Zworykin, V.K. and E.G. Ramberg. 1949. Photoelectricity and Its Applications. John Wiley and Sons, Inc., New York. 494 p.